

**INTEGRATED DESIGN AND APPLICATION  
OF INERTER ON VEHICLE SUSPENSION  
TO OPTIMAL OSCILLATION**

A DISSERTATION SUBMITTED TO THE  
GRADUATE SCHOOL OF ENGINEERING AND SCIENCE OF THE  
SHIBAURA INSTITUTE OF TECHNOLOGY

by

**TRAN THANH TUNG**

IN PARTIAL FULFILLMENT OF THE REQUIREMENTS  
FOR THE DEGREE OF

**DOCTOR OF ENGINEERING**

JUNE 2015



## **ACKNOWLEDGEMENT**

The first sincere words, I am grateful my supervisor Professor Hiroshi HASEGAWA, who had guided me how to get idea and research as well. He has supported me throughout my dissertation with his patience and knowledge. I attribute the level of my doctor degree to his encouragement.

During the doctor course, I have been guided whole-heartedly and thoughtfully by Professors, Advisors, Teachers and all Staff assistance of the Shibaura Institute of Technology in Japan. They used to hold workshops not only on technology but also on life support, which contribute to my knowledge at all.

Finally, I thank my family and my friends all over the world they have supported and encouraged me throughout all my studies at this program.

Sincerely,

**Tran Thanh Tung./.**



## **ABSTRACT**

This dissertation discusses the passive suspension vehicle models employing inerter mechanism. It contains three parts. In the first part of the thesis, we discuss the advantage of employing inerter on suspension through the analysis of the mechanical networks via specification of comfort and road holding. We apply classical suspension theory to show that a new suspension is necessary in quarter-car and half-car vehicle models, special interested in parallel suspension. In generally, a suspension system needs to be soft to insulate against road disturbances and hard to insulate against load disturbances. It cannot achieve with a traditional passive suspension that only considered to the stiffness and damper. In this study, we verify that the advantage suspension system with inerter not only improve comfort but also increase road holding.

In the second part of the thesis, we integrate suspension system with inerter on quarter-car models. We propose some new designs, which have some advantages for suspension system by improving vehicle oscillation. This part presents some issues related to new inerter mechanism designs and verification mathematical and computational model. We discuss some results of suspension dynamics which achieve through some modal parameter of inerter mechanisms using for some specific networks.

The final, we introduce optimization method to minimize cost functions for displacement, tire deflection with constraint function of suspension deflection limitation and the energy consumed when employ inerter. The advantage of research

is optimization modal parameter of inerter that can improve the vehicle oscillation on quarter-car model both displacement and tire deflection. On the other hands, this thesis verify results of optimal parameter that achieved through functions of the suspension modal parameters in mathematical and computational model in respectively. It shows the benefit of the inerter in proposal suspension system.

Throughout this dissertation, the multi-body simulation program is used for simulating of vehicle models in combination mathematical and computational model. As a result, the analysis and synthesis methods developed in this dissertation could be directly applied to complex models.

## TABLE OF CONTENTS

Acknowledgement .....	i
Abstract .....	iii
LIST OF FIGURES .....	ix
LIST OF TABLES .....	xiii
CHAPTER 1 Introduction.....	1
1.1    Comfort Specifications .....	2
1.2    Road-Holding Specifications .....	3
1.3    Suspension Limitations.....	4
1.4    Inerter Mechanism .....	5
1.5    Quarter-Car Performance Specifications .....	6
1.6    Review of Inerter Application .....	7
1.7    Motivation Research .....	12
1.8    Outline of the Dissertation.....	12
CHAPTER 2 Synthesis of Inerter Component .....	15
2.1    The Inerter.....	15
2.2    Vibration Absorption Problem.....	19
2.3    Synthesis Inerter Mechanism.....	20
2.3.1    Gear type inerter mechanism .....	20
2.3.2    Screw type inerter mechanism .....	21
2.3.3    Hydraulic type inerter mechanism.....	23
2.4    Summary and Comments.....	25
CHAPTER 3 Advantage of Inerter Apply on Quarter-car Model .....	27
3.1    Mathematical Model .....	27

3.1.1	Quarter-car Model.....	27
3.1.2	Suspension Model in Laplace Transformed .....	28
3.2	Quarter-car Model Analysis.....	31
3.2.1	Specification of Quarter-car Model .....	31
3.2.2	Mathematical Quarter-car Model Analysis.....	33
3.3	Parallel Suspension in Quarter-car Model .....	37
3.3.1	Performance Specifications: .....	38
3.3.2	Parallel Suspension Parameters Specification: .....	40
3.3.3	Parallel Suspension Modal Analysis.....	40
3.4	Results and Discussions.....	42
3.5	Summary and Comments.....	44
CHAPTER 4 Advantage of Inerter Apply on Half-car Model .....		45
4.1	Half-Car Model Analysis.....	45
4.2	Half-car Model Specification.....	47
4.3	Advantage Results on Half-car Model.....	49
4.4	Summary and Comments.....	51
CHAPTER 5 Verification Inerter Design Apply on Suspension System .....		53
5.1	Inerter Model Analysis .....	53
5.1.1	Conceptual Inerter Model .....	54
5.2	Mathematical Model .....	56
5.3	Computational Model .....	58
5.3.1	Inerter Modal Parameter .....	60
5.3.2	Updates to Model Parameters .....	62
5.4	Verification Process .....	63
5.4.1	Code Verification.....	65
5.4.2	Calculation Verification.....	66
5.4.3	Verification Results .....	67



5.5	Summary and Comments.....	71
CHAPTER 6 Optimization Process Apply on Suspension with Inerter .....		73
6.1	Response Surface Methodology (RSM) Introduction .....	73
6.1.1	Approximating Response Functions .....	74
6.1.2	The Sequential Nature of RSM.....	75
6.1.3	RSM and the Philosophy of Quality Improvement.....	76
6.1.4	Product Design and Formulation .....	77
6.1.5	Optimization Chart Flow .....	78
6.1.6	Optimization Process .....	78
6.2	Optimization Quarter-car Model .....	80
6.2.1	Optimal Displacement: .....	80
6.2.2	Optimal Tire Deflection:.....	82
6.2.3	Optimal Both Displacement and Tire Deflection: .....	83
6.3	Verification Optimal Modal Parameter .....	88
6.3.1	Verification Force Apply to Inerter .....	88
6.3.2	Verification Sprung mass Displacement.....	90
6.3.3	Verification Tire Deflection.....	92
6.4	Optimization Half-car Model.....	94
6.5	Summary and Comments.....	97
CHAPTER 7 Conclusions.....		99
7.1	Contributions of Dissertation.....	99
7.2	Future Research .....	101
APPENDIX A Simulation for Quarter-car Model USing Matlab r2014 .....		103
A.1	Function for Quarter-car Model.....	103
APPENDIX B Simulation for Half-car Model USing Matlab r2014 .....		105
B.1	Function for Half-car Model.....	108
APPENDIX C Computational Quarter-car Model AMESim REV 11 sl11.....		111

APPENDIX D.....	112
Software use in this dissertation .....	112
D.1    Matlab & Simulink: Version R2014.....	112
D.2    AMESim Rev 11 SL11 .....	112
List of Publication.....	117

## LIST OF FIGURES

<b>Figure 2-1:</b> A free-body diagram of a one-port (two-terminal) mechanical element or network with force–velocity pair [14].	15
<b>Figure 2-2:</b> Schematic of a mechanical model of an inerter [18].	17
<b>Figure 2-3:</b> Circuit symbols and correspondences with defining equations [18].	19
<b>Figure 2-4:</b> Vibration absorption problem [17].	20
<b>Figure 2-5:</b> Gear type inerter mechanism [15].	20
<b>Figure 2-6:</b> Screw type inerter mechanism [15].	21
<b>Figure 2-7:</b> Hydraulic type inerter mechanism [16].	24
<b>Figure 3-1:</b> The base, the parallel and the series quarter-car model in respectively...	27
<b>Figure 3-2:</b> The quarter-car model with suspension function represented in Laplace transformed.	29
<b>Figure 3-3:</b> The conventional parallel spring-damper arrangement.	30
<b>Figure 3-4:</b> The parallel spring-damper augmented by an inerter in parallel.	30
<b>Figure 3-5:</b> The parallel spring-damper series with the parallel spring-inerter.	30
<b>Figure 3-6:</b> Vibration sources and input to the suspension [28].	32
<b>Figure 3-7:</b> The base, parallel and series quarter-car model in frequency response of acceleration from road disturbance $Z_r$ to sprung-mass $Z_{s\_dd}$ .	34
<b>Figure 3-8:</b> Comparison base and parallel quarter-car model in frequency response from $Z_r$ to $Z_{s\_dd}$ with the change of $b\_value$ .	35
<b>Figure 3-9:</b> Comparison base and series quarter-car model in frequency response from $Z_r$ to $Z_{s\_dd}$ with the change of $b\_value$ .	35
<b>Figure 3-10:</b> Sprung-mass acceleration results of base, parallel and series quarter-car model in time domain.	36
<b>Figure 3-11:</b> Sprung-mass displacement results of base, parallel and series quarter-car model in time domain.	36

<b>Figure 3-12:</b> Sprung-mass displacement results of base and parallel quarter-car model with change $b\_value$ . .....	37
<b>Figure 3-13:</b> The base and parallel quarter-car model with suspension function represented in Laplace Transformed respectively. ....	37
<b>Figure 3-14:</b> The conventional and parallel suspension with inerter.....	38
<b>Figure 3-15:</b> Frequency response function $TZ_s(s)$ and $TZ_t - def(s)$ of base and parallel quarter-car model with the change of inertance $b$ value in respectively.....	41
<b>Figure 3-16:</b> Comparative sprung mass displacement of base, parallel quarter-car model respectively. ....	42
<b>Figure 3-17:</b> Comparative tire deflection of base, parallel quarter-car model respectively. ....	44
<b>Figure 4-1:</b> The half-car model.....	46
<b>Figure 4-2:</b> The simulation of half-car model to calculate rolling and displacement. ....	48
<b>Figure 4-3:</b> The result of sprung mass displacement compare old and new half-car model.....	49
<b>Figure 4-4:</b> The result of rolling angle compare old and new half-car model. ....	50
<b>Figure 5-1:</b> Path from conceptual model to computational model [29].....	54
<b>Figure 5-2:</b> Theory structural inerter element [18]. ....	55
<b>Figure 5-3:</b> The conventional and parallel mathematical quarter-car model.....	58
<b>Figure 5-4:</b> The computational parallel suspension on quarter-car model. ....	59
<b>Figure 5-5:</b> Gear component with 3 ports.....	60
<b>Figure 5-6:</b> Helical rack and pinion. ....	61
<b>Figure 5-7:</b> Rotary load with two shafts without friction. ....	62
<b>Figure 5-8:</b> Verification & Validation activities and products [29].....	64
<b>Figure 5-9:</b> Verification process [29].....	65
<b>Figure 5-10:</b> Quarter-car employing inerter represent in mathematical model. ....	66
<b>Figure 5-11:</b> Comparison force apply on computational and mathematical Inerter. ..	68
<b>Figure 5-12:</b> Comparison sprung mass displacement among conventional, mathematical and computational model. ....	69

<b>Figure 5-13:</b> Comparison RMS sprung mass displacement among conventional, mathematical and computational model. ....	70
<b>Figure 6-1:</b> The response surface methodology optimization chart flow. ....	78
<b>Figure 6-2:</b> The approximate optimization process. ....	79
<b>Figure 6-2:</b> Comparative sprung mass displacement of base, parallel and optimal model in respectively. ....	85
<b>Figure 6-3:</b> Comparative tire deflection of base, parallel and optimal model in respectively. ....	86
<b>Figure 6-4:</b> Comparative sprung mass displacement and tire deflection of base and optimal quarter-car model in respectively.....	87
<b>Figure 6-6:</b> Comparison RMS force between optimization of mathematical and computational inerter. ....	89
<b>Figure 6-7:</b> Comparison RMS sprung mass displacement among conventional, mathematical and computational model respectively. ....	91
<b>Figure 6-8:</b> Comparison RMS tire deflection among conventional, mathematical and computational model respectively.....	93
<b>Figure 6-9:</b> Results of optimization rolling angle for half-car models. ....	96
<b>Figure A-1:</b> Simulink of conventional quarter-car model. ....	103
<b>Figure A-2:</b> Simulink of new and optimal quarter-car model. ....	103
<b>Figure B-3:</b> Simulink of half-car model. ....	105
<b>Figure B-4:</b> Simulink of sprung mass module. ....	106
<b>Figure B-5:</b> Simulink of un-sprung mass module.....	106
<b>Figure B-6:</b> Simulink of tire module.....	107
<b>Figure B-7:</b> Simulink of conventional suspension module.....	107
<b>Figure B-8:</b> Simulink of new parallel suspension module.....	108
<b>Figure B-9:</b> Simulink of optimal suspension module. ....	108
<b>Figure C-10:</b> The computational quarter-car model with screw inerter and hydraulic inerter in respectively.....	111



## LIST OF TABLES

<b>Table 3-1:</b> The specification of Formula SAE quarter-car model. ....	31
<b>Table 3-2:</b> The specification of parallel suspension with inerter. ....	40
<b>Table 3-3:</b> Comparison the RMS sprung mass displacement of base, parallel quarter-car model. ....	43
<b>Table 3-4:</b> Comparison the RMS tire deflection of base, parallel quarter-car model. ....	44
<b>Table 4-1:</b> The specification of Formula SAE half-car model. ....	47
<b>Table 4-2:</b> The comparison rolling angle peak point results. ....	50
<b>Table 5-1:</b> Gear component parameters index. ....	60
<b>Table 5-2:</b> Helical rack and pinion component parameters index. ....	61
<b>Table 5-3:</b> Rotary parameter . ....	62
<b>Table 5-4:</b> Comparison RMS force apply to mathematical and computational inerter respectively. ....	69
<b>Table 5-5:</b> Comparison improvement RMS sprung mass displacement of conventional, mathematical and computational model in respectively. ....	71
<b>Table 6-1:</b> The boundary of design variables. ....	80
<b>Table 6-2:</b> The comparative modal parameters to optimal sprung mass displacement. ....	82
<b>Table 6-3:</b> The comparative modal parameters to optimal tire deflection. ....	83
<b>Table 6-4:</b> The comparative modal parameters to optimal both displacement and tire deflection. ....	84
<b>Table 6-5:</b> Comparison the RMS sprung mass displacement results. ....	85
<b>Table 6-6:</b> Comparison the RMS tire deflection results. ....	87
<b>Table 6-7:</b> Comparison both RMS sprung mass displacement and tire deflection results. ....	88

<b>Table 6-8:</b> Comparison RMS force apply to optimal mathematical and computational inerter respectively.....	90
<b>Table 6-9:</b> Comparison RMS of sprung displacement among convetional and optimal mathematical, optimal computational inerter respectively.....	92
<b>Table 6-10:</b> Comparison RMS of tire deflection among convetional and optimal mathematical, optimal computational inerter respectively. ....	94
<b>Table 6-11:</b> The boundary of design variables.....	94
<b>Table 6-12:</b> The comparative modal parameters for half-car model. ....	95
<b>Table 6-13:</b> The comparison rolling peak results.....	96



## **CHAPTER 1**

### **INTRODUCTION**

Passive, semi-active and active suspension systems have been utilized to improve ride comfort of vehicles and their effectiveness has also been demonstrated. However, it is not easy to improve dynamics stability with passive suspension systems. To achieve it, several control methods have been proposed, but most of them relate the active suspension [1] [2] [3].

In the automotive field, vehicle and human body performance specifications are subjects where many works have been published and still are open research areas covering different engineering domains [4]. Briefly speaking, to define these performances, automotive engineers have first to formulate requirements in classical words then to turn them into mathematical expressions and introduce consistent and repetitive metrics to quantify these characteristics. Usually, the first step is straightforward since it comes from driver feelings and expectation. The second step is usually much harder since it is very dependent on the engineering general approach (time, frequency...), and may turn out to be non-representative to all drivers. Some metrics for performance evaluation have been selected according to researchers, general observations and discussions with automotive experts from both industry and academy. The researchers stress that other relevant metrics should also be used and may be preferred according to other fields, but, since the proposed ones are derived in both time and frequency domains, they are representative of a large spectrum of behaviors and can be considered as reliable and consistent for our purpose. Moreover,

even if other metrics may be introduced, the researchers should notice that the interest of the proposed metrics rely on their simplicity and complementary.

As a consequence, the model used in this thesis is the classical quarter-car model. Suspension characteristics also affect other ground vehicle dynamics such as roll, pitch, longitudinal, but also yaw, therefore the suspension parameter is also a matter of global chassis improvement [5] [6].

## **1.1 Comfort Specifications**

When comfort characteristics are considered, it mainly concerns the passenger's comfort. This very subjective feeling is a combination of different factors such as:

- The driver's state (e.g. feelings, age, health, general abilities etc.) and environment (e.g. weather) which are not controllable.
- The chassis vibrations, noise, etc. which are controllable by an adequate suspension and control law design.

From a general viewpoint, comfort feeling, characterized by the road unevenness filtering, has an impact on the driver reaction time, accuracy, situation evaluation and decision abilities, which makes this objective particularly active in the automotive community [7].

Since the driver comfort study is a complex and subjective concept, an entire chapter may be required to describe driver vibration models, sensitive zones, etc. Roughly speaking, in the literature, comfort analysis is mainly treated as non-comfort analysis; such studies are usually held by modeling the human body as a complex system composed of masses linked by spring and damper elements, modeling the muscles [8]. Then, according to this kind of model, studies indicate some sensitive frequency zones (related e.g. to the heart, the head, etc.) having resonance or gain

amplifications around some specific frequencies according to different disturbances such as the steering wheel vibrations or the road irregularities.

The comfort characteristics are considered, it mainly related to displacement, chassis vibration, noise, etc. It has an impact on the driver reaction time, accuracy, situation evaluation and decision abilities, which makes this objective particularly active in the automotive community. According to these kind of models, they indicate some sensitive frequency zones related to the heart, the head, etc. having resonance or gain amplifications around some specific frequencies according to different disturbances such as the road irregularities [9].

In this study, the comfort is not directly discussed, but evaluated through the chassis analysis as sprung mass displacement. The comfort feeling analysis is performed by analyzing some specific frequencies of the vertical behavior of the quarter-vehicle model. We focus on the analysis of simpler variables behavior with respect to road unevenness, such as vertical acceleration  $\ddot{Z}_s$  and displacement  $Z_s$  of the chassis. Then an improvement on these variables will imply comfort improvement with mathematical objective is:

$$\min \ddot{Z}_s(t) := \min Z_s(t) \quad \text{Eq. 1-1}$$

## 1.2 Road-Holding Specifications

Compared to the human comfort, road-holding is a vehicle property which characterizes the ability of the vehicle (and more specifically, of the wheels) to keep contact with the road and maximize wheel tracking to road unevenness, i.e. to filter the wheel trepidations generated by road irregularities, and, to guarantee road contact whatever the road profile and load transfer situations (e.g. in difficult cornering situations). This contact property is essential since wheel load is strongly related to longitudinal and lateral force descriptions which are essential in all vehicle dynamics.

These functions are highly nonlinear and complex to define; in fact, they will not be treated in other books and assumed as constant, for more detail, the reader is encourage to refer [10] [11] [12] [13].

Road-holding is a vehicle property which characterizes the ability of the vehicle to keep contact with the road and maximize wheel tracking to road unevenness. In a very simplified manner, the longitudinal  $F_{tx}$  lateral  $F_{ty}$  forces of each tire as follows:

$$F_{tx} = F_n \mu_x \quad \text{Eq. 1-2}$$

$$F_{ty} = F_n \mu_y \quad \text{Eq. 1-3}$$

Where  $\mu_x$  and  $\mu_y$  are the nonlinear functions, dependent on the slip ratio, the slip angle and the road roughness characteristics.

These forces are also affine functions of  $F_n$ , the normal load, defined as:

$$F_n = (M_s + M_u)g - k_t(Z_u - Z_r) \quad \text{Eq. 1-4}$$

Where  $M_s$  and  $M_u$  are the sprung and unsprung masses,  $Z_u$  is displacement of unsprung mass,  $Z_r$  is road disturbance,  $k_t$  is the vertical tire stiffness characteristic and tire deflection:

$$Z_{t-def} = Z_u - Z_r \quad \text{Eq. 1-5}$$

Because  $(M_s + M_u)g > 0$  and  $k_t > 0$  then:

$F_n$  max when tire deflection  $Z_{t-def} = Z_u - Z_r$  go to minimization.

### 1.3 Suspension Limitations

When evaluating a suspension system and its associated control algorithm, to take into account the static suspension stroke limitations  $Z_{sus} = Z_s - Z_u$  which should always remain in between the limitations defined by the technology, i.e. then:

$$\min Z_{sus} \leq Z_{sus} \leq \max Z_{sus}$$

Where  $\min Z_{\text{sus}}$  and  $\max Z_{\text{sus}}$  are the suspensions deflection limits. This constraint is very important for practical applications, in order to preserve the mechanical suspension system.

#### **1.4 Inerter Mechanism**

To improve vehicle oscillation, this study proposes a design of passive suspension system taking with new component element named "inerter" into consideration the both sensitive of the sprung mass and tire deflection vehicle behaviour when have road disturbance [14]. It can improve both displacement and tire deflection of vehicle proposed by optimizing the modal parameters of suspension and tire. In order to verify the effectiveness of the proposed method, a quarter-car model that has variable stiffness, damping and inerter in suspension system is constructed and the numerical simulations are carried.

For modelling of an inerter, it was defined to be a mechanical two-terminal, one-port device with the property that the equal and opposite force applied at the nodes is proportional to the relative acceleration between the nodes. For example, the gear type inerter mechanism including a gear set and rack, it has two terminals at the rack and the base body. The dynamic equation of an inerter is derived as  $F=b*a$ , wherein  $F$ ,  $b$  and  $a$  represent the applied force, the inerter coefficient (called inertance) and the relative acceleration of two terminals, respectively. The inertance is calculated from the radius and inertia of flywheel. Another objective is presented to reduce friction force and system energy dissipation is screw type inerter mechanism. It can be reduce conventional backlash general by gear transmission [15]. In other hands, hydraulic type inerter is mechanism which comprises a hydraulic cylinder. A hydraulic motor connected to hydraulic cylinder with an output shaft for converting

the linear motion to rotary motion and an inerter body disposed on the output shaft. This system subjects to high external force loads and controllability [16].

Let focus attention first on the familiar two-terminal modeling elements: spring, damper and inerter. Each is an ideal modeling element, with a mathematical definition [17] [18] [19]. It is useful to discuss on mechanical networks, which give some hint toward the inerter idea, in order to highlight the new passive suspension system.

### 1.5 Quarter-Car Performance Specifications

Considering the previous remarks, and considering the quarter-car model given, the following signals are considered for performance analysis and characterization of a suspension system:

- To evaluate the comfort, the vertical displacement  $Z$  (or acceleration  $\ddot{Z}$ ) of the chassis is analyzed.
- To evaluate the road-holding, the tire deflection ( $Z_{t-def}$ ) is analyzed.
- Eventually, the deflection limits ( $minZ_{sus}$  and  $maxZ_{sus}$ ) could be analyzed.

Note that in this thesis, this point will not be dealt with, since it involves linear suspension spring description.

The frequency responses of both main transfer functions under discussion in this thesis, namely,  $F_Z$  and  $F_{Z_{t-def}}$  are transfer function from road disturbance to sprung mass and tire deflection in respectively. Then let us define the comfort and road-holding performances as follows.

**Comfort:** The vibration isolation between [0; 20]Hz is evaluated by the transfer function  $F_Z$ . Ideally, the vertical displacement of the chassis should be the same as the one of the road for low frequencies (lower than around 1Hz) and

attenuated for high frequencies (higher than 1Hz), in order to filter undesirable vibrations. In practice, for low disturbances [20].

**Road-Holding:** As indicated before, it is evaluated using the transfer function  $F_{Z_t-def}$  over the frequency range of [0; 30]Hz. For a good road-holding, the tire deflection should be attenuated for low frequencies, and filtered around the resonance frequency of the wheel and over. Moreover, especially for high frequencies, the wheel should always remain linked to the road.

Note that these objectives are consistent with the ones given in previous suspension analysis works [21] [22]. The comfort and road-holding performances objectives are illustrated, considering the passive quarter-car model using the motorcycle parameters.

**Deflection:** The deflection signal should remain in the linear zone of the suspension system to avoid the end-stop zone leading to discontinuities. This consideration is very important especially when the comfort objective is to be reached.

Note that in this study, frequency limits will be fixed to 30Hz. This choice is justified by the fact that, practically, higher frequencies are filtered by the vehicle mechanical elements.

Therefore, it is not of great importance to extend the analysis over that frequency. Moreover, according to the quarter-car definition given in this thesis, this frequency limit is enough to describe all the interesting behaviors, the two masses resonance peaks, the static gain, the attenuation area, etc.

## 1.6 Review of Inerter Application

During development of inerter, McLaren invented a decoy name for the inerter (they call "J-damper") to keep the technology secret from its competitors for as long

as possible. In fact, the device was first conceived by its creator, Professor Malcolm Smith, as long ago as 1997. The suspension device for use in F1 car with Inerter has been developed in secret by McLaren and Cambridge University since 2005 under a confidential arrangement between the team and university. It is used not only to improve mechanical grip but can offer greater flexibility in a vehicle's suspension system. Looks like that in same time Ferrari was developing same system by themselves, and without any outside help.

The fact that the Inerter is an inerter was revealed in the Autosport article by Craig Scarborough, a motor sport correspondent from Autosport magazine. Autosport ran an article on May 29, 2008, which revealed the Cambridge connection and that the Inerter was an inerter. Cambridge Enterprise, the commercialization office of the University of Cambridge, has now entered into a license agreement with Penske Racing Shocks enabling Penske to supply inerter to any team in Formula One.

Inerter is the legal version of mass damper and is found in the third, transverse damper on the rear suspension of the cars. Reacting to the acceleration of the suspension, the Inerter absorbs the loads that would otherwise not be controlled by the velocity sensitive conventional dampers. Inerter absorbs excess energy from tires and suspension to make the load through the contact patch more predictable and hence more stable at the point in time when stability is most crucial. Normal damper dissipate energy mostly through heat, and Inerter absorbs energy. Mass inside Inerter is attached to a threaded shaft within the transverse damper so it is effectively out of sight.

The inerter is a device which provides a force proportional to the relative acceleration between its attachment points ("terminals") which must be freely and



independently movable in space. A typical realization incorporates a flywheel which rotates in proportion to the relative displacement between the terminals. The first publication on the subject, in which the word "inertor" was coined [14] and a patent on the device had previously been filed by the Cambridge University.

It is known that the correspondence is perfect in the case of the spring and damper. A fact which is also known, but frequently glossed over, is that there is a restriction in the case of the mass. All the above elements except the mass have two "terminals", for a mechanical element the terminals are the attachment points which should be freely and independently movable in space. In contrast, the mass element has only one such terminal the centre of mass.

The inertor is in fact a spinning mass on the damper rod inside a damper body. The inertor looks superficially like a conventional shock absorber, with an attachment point at each end. For example, one end may be attached to the car body and the other to the suspension assembly. A plunger slides in and out of the main body of the inertor as the car moves up and down. This causes the rotation of a flywheel inside the device in proportion to the relative displacement between the attachment points. The result is that the flywheel stores rotational energy as it spins. In combination with the springs and dampers, the inertor reduces the effect of the oscillations and thus helps the car to retain a better grip on the road. Looks like no any springs or hydraulics or MR fluid is involved. It works much like the Renault's well known Mass damper to take the energy from the tires movement to maximize contact patch/area/load.

As it's a recognizable part of the suspension fitted in place of the third damper, works to improve the use of the tires as suspensions purpose and works only in response to suspension loads, it may be seen as legal. The fact that the device is light, small and well contained compared to the bigger masses placed in the nose cone of

Renault, probably means this will remain legal. Inerter can't work without rest of suspension system (dampers and springs).

Standard suspension systems are based around two components - springs and shock absorbers (dampers). Together, these contribute to the car's ride and handling. No matter how the system is tuned, however, there is always a compromise taking place between handling, comfort and grip. Even in F1 cars, where comfort is not important, the suspension needs to be set to allow both sensitive handling, which requires a harder suspension, and a good mechanical grip, for which the suspension would normally be softer. The upshot is that there is still some oscillation as the load on the tires varies, which impedes the vehicle's grip and therefore slows it down.

Think of the car's suspension's reaction to the ground as acting in a sine wave motion. The wave would obviously be damped over time by itself, but this time is too long. The reaction from the ground would cause the Inerter rotating mass to react in a sine wave motion (speeding up its rotation) and damp over time by itself. The two reactions do not coincide, it means the car doesn't bounce up while the Inerter speed up, so they counteract each other. Obviously the car's reaction through the suspension outweighs the mass reaction, but the spinning mass will still dampen the car's reaction to the ground through its countering force. An F1 car has a very small degree of suspension travel compared to a road car. Its purposes are not just to make the car ride well over bumps, but to improve traction and aid aerodynamic performance.

Today in all modern road car, independent suspensions, in which the wheels are each allowed to move on their own is used. If both the front and the back wheels use an independent suspension, then a car can be said to have four-wheel independent suspension. One of the most common designs used on the front suspension is the McPherson strut, which is named after its inventor, Earle S. McPherson of General

Motors. Invented in 1947, this design is still common today. Another common design for front suspensions is the double wishbone or double A arm suspension. In this design, two wishbone (Y) shaped supports are attached to each wheel, joining the wheel at one point and the frame at two points. Each of these basic designs has been modified in a number of different ways to produce a range of suspension options. All of these designs, however, employ the same basic principles to produce a safe and comfortable ride.

The frame is the rigid structure that supports the main weight of the car. This part of the car is referred to as the sprung mass because it rests on springs. These springs absorb the increased vertical velocity of the wheels as they travel over bumps. The unsprung mass is the weight of the car below the frame: wheels, tires, axles, suspension arms, brakes etc.

The stiffness of the springs affects the performance of the vehicle. If a car is loosely sprung, it will easily absorb bumps in the road, providing a very smooth ride. However, the handling of the car won't be as good, as the vehicle body will be prone to moving forward, backward, and side to side. Tightly sprung cars, while offering bumpy rides, maneuver more effectively. Car manufacturers aim to find a balance between these qualities. Springs absorb energy easily; however, they don't dissipate it so well. As soon as you release a compressed spring, it snaps back in the reverse direction and continues to oscillate until all the energy has been dissipated. If suspensions relied entirely on springs, you would have a very bumpy and uncontrollable ride. To account for this, springs are usually paired with dampers, or shock absorbers. These devices use hydraulics to turn kinetic energy (motion) into thermal energy (heat). This way, the energy stored in the spring dissipates quickly, without causing unnecessary motion in the body of the car. A typical shock absorber

is, in essence, a piston inside oil filled tube. The piston is attached to a casing, which is in turn attached to the spring. As the spring moves, it pushes the piston up or down, compressing the oil inside the pressure tube. Tiny valve perforations in the pressure tube allow the oil to slowly escape into the reserve cylinder.

The system is designed to provide enough resistance to absorb all of the energy from the spring, but for more capacity energy from oscillation, we apply inerter to suspension with a normal car. Otherwise, a road car has a bigger degree of suspension travel compared to a racing car. Its purposes make the car ride well over bumps and also make good handling.

## **1.7 Motivation Research**

The purposes of formula one car are not just to make the car ride well over bumps, but to improve traction and aid aerodynamic force performance. Even in formula cars, where comfort is not important, the suspension needs to be set to allow both sensitive handling, which requires a harder suspension, and a good mechanical grip. However, a normal car concern to taking place between handling, comfort and grip. A normal car need to be soft against road disturbance and hard against load disturbance when it turning or breaking.

As previous reviews, inerter only applies to formula one car which has advance on road holding at high speed. But this dissertation proposes are verify an advantage of employing inerter to suspension to verification process and optimization process structure to get both benefit of comfortable and road holding in the next chapters.

## **1.8 Outline of the Dissertation**

This dissertation is organized as follows:

## **Chapter 1: Introduction**

## **Chapter 2: Synthesis of Inerter Component**

This chapter is concerned with the problem of synthesis of passive mechanical one-port networks. One of the main contributions of this thesis is the introduction of a device, which will be called the inerter, which is the true network dual of the spring. This contrasts with the mass element which, by definition, always has one terminal connected to ground. The inerter need not have large mass. This allows any arbitrary positive-real impedance to be synthesized mechanically using physical components which may be assumed to have small mass compared to other structures to which they may be attached. The possible application of the inerter is considered to a vibration absorption problem, a suspension strut design, and as a simulated mass.

## **Chapter 3: Advantage of Inerter apply on Quarter-car Model**

This chapter introduces the mechanical systems that presents the vehicle models as corresponding networks. The passivity suspension of the network can then be checked by the positive realness of its transformation matrices. An analysis procedure combined with suspension model which is employed to show the necessity of implementing inerter in order to achieve certain performance requirements. This chapter applies the disturbance response to the linear quarter-car model employing inerter with various valuable. The results are compared with the difference structure and illustrate our systematic approach for vehicle passive suspension design. The achievable results are shown to reduce vehicle oscillation after the design.

## **Chapter 4: Advantage of Inerter apply on Half-car Model**

This chapter extend the application of inerter to the linear half-car model, and discusses the “simplicity” conditions which decompose the half-car into two quarter-car models. The procedure of successive design, which improves stable oscillation and rolling angle for vehicle.

#### **Chapter 5: Verification Inerter Design Apply on Suspension System**

This chapter we propose verification process which present some issues related to inerter mechanism designs such as: gear type inerter employ to suspension system as parallel quarter-car model. We discuss some results on verification modal parameter which can be achieved through inerter mechanisms using for some specific networks.

#### **Chapter 6: Optimization Process Apply on Suspension with Inerter**

This chapter we introduce the approximate optimization method, Sequential Quadratic Programming (SQP) with Response Surface Method (RSM). We made RSM using the OA to optimize modal parameters of the passive suspension system with inerter. The new modal parameters are represented for optimization suspension system and they called:  $k_{opt}$ ,  $c_{opt}$ ,  $b_{opt}$  and  $k_{t-opt}$ .

#### **Chapter 7: Concluding Remark**

This chapter summaries the main contributions of this dissertation and outlines for further research.

## CHAPTER 2

### SYNTHESIS OF INERTER COMPONENT

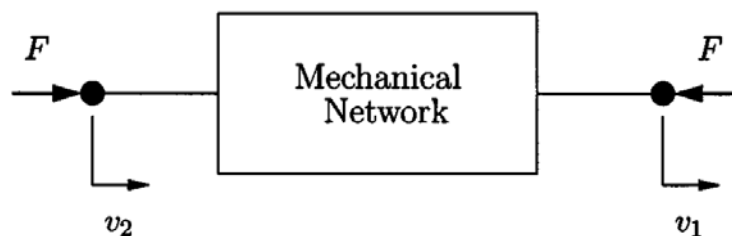
#### 2.1 The Inerter

The define of inerter to be a mechanical two-node (two-terminal), one-port device with the property that the equal and opposite force applied at the nodes is proportional to the relative acceleration between the nodes. That is, in the notation of **Figure 2-1**.

$$F = b(\dot{v}_2 - \dot{v}_1) \quad \text{Eq. 2-1}$$

The constant of proportionality is called the inertance and has units of kilograms. The stored energy in the inerter is equal to:

$$E = \frac{1}{2}b(v_2 - v_1)^2 \quad \text{Eq. 2-2}$$



**Figure 2-1:** A free-body diagram of a one-port (two-terminal) mechanical element or network with force–velocity pair [14].

Naturally, such a definition is vacuous unless mechanical devices can be constructed which approximate the behavior of the ideal inerter. To be useful, such devices also need to satisfy certain practical conditions which we list as follows.

1 - The device should be capable of having a small mass, independent of the required value of inertance.

2 - There should be no need to attach any point of the physical device to the mechanical ground.

3 - The device should have a finite linear travel which is specifiable, and the device should be subject to reasonable constraints on its overall dimension.

4 - The device should function adequately in any spatial orientation and motion.

Condition (2) is necessary if the inerter is to be incorporated in a free-standing device which may not easily be connected to a fixed point in an inertial frame, e.g., a suspension strut which is connected between a vehicle body and wheel hub. We mention that conditions of the above type hold for the ordinary spring and damper.

The aforementioned reliability conditions can indeed be satisfied by a mechanical device which is easy to construct. A simple approach is to take a plunger sliding in a cylinder which drives a flywheel through a rack, pinion, and gears show in **Figure 2-2**.

Note that such a device does not have the limitation that one of the terminals be grounded, i.e., attached to a fixed point in an inertial frame. To approximately model the dynamics of the device, let  $r_1$  be the radius of the rack pinion,  $r_2$  the radius of the gear wheel,  $r_3$  the radius of the flywheel pinion,  $\gamma$  the radius of gyration of the flywheel,  $m$  the mass of the flywheel, and assume the mass of all other components is negligible. Assuming  $v_1 = 0$  we can check that the following relation holds:

$$F = (m\alpha_1^2\alpha_2^2)\dot{v} \quad \text{Eq. 2-3}$$

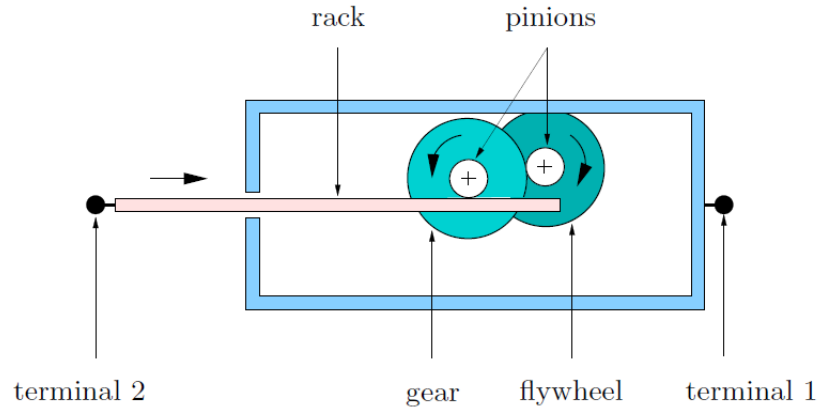
where  $\alpha_1 = \frac{\gamma}{r_3}$  and  $\alpha_2 = \frac{r_2}{r_1}$ .



If  $v_1 \neq 0$  the direct inertial effect of the flywheel mass comes into play, but this will only change **Eq. 2-3** by a small proportion providing  $\alpha_1^2 \alpha_2^2$  is large.

To a first approximation, such an effect can be neglected, as is commonly done for springs and dampers. Note that even with relatively modest ratios  $\alpha_1 = \alpha_2 = 3$  the inertance is a factor of 81 times the mass. It is clearly feasible to introduce additional gearing; an extra gear wheel and pinion with ratio  $\alpha_3$  will multiply the inertance by a factor  $\alpha_3^2$ .

The remaining conditions (2-4) are also satisfied by the realization of **Figure 2-1**. In the case of gyroscopic effects being an issue under condition (4), a system of counter-rotating flywheels could be introduced.



**Figure 2-2:** Schematic of a mechanical model of an inerter [18].

It is useful to discuss two references on mechanical networks, which give some hint toward the inerter idea, in order to highlight the new contribution here. We first mention [23] which describes a procedure whereby an electrical circuit is first modified by the insertion of ideal one-to-one transformers so that all capacitors then have one terminal grounded. This then allows a mechanical circuit to be constructed with levers, which has similar dynamic properties to the electrical one while not being properly analogous from a circuit point of view. Another difficulty with this approach

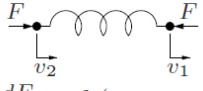
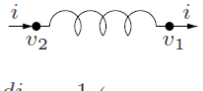
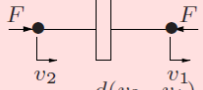
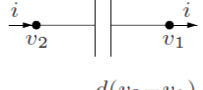

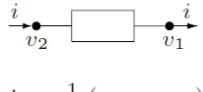
is with condition (2) since a pair of terminals of the transformer need to be connected to the mass and the ground.

Second, we highlight the paper of Schönfeld [24], which is principally concerned with the treatment of hydraulic systems as distinct from mechanical systems and the interpretation of acoustic systems as mixed mechanical–hydraulic systems, a work which appears to have been unfairly neglected. In connection with mechanical–electrical analogies, the possibility of a biterminal mechanical inertance is mentioned. The idea is essentially to place a mass at the end of a lever, connected with links to the two terminals, while increasing the lever length and decreasing the value of mass arbitrarily but in fixed ratio. Although this in principle deals with condition (1) and (2), there is a problem with (3) due to the large lever length required or the vanishing small available travel. A variant on this idea has similar difficulties as well as a problem with condition (4). It is perhaps the obvious limitations of these devices that have prevented the observation from being developed or formalized.

In the light of the previous definition of the ideal inerter, it may sometimes be an advantage to reinterpret combinations of system elements as acting like an inerter. For example, in paper [25] two masses are connected together by means of a lever arrangement that interpreted as a 2-port transformer connected to a 1-port inertia element in the bond graph formalism.

If this system is linearized for small displacements then the behavior is the same as if an inerter were connected between the two masses. Of course, such an arrangement has problems with condition (3). Indeed, if large values of inertance were required for a moderate amount of travel then the lever lengths and ratios would be impractical. A table of the circuit symbols of the six basic electrical and

mechanical elements, with the newly introduced inerter replacing the mass, is shown in Fig. 4. The symbol chosen for the inerter represents a flywheel.

Mechanical	Electrical
 $Y(s) = \frac{k}{s}$ $\frac{dF}{dt} = k(v_2 - v_1)$ spring	 $Y(s) = \frac{1}{Ls}$ $\frac{di}{dt} = \frac{1}{L}(v_2 - v_1)$ inductor
 $Y(s) = bs$ $F = b \frac{d(v_2 - v_1)}{dt}$ inerter	 $Y(s) = Cs$ $i = C \frac{d(v_2 - v_1)}{dt}$ capacitor
 $Y(s) = c$ $F = c(v_2 - v_1)$ damper	 $Y(s) = \frac{1}{R}$ $i = \frac{1}{R}(v_2 - v_1)$ resistor

**Figure 2-3:** Circuit symbols and correspondences with defining equations [18].

## 2.2 Vibration Absorption Problem

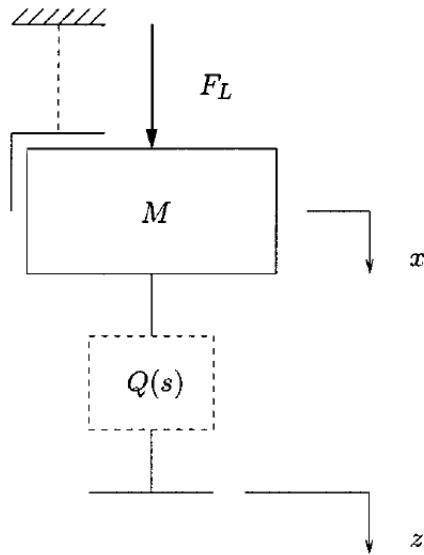
Suppose we wish to connect a mass  $M$  to a structure so that steady sinusoidal vibrations of the structure at a constant frequency  $\omega_0$  do not disturb the mass. The problem is posed as in **Figure 2-4** where the mass is connected to the structure by a device whose mechanical admittance is  $Q(s)$ . The mass may be subjected to a force  $F_L$  and the displacement of the mass and the structure are  $x$  and  $z$ , respectively. We seek to design and realize a positive-real  $Q(s)$  so that if  $z = \sin(\omega_0 t)$  then  $x(t) \rightarrow 0$  as  $t \rightarrow \infty$ .

The equation of motion for the mass in the Laplace transformed domain is:

$$Ms^2 \hat{x} = \hat{F}_L + sQ(s)(\hat{z} - \hat{x}) \quad \text{Eq. 2-4}$$

whence

$$\hat{x} = \frac{1}{Ms^2 + sQ(s)} \hat{F}_L + \frac{Q(s)}{Ms + Q(s)} \hat{z} \quad \text{Eq. 2-5}$$

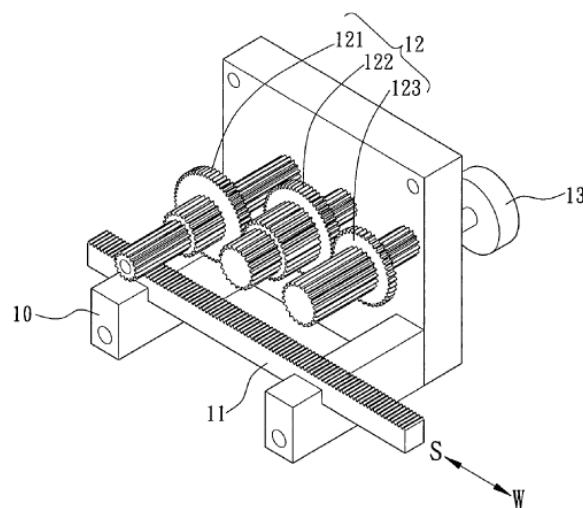


**Figure 2-4:** Vibration absorption problem [17].

where  $\hat{\cdot}$  denotes Laplace transform. It is evident that the mass will be impervious to a steady sinusoidal disturbance at  $z$  providing  $\frac{Q(s)}{Ms+Q(s)}$  has a zero at  $s = j\omega_0$ , and that this will hold providing  $Q(s)$  has a zero at  $s = j\omega_0$ .

## 2.3 Synthesis Inerter Mechanism

### 2.3.1 Gear type inerter mechanism

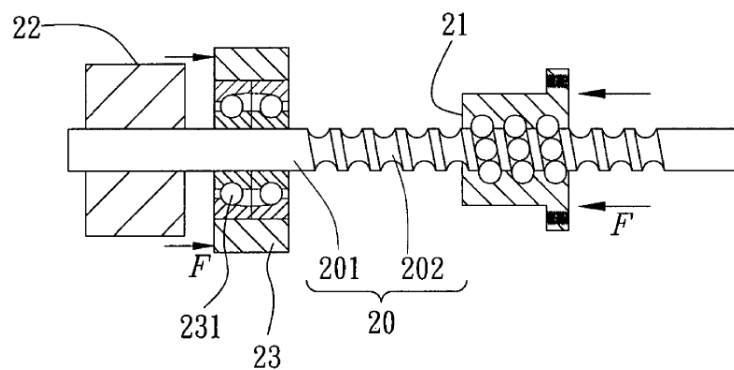


**Figure 2-5:** Gear type inerter mechanism [15].

The gear type inerter mechanism including a gear set and rack, it has two terminals at the rack and the base body. The dynamic equation of an inerter is derived as  $F=b*a$ , wherein  $F$ ,  $b$  and  $a$  represent the applied force, the inerter coefficient (called inertance) and the relative acceleration of two terminals, respectively. The inertance is calculated from the radius and inertia of flywheel as above.

### 2.3.2 Screw type inerter mechanism

Although we have design of gear type inerter mechanism and to obtain theories, but the friction force between gears can be large and the backlash exists. It means two gears cannot be tightly assembled, therefore making phase draggle. So another objective is presented to reduce friction force and system energy dissipation is screw type inerter mechanism. It can be reduce conventional backlash general by gear transmission.



**Figure 2-6:** Screw type inerter mechanism [15].

As shown in **Figure 2-6**, if two forces  $F$  are applied to the connection body (23) and the nut (21) in opposite directions parallel to the axis of the screw (20) so as to allow the connection body to have horizontal displacement relative to the nut (21) and in parallel with the axis of the screw and it is brought to rotate around its axis due to interaction between the bearings and threads. Further, the inertia

body (22) is fixed to the limit portion (20-1) of the screw, and the axis of the screw serves as the rotation axis of the inertia body. When the screw rotates around its axis, the inertia body is brought to rotate. In addition, when the screw rotates, the connection body will not rotate due to action of the bearings (23-1), and horizontal and vertical positions of the connection body relative to the screw do not change.

The horizontal displacement of the connection body relative to the nut is in parallel with the axis of the screw, and can be in a positive direction or in a negative direction, which brings the screw to rotate clock-wisely or counter clock-wisely. The directions of the horizontal displacement and the screw rotation can be determined according to design of the thread. The relationship between the horizontal displacement of the connection body and the nut and angular displacement of the screw can also be determined according to design of the thread.

Now the relative displacement of the connection body and the nut is analyzed according to the inerter theory. The nut and the connection body can be considered as two terminals of the inerter. According to the equation, a suitable screw type inerter mechanism can be designed by adjusting the screw pitch or the inertia of the rotation bodies. Following, the equation force is obtained:

$$F = b(\dot{v}_2 - \dot{v}_1) \quad \text{Eq. 2-6}$$

Wherein  $\dot{v}_2$  and  $\dot{v}_1$  are the relative acceleration of the two terminals, b is the inertance.

$$b = I(2\pi P) \quad \text{Eq. 2-7}$$

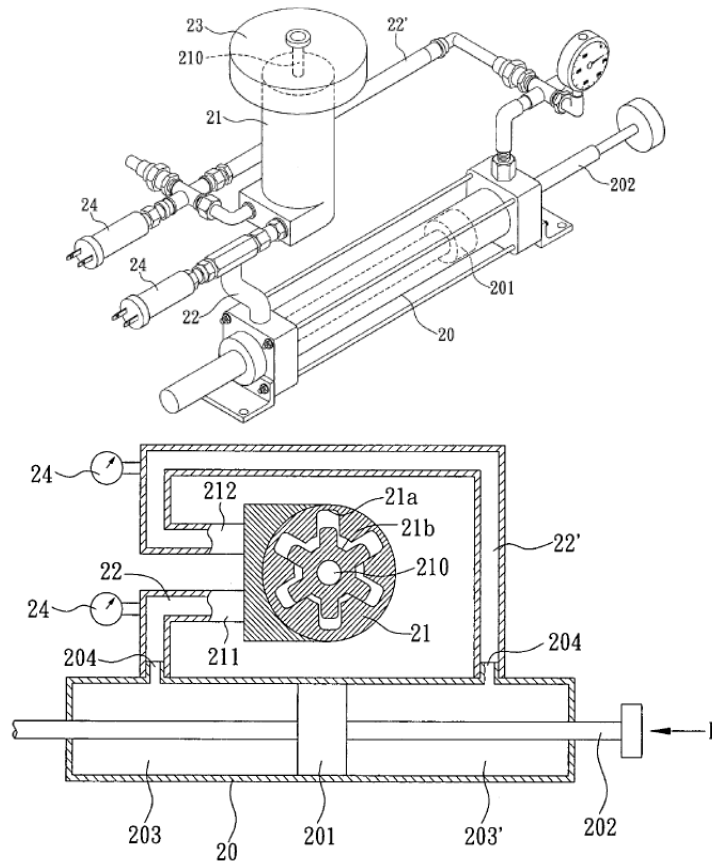
I is the total mass moments of inertia of the inertia body and the screw

P is the screw pitch

### 2.3.3 Hydraulic type inerter mechanism

This is another objective of research, hydraulic type inerter mechanism which comprises a hydraulic cylinder. A hydraulic motor connected to hydraulic cylinder with an output shaft for converting the linear motion to rotary motion and an inerter body disposed on the output shaft. This system subjects to high external force loads and controllability.

Referring to **Figure 2-7**, an external force  $F$  is applied to one end of the piston rod (20-2) for pushing the piston (20-1) inwards to create rectilinear motion inside the hydraulic cylinder (20), thus increasing the pressure of the working fluid inside compartment (20-3) to the inlet (21-1) of the hydraulic motor (21) through pipe body (22) and thereby forming a high pressure zone at the inlet (21-1) of the hydraulic motor. Then, the working liquid flows from the outlet (21-2) back to compartment (20-3') of the hydraulic cylinder through pipe body (22'), thereby forming a low pressure zone at outlet of the hydraulic motor. Consequently, a pressure difference is formed between the inlet and the outlet of the hydraulic motor, wherein such a pressure difference can be calculated from difference of the readings of the two manometers (24). The pressure difference is capable of driving the hydraulic motor to revolve, and thus drives the output shaft (21-0), so as to drive the inertia body (23) to rotate. Consequently, the rectilinear motion is converted to rotary motion, and the external force is converted to rotate the flywheel, thereby attaining inerter characteristics. Moreover, if the external force is applied to the opposite end of the piston rod, the piston moves in an opposite direction and the hydraulic motor rotates reversely, thereby being a reversible process.



**Figure 2-7:** Hydraulic type inerter mechanism [16].

For an ideal inerter, inertance  $b$  can be calculated as follows:

$$b = I(A/D)^2 \quad \text{Eq. 2-8}$$

In which:

$I$  is the inertia of the flywheel.

$A$  is the area of the piston.

$D$  is displacement volume of motor.

Moreover, since the inertance of the inerter mechanism of the invention is changeable by adjusting the moment of inertia of the inertia body, the moment of inertia of the inertia body can be adjusted by changing the mass  $m$  of inertia body or the distance  $r$  between the masses comprising the inertia body and the center of the rotating shaft.



The moment of inertia of a multi-particle inertia body is the sum of each particle mass multiplied by the square of distance between each particle and the rotating shaft. Therefore, changing the mass of each particle of the inertia body or the distance between particles and the rotation shaft will change moment of inertia of the inertia body, and consequently will change the inertance of the inerter mechanism. The following two embodiments are examples of changing the mass of particles of the inertia body or the distance between particles of inertia body and the rotation shaft, thereby changing the moment of inertia of an inertia body. We use the familiar of two-terminal modeling elements: spring, damper and inerter to simulate passive suspension model, mathematical model and physical model of quarter-car.

#### **2.4 Summary and Comments**

In this chapter, we described the inerter mechanism and discussed vehicle suspension components as their corresponding networks. Then we showed how to check the passive suspension in Laplace transformation  $Q(s)$ . For inerter models, we synthesis some kinds of mechanism as: gear type, screw type and hydraulic type of inerter which can employ on suspension system. This component will be shown detail in Chapter 3 for the analysis and design of quarter-car model.



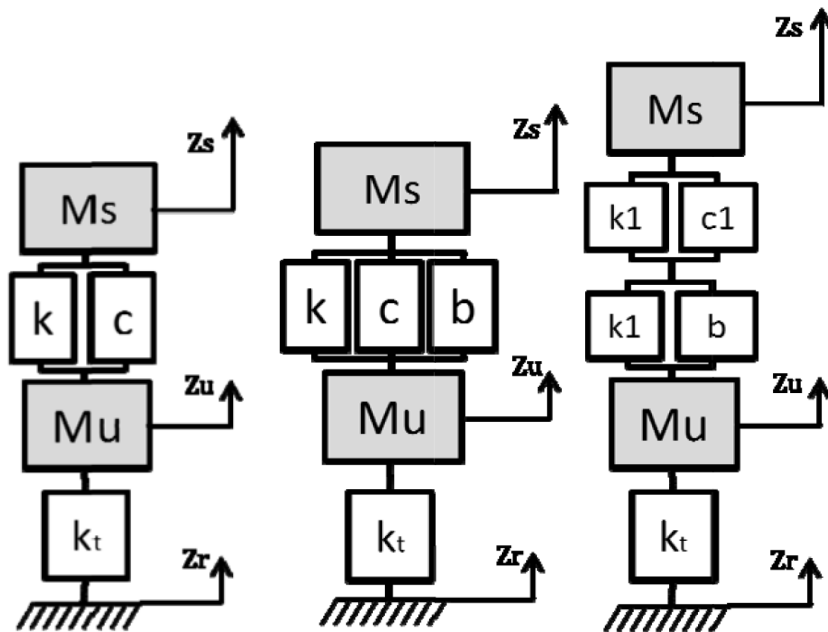
## CHAPTER 3

### ADVANTAGE OF INERTER APPLY ON QUARTER-CAR MODEL

#### 3.1 Mathematical Model

##### 3.1.1 Quarter-car Model

Base on the conventional quarter- car model, we design two structures are called quarter-car suspension parallel and series structure model show in **Figure 3-1**. This model will change from normal passive suspension to new suspension with stiffness, damping and inerter in parallel or series. We study about the vertical displacement of sprung mass in some kinds of simulations.



**Figure 3-1:** The base, the parallel and the series quarter-car model in respectively.

For the quarter-car model, the suspension strut provides an equal and opposite force on the sprung and un-sprung masses by means of the positive real admittance function which relates the suspension force to the strut velocity through spring, damper and inerter. We define them as the following equations.

Base quarter-car model dynamics equation in time-domain:

$$M_s \ddot{Z}_s(t) = F_k(t) + F_c(t) \quad \text{Eq. 3-1}$$

$$M_u \ddot{Z}_u(t) = F_{kt}(t) - (F_k(t) + F_c(t)) \quad \text{Eq. 3-2}$$

Where:

$$F_k(t) = k(Z_u(t) - Z_s(t)) \quad \text{Eq. 3-3}$$

$$F_c(t) = c(\dot{Z}_u(t) - \dot{Z}_s(t)) \quad \text{Eq. 3-4}$$

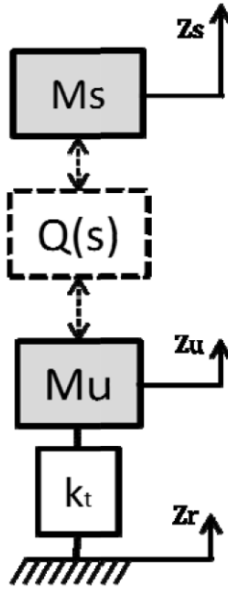
$$F_{kt}(t) = k_t(Z_r(t) - Z_u(t)) \quad \text{Eq. 3-5}$$

State-space representation:

$$\begin{bmatrix} \ddot{Z}_s \\ \dot{Z}_s \\ \ddot{Z}_u \\ \dot{Z}_u \end{bmatrix} = \begin{bmatrix} -\frac{c}{M_s} & -\frac{k}{M_s} & \frac{c}{M_s} & \frac{k}{M_s} \\ 1 & 0 & 0 & 0 \\ \frac{c}{M_u} & \frac{k}{M_u} & -\frac{c}{M_u} & -\frac{k+k_t}{M_u} \\ 0 & 0 & 1 & 0 \end{bmatrix} \begin{bmatrix} \dot{Z}_s \\ Z_s \\ \dot{Z}_u \\ Z_u \end{bmatrix} + \begin{bmatrix} 0 \\ 0 \\ \frac{k_t}{M_u} \\ 0 \end{bmatrix} Z_r \quad \text{Eq. 3-6}$$

### 3.1.2 Suspension Model in Laplace Transformed

We summarize the approach of the suspension design problem was formulated modal parameter to improve vertical displacement. The solution of the optimization problem made use structure of new quarter-car model that improve from traditional passive suspension system in adding inerter elements. In some previous researching, the good and simple structure was able to come up with new network topologies involving inerter [26]. To solving these problems, we use Laplace transform function as the ways to represent for suspension system in cases study by  $Q(s)$  present for parallel and series suspension system in respectively.



**Figure 3-2:** The quarter-car model with suspension function represented in Laplace transformed.

The equations of motion in the Laplace transformed domains are:

$$M_s s^2 \widehat{Z}_s = -sQ(s)(\widehat{Z}_s - \widehat{Z}_u) \quad \text{Eq. 3-7}$$

$$M_u s^2 \widehat{Z}_u = sQ(s)(\widehat{Z}_s - \widehat{Z}_u) + k_t(\widehat{Z}_r - \widehat{Z}_u) \quad \text{Eq. 3-8}$$

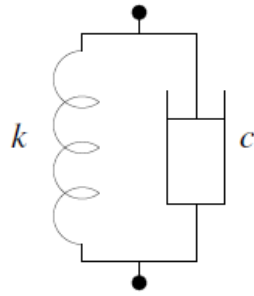
We can compute the relevant transfer functions as follows:

The transfer functions from the road disturbance  $z_r$  to the displacement of the sprung mass  $z_s$ :

$$T_{Z_r \rightarrow Z_s} = \frac{k_t Q(s)}{M_s s(M_u s^2 + k_t) + ((M_u + M_s)s^2 + k_t)Q(s)} \quad \text{Eq. 3-9}$$

The transfer functions from the road disturbance  $z_r$  to the acceleration of the sprung mass  $\ddot{z}_s$ :

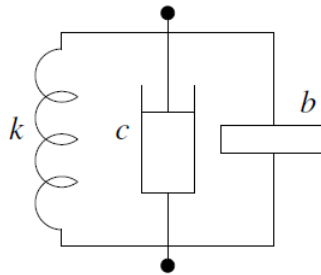
$$\begin{aligned} T_{Z_r \rightarrow \ddot{Z}_s} &= s^2 T_{Z_r \rightarrow Z_s} \\ &= \frac{s^2 k_t Q(s)}{M_s s(M_u s^2 + k_t) + ((M_u + M_s)s^2 + k_t)Q(s)} \end{aligned} \quad \text{Eq. 3-10}$$



**Figure 3-3:** The conventional parallel spring-damper arrangement.

The conventional suspension function represented in Laplace transformed:

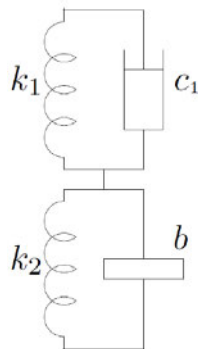
$$Q(s) = Y_k + Y_c = \frac{k}{s} + c \quad \text{Eq. 3-11}$$



**Figure 3-4:** The parallel spring-damper augmented by an inerter in parallel.

The parallel suspension function represented in Laplace transformed:

$$Q(s) = Y_k + Y_c + Y_b = \frac{k}{s} + c + bs \quad \text{Eq. 3-12}$$



**Figure 3-5:** The parallel spring-damper series with the parallel spring-inerter.

The series suspension function represented in Laplace transformed:

$$Q(s) = \left( \frac{1}{Y_c + Y_{k_1}} + \frac{1}{Y_b + Y_{k_2}} \right)^{-1} = \left( \frac{1}{c + \frac{k_1}{s}} + \frac{1}{bs + \frac{k_2}{s}} \right)^{-1} \quad \text{Eq. 3-13}$$

### 3.2 Quarter-car Model Analysis

#### 3.2.1 Specification of Quarter-car Model

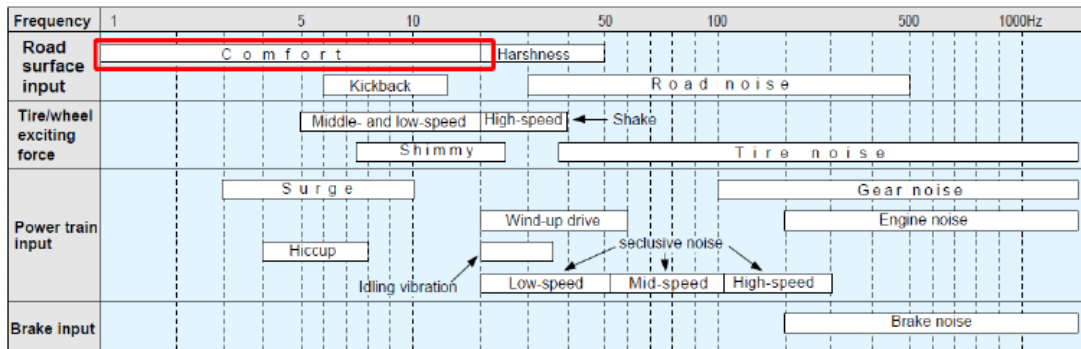
For the evaluation of the displacement of the sprung mass, we use a hump road profile and there is no load disturbances applied on the sprung mass. Base on previous study [27], we have modal parameters for passive suspension system as:

**Table 3-1:** The specification of Formula SAE quarter-car model.

Symbols	Parameters	Values
$M_s$	Mass of body	63 kg
$M_u$	Mass of tire	12 kg
$k$	Stiffness coefficient	24000 N/m
$k_1, k_2$	Stiffness coefficient	48000 N/m
$c$	Damping coefficient	1200 Ns/m
$c_1$	Damping coefficient	2400 Ns/m
$b$	Mass of inertance	20 kg
$k_t$	Stiffness coefficient of tire	70000 N/m
$H_0$	Road disturbance hump	0.05 m

We have looked at suspension and steering systems in regard to vehicle vibration characteristics affecting vehicle-mounted equipment. **Figure 3-6** shows related vehicle vibration and noise classified according to source input and source frequency.

Just as in the suspension system, most vibration affecting the handling does not act directly on the steering system, but is amplified in the tires and suspension system. Other vibration phenomena include power steering vibration, kickback due to uneven road disturbance, and dynamic unbalance of rotating parts such as the wheels and the braking system.



**Figure 3-6:** Vibration sources and input to the suspension [28].

Low-speed shimmy is generated by self-induced vibration accumulating within the steering system, and occurs at the low vehicle speeds of 20 to 60 kilometers per hour. Displacement is large, and the shimmy has a greater tendency to occur in worn tires or tires with low air pressure.

High-speed shimmy is mainly caused by static or dynamic unbalance of the tires on the wheels. Other causes include disk wheel eccentricity, the wheel not being vertically plumb, and non-uniformity of the tires. Unbalance of the tires on the wheels causes peak vibration in the vicinity of 10 Hz to 30 Hz. Displacement is small, but with worn tires or low air pressure in the tires, displacement becomes large.

Kickback occurs when driving on a bad road surface causes both vertical and horizontal vibration to the drive tires. That vibration is transmitted to the tire rods, causing the steering wheel to turn suddenly. This vibration occurs in the drive wheels



on front-wheel drive cars, giving a greater tendency for longitudinal changes in force than with rear-wheel-drive cars.

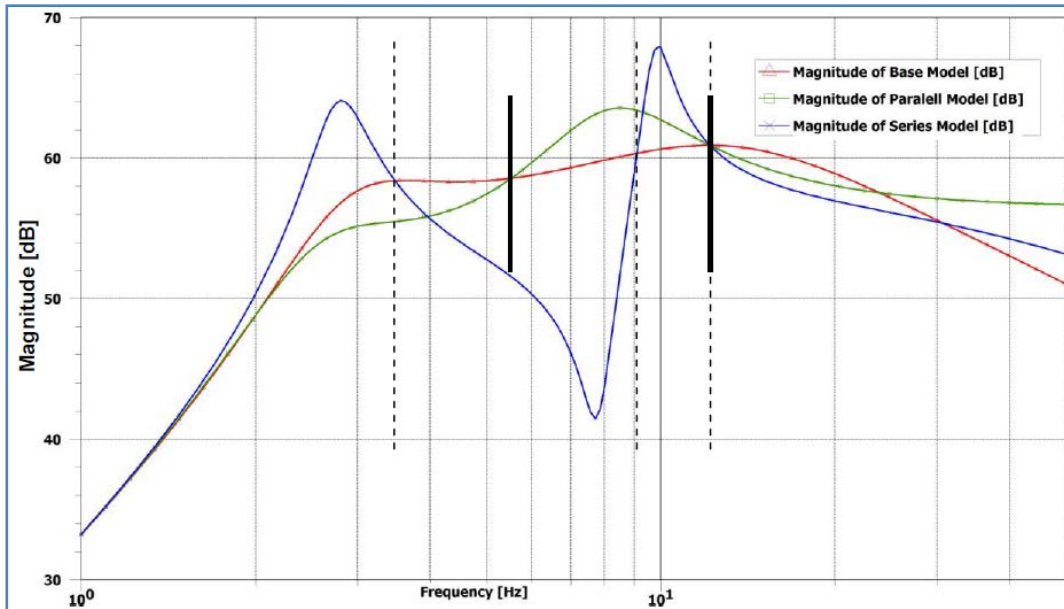
Tire vibration factors seen from the characteristics of static springs; include vertical springs, lateral springs, longitudinal springs, and torsion springs. Longitudinal stiffness is strongly related to actual vibration, and becomes harder roughly in proportion to the increase in air pressure. Natural tire frequency results from the fact that an elastic body filled with air has an individual vibration mode.

In this study, we focus to analyze the effect from road disturbance to kickback and comfort via displacement and acceleration of sprung mass. The frequency domain to estimate from 1-20 Hz, it is the main reason that we not mention about other kinds of road disturbances.

### 3.2.2 Mathematical Quarter-car Model Analysis

The present numerical discussion consists in analyzing the previous model properties on a numerical example. The model used in the following simulations is the simple LTI passive one, as given in definition with the Formula SAE car parameters given in **Table 3-1**. Since the main objective is to analyze passive suspensions, suspensions with inerter employed and changeable, the analysis carried in this section is centered on the behavior of the passive system for varying inertance  $b$  values.

**Figure 3-7** illustrates the pole location of the passive quarter-car model for different models, with  $b$  values 20 kg. First, according to this figure, it is notable that whatever the frequency smaller than 5 Hz, parallel model is better than base model while the series model is unstable. The quarter-car system remains stable with parallel structure. However, from 5 Hz to 12 Hz, the parallel model is not good as base model, and the series model is remaining unstable.



**Figure 3-7:** The base, parallel and series quarter-car model in frequency response of acceleration from road disturbance  $Z_r$  to sprung-mass  $Z_{s,dd}$ .

Then in parallel structure, by increasing the  $b$  value, the acceleration response magnitude poles module reduces. More specifically see in **Figure 3-8**.

When  $b = 10$  kg, the poles are located on the imaginary axis and start to reduce in 1-5 Hz.

When  $b \rightarrow 50$  kg, the poles tend to be located is continuous reduce in this frequency.

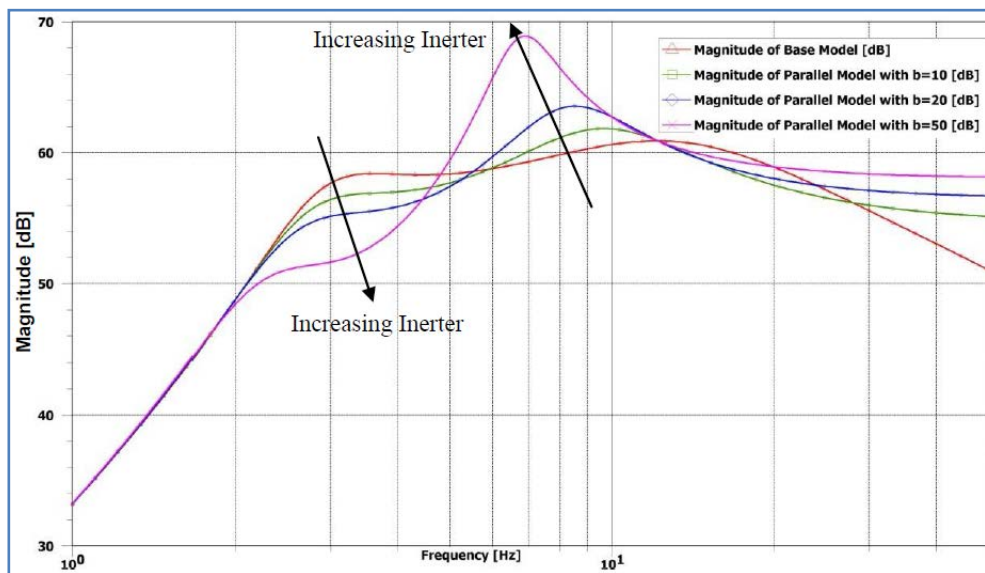
From the figure, it is interesting to note the following points:

On **Figure 3-8**, as expected and accordingly to the pole location analysis provided with **Figure 3-7**, increase the inertance  $b$  value in parallel model will reduce the resonance peaks, leading to an oscillatory behavior. But, in other frequency phase, the system is not good.

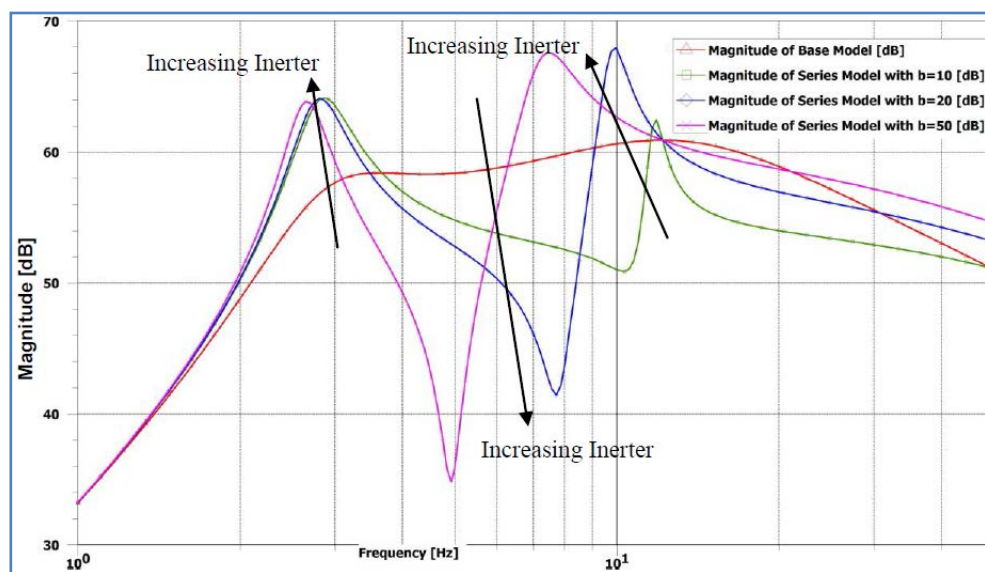
On **Figure 3-9**, the system is unstable with series model. As previously explained, some of these reason when we change  $b$  value, we cannot verify the behavior of model. Indeed on this figure, where analysis is shown for varying  $b$  value

and fixed stiffness values, damper value, from 1 to 20 Hz, the system seem to be not good at all.

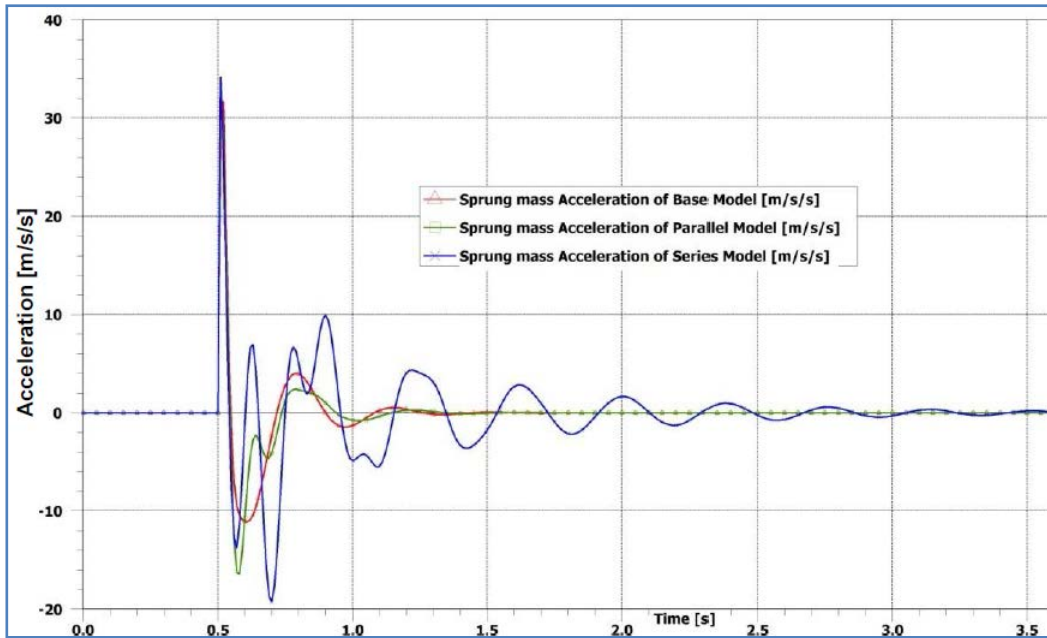
Finally, for improve suspension system in oscillation, we suggest using parallel structure to optimize quarter-car and then is half-car model respectively.



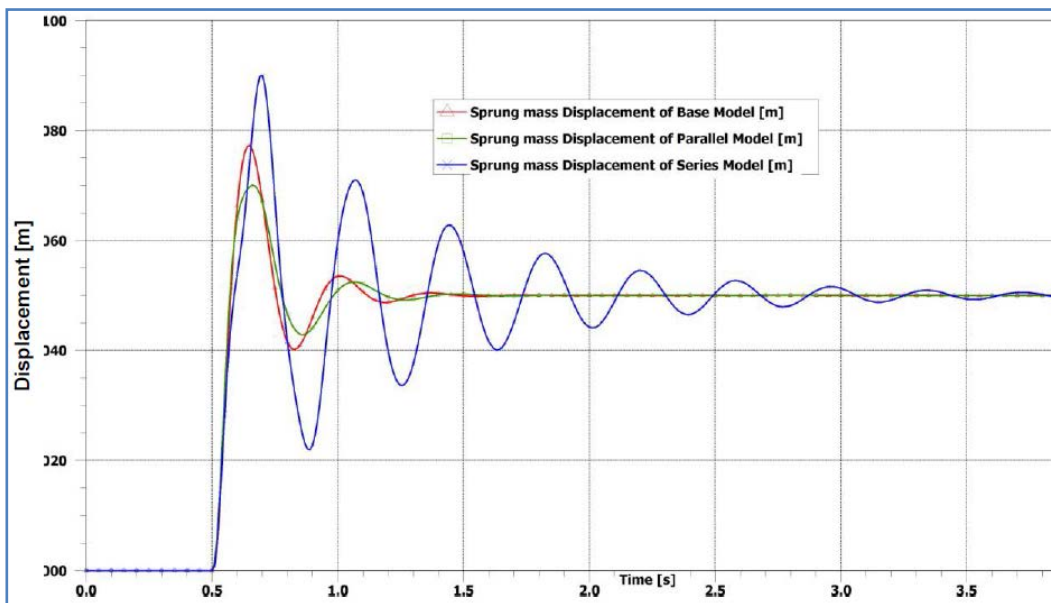
**Figure 3-8:** Comparison base and parallel quarter-car model in frequency response from  $Z_r$  to  $Z_{s\_dd}$  with the change of  $b\_value$ .



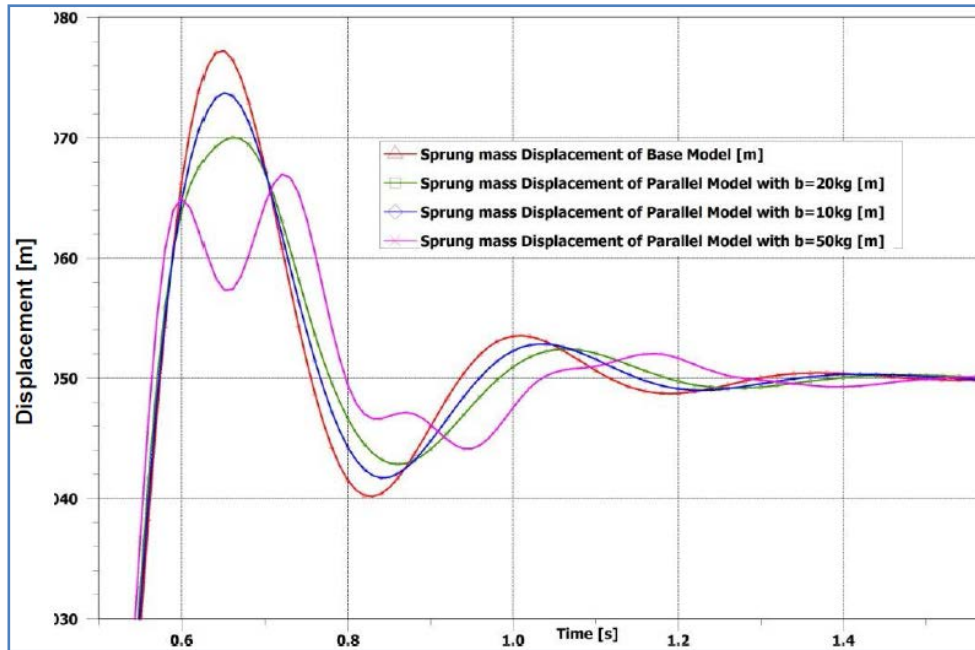
**Figure 3-9:** Comparison base and series quarter-car model in frequency response from  $Z_r$  to  $Z_{s\_dd}$  with the change of  $b\_value$ .



**Figure 3-10:** Sprung-mass acceleration results of base, parallel and series quarter-car model in time domain.



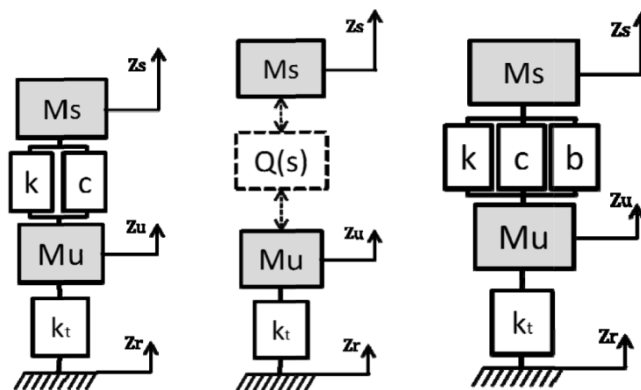
**Figure 3-11:** Sprung-mass displacement results of base, parallel and series quarter-car model in time domain.



**Figure 3-12:** Sprung-mass displacement results of base and parallel quarter-car model with change  $b$ \_value.

The figures show that the inerter has an advantage in frequency from 2 to 5Hz, then disadvantage from 6 to 12Hz with parallel suspension. The parallel suspension model is more stable than the series suspension model. Frequency response function is the basis of design suspension system with some points above.

### 3.3 Parallel Suspension in Quarter-car Model



**Figure 3-13:** The base and parallel quarter-car model with suspension function represented in Laplace Transformed respectively.

The equations of motion in the Laplace transformed domains are **Eq. 3-7** and **Eq. 3-8**.

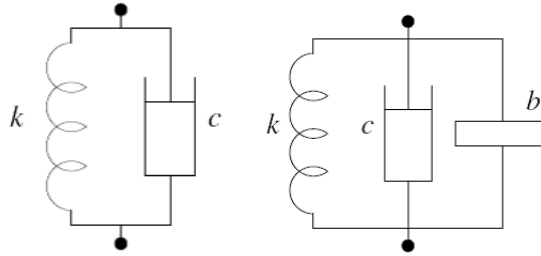
We can compute the relevant transfer functions as follows:

The transfer functions from the road disturbance  $Z_r$  to the displacement of the sprung mass  $Z_s$  is:

$$T_{Z_s} = \frac{k_t Q(s)}{M_s s(M_u s^2 + k_t) + ((M_u + M_s)s^2 + k_t)Q(s)} \quad \text{Eq. 3-14}$$

The transfer functions from the road disturbance  $Z_r$  to tire deflection  $Z_{t-def}$  is:

$$T_{Z_{t-def}} = \frac{-s^2 [M_s M_u s + (M_s + M_u)Q(s)]}{M_s s(M_u s^2 + k_t) + ((M_u + M_s)s^2 + k_t)Q(s)} \quad \text{Eq. 3-15}$$



**Figure 3-14:** The conventional and parallel suspension with inerter.

The conventional and parallel suspension function represented in Laplace transformed respectively:

$$Q(s) = Y_k + Y_c = \frac{k}{s} + c \quad \text{Eq. 3-16}$$

$$Q(s) = Y_k + Y_c + Y_b = \frac{k}{s} + c + bs \quad \text{Eq. 3-17}$$

### 3.3.1 Performance Specifications:

Considering the previous literature review and considering the quarter-car model given above, the following signals are considered for performance analysis and characterization of a suspension system:

To evaluate the comfort, the vertical displacement  $Z_s$  of the chassis is analyzed.

To evaluate the road-holding, the tire deflection  $Z_{t-def}$  is analyzed.

The suspension deflection limits  $\min Z_{sUS}$  and  $\max Z_{sUS}$  could be analyzed as the constraint function.

Frequency responses of both main transfer functions under discussion in this paper are  $T_{Z_s}$  and  $T_{Z_{t-def}}$  then we define the sprung mass displacement and tire deflection performances. We have looked at suspension in regard to vehicle vibration characteristics affecting vehicle equipment. **Figure 3-6** shown relation of vehicle vibration and noise classified according to source input and source frequency.

In this study, we focus to analyze the effect from road disturbance to kickback and comfort via displacement of sprung mass and tire deflection. The frequency domain to estimate from 1 to 20Hz, it is the main reason that we not mention about other disturbances.

For sprung mass displacement, the vibration isolation between [0; 20] Hz is evaluated by the transfer function  $T_{Z_s}(s)$ .

For tire deflection, it is evaluated using the transfer function  $T_{Z_{t-def}}(s)$  over the frequency range of [0; 30] Hz. A good road-holding, the tire deflection should be attenuated for low frequencies, and filtered around the resonance frequency of the wheel and over. Moreover, especially for high frequencies, the wheel should always remain linked to the road.

Suspension deflection is signal that should remain in the linear zone of suspension system to avoid limitation points. In this case, frequency limit is 30 Hz, this is the fact that high frequencies are filtered by vehicle mechanical elements.

### 3.3.2 Parallel Suspension Parameters Specification:

For the evaluation of sprung mass displacement and tire deflection, we use a bump road profile and there is no load disturbances applied on the sprung mass. Based on previous study, we have modal parameters for passive suspension system as:

**Table 3-2:** The specification of parallel suspension with inerter.

Symbols	Parameters	Values
$M_s$	Mass of body	63 [kg]
$M_u$	Mass of tire	12 [kg]
$k$	Stiffness coefficient	24000 [ $\text{Nm}^{-1}$ ]
$c$	Damping coefficient	1200 [ $\text{Nsm}^{-1}$ ]
$b$	Mass of inertance	20 [kg]
$k_t$	Stiffness coefficient of tire	70000 [ $\text{Nm}^{-1}$ ]
$H_0$	Bump road disturbance	0.05 [m]

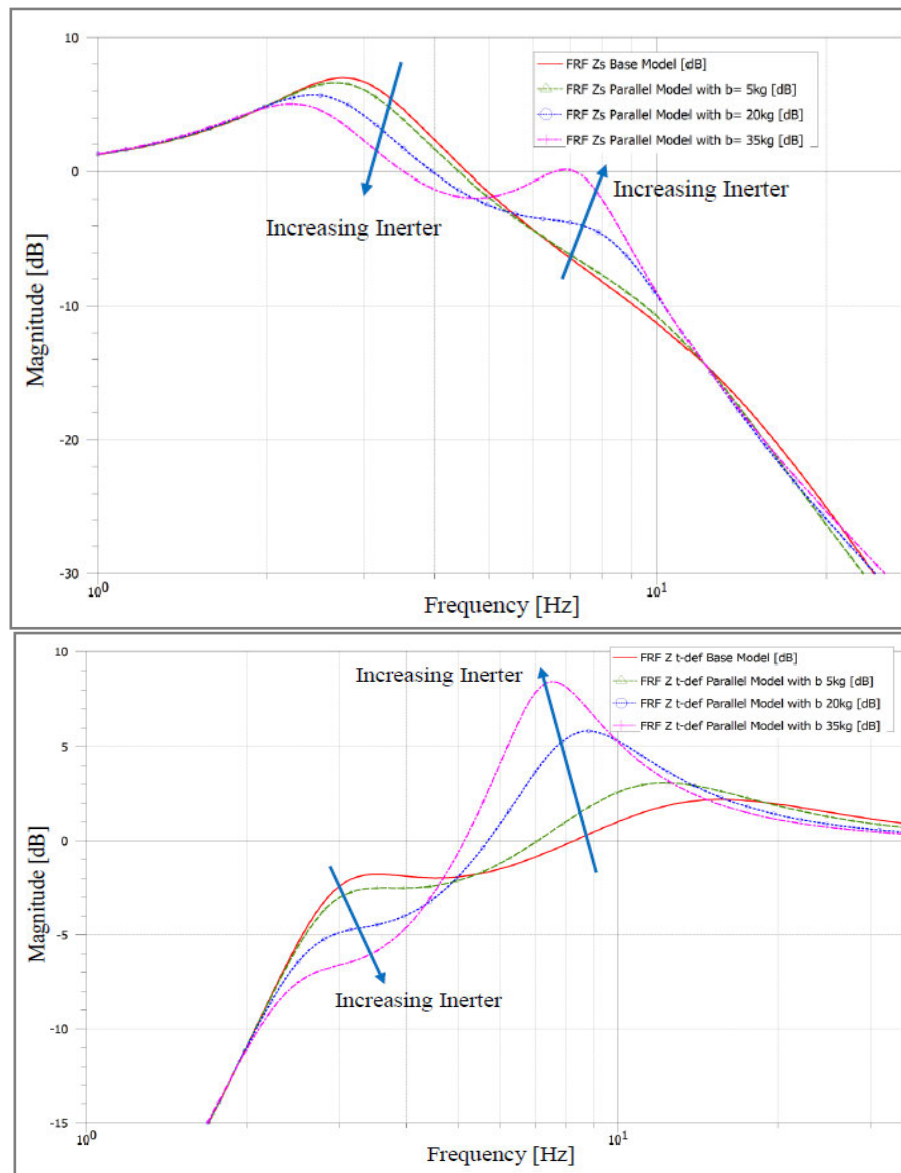
### 3.3.3 Parallel Suspension Modal Analysis

The present numerical discussion consists in analyzing the previous model properties on a numerical example. The model used in the following simulations is the simple linear passive one, as given in definition with the Formula SAE car parameters given in **Table 3-2**. Since the main objective is to analyze passive suspensions, suspensions with inerter employed and changeable, the analysis carried in this section is sprung mass displacement and tire deflection of the passive system for varying inertance  $b$  values.

**Figure 3-15** illustrates the pole location of the passive quarter-car model for different models when we apply inerter in parallel model. First, according to this figure, it is notable that whatever the frequency smaller than 5 Hz, parallel model is better than base model in both displacement and tire deflection response frequency



performance. The quarter-car system remains stable with parallel structure. However, from 5 Hz to 12 Hz, the parallel model is not good as base model.



**Figure 3-15:** Frequency response function  $T_{Z_s}(s)$  and  $T_{Z_{t-def}}(s)$  of base and parallel quarter-car model with the change of inerte b value in respectively.

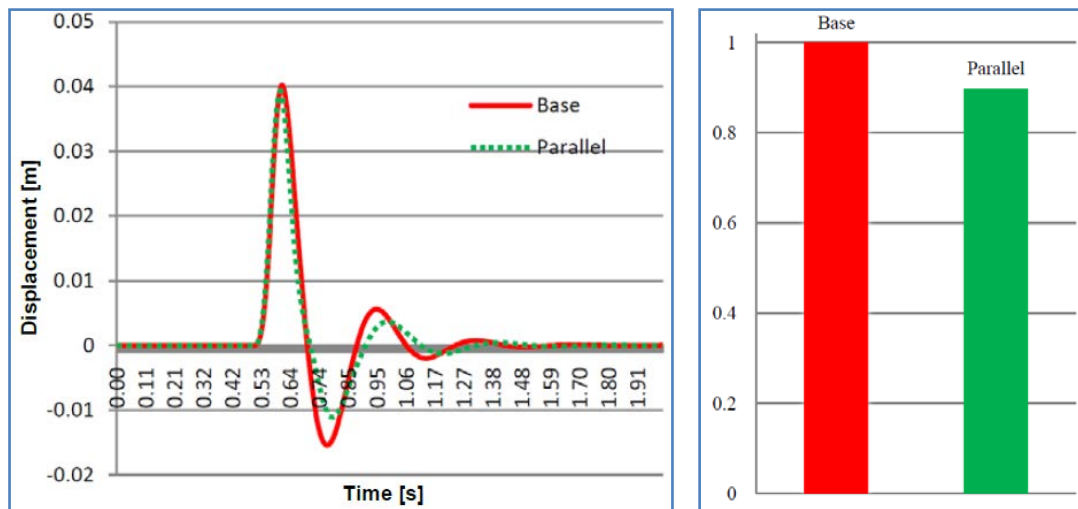
Then in parallel structure, by increasing the b value, the displacement and tire deflection response magnitude poles module reduces.

When  $b = 5$  kg, the poles start to reduce in 1-5 Hz.

When  $b \rightarrow 35$  kg, the poles tend to be located is continuous reduce in this frequency.

It is interesting to note the following points, as expected and accordingly to the pole location analysis provided above, increasing inertance  $b$  value reduce the resonance peaks, leading to an oscillatory behavior. But, in other frequency phase, the system is not good. To improving suspension system in oscillation, we suggest using parallel structure to optimize quarter-car model.

### 3.4 Results and Discussions



**Figure 3-16:** Comparative sprung mass displacement of base, parallel quarter-car model respectively.

The results confirm that the suspension system with inerter effects to the sprung mass displacement, the time histories of the displacement in respectively. The **Figure 3-16** shown that the displacement is reduced by comparison between base and parallel models. The parallel suspension model presented as dot line curve suggesting that the structure of the suspension employing inerter is better than conventional model in displacement.

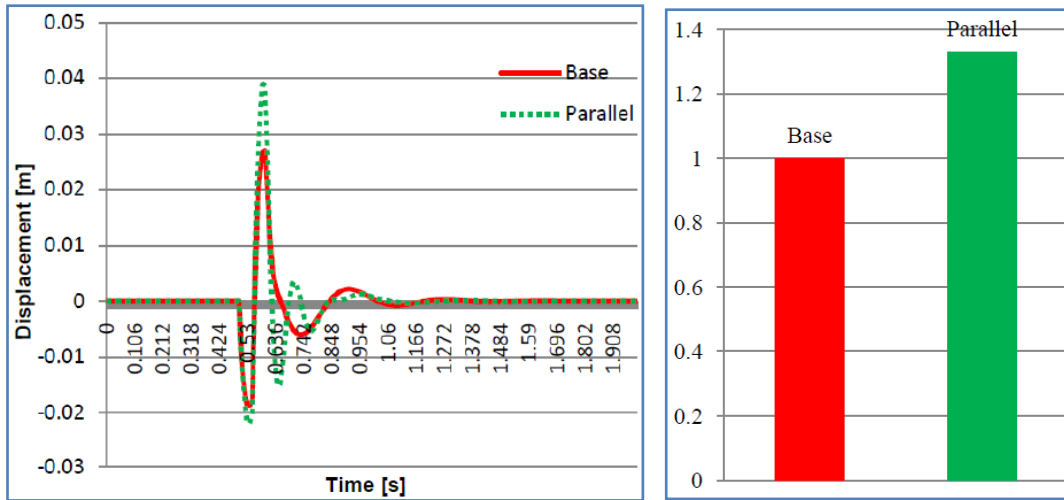
**Table 3-3** is comparing between base and parallel model, we found that correspondences between these RMS of displacement variables of sprung mass is summarized below. If we only apply inerter to base suspension system, we can get a better RMS displacement improve more than 10 percent with constant spring and damper parameter. These results verified that apply inerter on traditional suspension system will reduce displacement of sprung mass and improve comfortable.

**Table 3-3:** Comparison the RMS sprung mass displacement of base, parallel quarter-car model.

Model	RMS( $Z_s$ ) [m]	Improvement
Base model	0.369	0%
Parallel model	0.331	10.32%

On the other hands, **Figure 3-17** shown if sprung mass displacement is good at almost parameters of parallel model then the tire deflection is hard to get better RMS value. If we only apply inerter to base model under parallel suspension with no change of tire stiffness, spring and damper parameters, the RMS value of tire deflection is increase more than 33 percent compare with base model show on **Table 3-4**. It means that tire deflection is not good for tire grip to contact the road. Otherwise, we have to optimal this value by change the quarter ca parameter, it will be shown in next chapter.

The red line present for tire deflection of base model while dot blue line is parallel model employing inerter. The **Figure 3-17** show that the tire grip is strike with some of pick point, it is a little hard to contact on the road.



**Figure 3-17:** Comparative tire deflection of base, parallel quarter-car model respectively.

**Table 3-4:** Comparison the RMS tire deflection of base, parallel quarter-car model.

Model	RMS(Zt-def) [m]	Improvement
Base model	0.206	0%
Parallel model	0.274	-33.06%

### 3.5 Summary and Comments

In this chapter, we considered the quarter-car model with inerter employing as parallel and series in suspension, which compare with a conventional model to reduce both sprung displacement and tire deflection under road bump disturbance. Firstly, we discussed among the conventional, parallel and series model based on the passive suspension system. Then through the analysis it was shown that a passive suspension apply inerter in parallel has good sprung mass displacement in general performance specification. But it do not show clear advantage for tire deflection, thus the parallel suspension design with inerter will later be performed by optimization process in Chapter 6.

## CHAPTER 4

### ADVANTAGE OF INERTER APPLY ON HALF-CAR MODEL

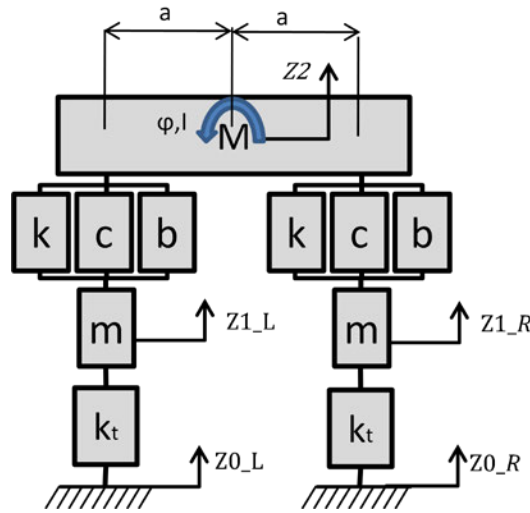
#### 4.1 Half-Car Model Analysis

We summarize the approach of the suspension design problem was formulated as an optimal modal parameter to improve rolling angle through displacement variables. The solution of the optimization problem uses structure of new half-car model that is improved from traditional passive suspension system in adding inerter elements. In this chapter, we shall apply the training parameterization method to the half-car model.

In this part, we made simulations creating mathematical model with inerter in the linear half-car model. The vehicle model has an input road disturbance to right sides, and the main outputs are rolling angle  $\varphi$  and sprung mass displacement  $Z_2$ . Several subsystems of model performance are considered such as sprung mass, un-sprung mass, suspension and tire. To optimizing suspension problems, we used these simulation results as the initial values that results represent for the picks of rolling angle  $Max\varphi$  and sprung mass displacement  $MaxZ_2$ .

We shall apply the training parameterization method to the half-car model. The half-car model represented in **Figure 4-1**: The half-car model. is the simple model to consider for suspension design. It consists of the sprung mass  $M$ , the un-sprung mass  $m$  and the tire model represented by stiffness  $k_t$ . The suspension strut provides an equal and opposite force on the sprung and un-sprung masses by means of

the positive-real admittance function which relates the suspension force to the strut velocity through spring, damper and inerter.



**Figure 4-1:** The half-car model.

For the half-car model, we define it as the following equations. The module of sprung mass body was represented by these equations:

$$M\ddot{z}_2(t) = (F_{kL}(t) + F_{cL}(t) + F_{bL}(t)) + (F_{kR}(t) + F_{cR}(t) + F_{bR}(t)) \quad \text{Eq. 4-1}$$

$$I\ddot{\varphi}(t) = a(F_{kL}(t) + F_{cL}(t) + F_{bL}(t)) - a(F_{kR}(t) + F_{cR}(t) + F_{bR}(t)) \quad \text{Eq. 4-2}$$

$$I = Ma^2/3 \quad \text{Eq. 4-3}$$

The module of suspension systems were represented as:

$$F_{kL}(t) = k(Z_{1L}(t) - (Z_2(t) - a\varphi(t))) \quad \text{Eq. 4-4}$$

$$F_{cL}(t) = c(\dot{Z}_{1L}(t) - (\dot{Z}_2(t) - a\dot{\varphi}(t))) \quad \text{Eq. 4-5}$$

$$F_{bL}(t) = b(\ddot{Z}_{1L}(t) - (\ddot{Z}_2(t) - a\ddot{\varphi}(t))) \quad \text{Eq. 4-6}$$

$$F_{kR}(t) = k(Z_{1R}(t) - (Z_2(t) + a\varphi(t))) \quad \text{Eq. 4-7}$$

$$F_{cR}(t) = c(\dot{Z}_{1R}(t) - (\dot{Z}_2(t) + a\dot{\varphi}(t))) \quad \text{Eq. 4-8}$$

$$F_{bR}(t) = b(\ddot{Z}_{1R}(t) - (\ddot{Z}_2(t) + a\ddot{\varphi}(t))) \quad \text{Eq. 4-9}$$

The un-sprung mass module as:

$$m\ddot{Z}_{1L}(t) = F_{ktL}(t) - (F_{kL}(t) + F_{cL}(t) + F_{bL}(t)) \quad \text{Eq. 4-10}$$

$$m\ddot{Z}_{1R}(t) = F_{ktR}(t) - (F_{kR}(t) + F_{cR}(t) + F_{bR}(t)) \quad \text{Eq. 4-11}$$

The tire module as:

$$F_{ktL}(t) = k_t(Z_{0L}(t) - Z_{1L}(t)) \quad \text{Eq. 4-12}$$

$$F_{ktR}(t) = k_t(Z_{0R}(t) - Z_{1R}(t)) \quad \text{Eq. 4-13}$$

For the evaluation of the rolling angle we use a hump road profile. The hump has height  $H_{0\_R}$  (on the right side) and flat on the left side. The hump initially appears after 1 second when run simulation then the right wheel impact while the left wheel has no disturbance. There is no load disturbances applied on the sprung mass.

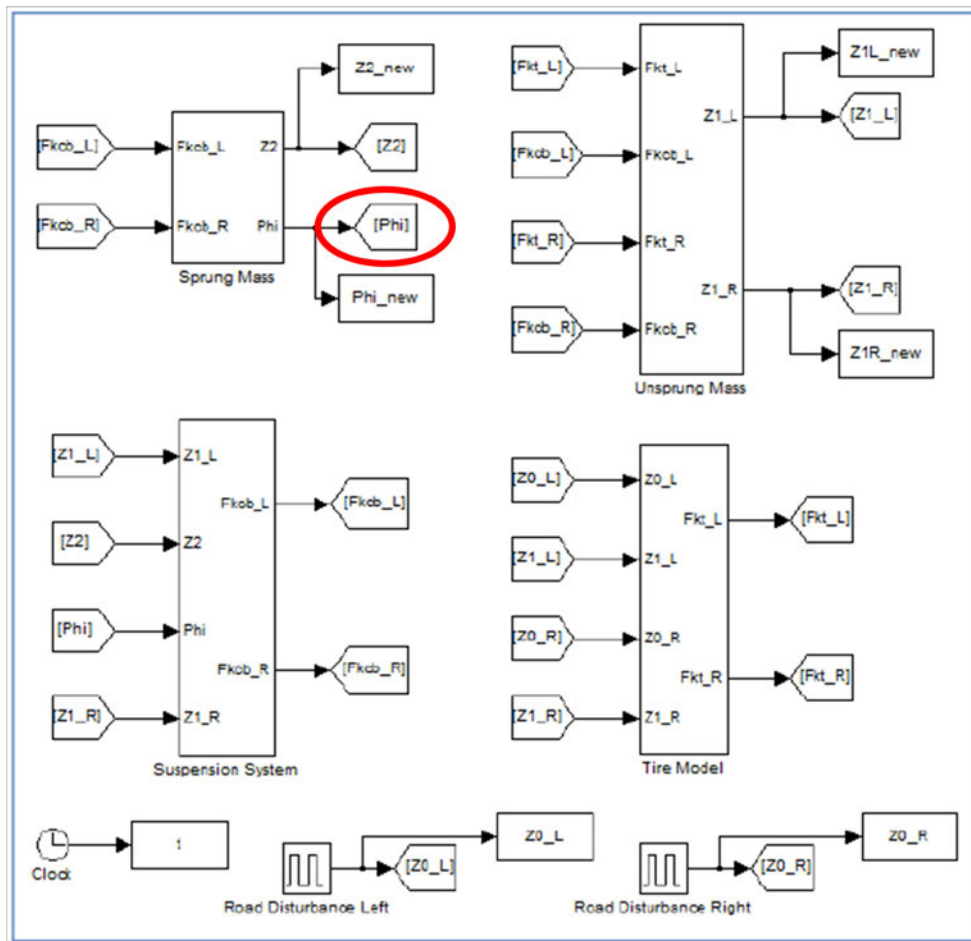
## 4.2 Half-car Model Specification

Base on previous study, we have modal parameters for passive suspension system as:

**Table 4-1:** The specification of Formula SAE half-car model.

Symbols	Parameters	Values
M	Mass of body	126 kg
m	Mass of tire	12 kg
I	Roll moment of inertia	15.1 kgm <sup>2</sup>
k	Stiffness coefficient	24000 N/m
c	Damping coefficient	1200 Ns/m
b	Mass of inertance	20 kg
$k_t$	Stiffness coefficient of tire	70000 N/m
a	Half length of track	0.6 m
$H_{0\_R}$	Road disturbance hump	0.1 m

In this part, we made simulations creating two models called: old\_model on basic suspension system and new\_model with inerter. The methodology used of a linear half-car model which is constructed in the simulation toolboxes. The vehicle model has an input road disturbance right sides, the main output is rolling angle ( $\phi$ ) and sprung mass displacement ( $Z_2$ ). Several subsystems of model performance are considered such as sprung mass, un-sprung mass, suspension and tire showed in **Figure 4-1**. For each aspect of performance we will propose time-domain performance measures that are evaluated after a simulation run. To optimizing suspension problems, we used these simulation results as the initial values. The results represent for the peaks of rolling angle  $\text{Max}\phi$  and sprung mass displacement  $\text{Max}Z_2$ .

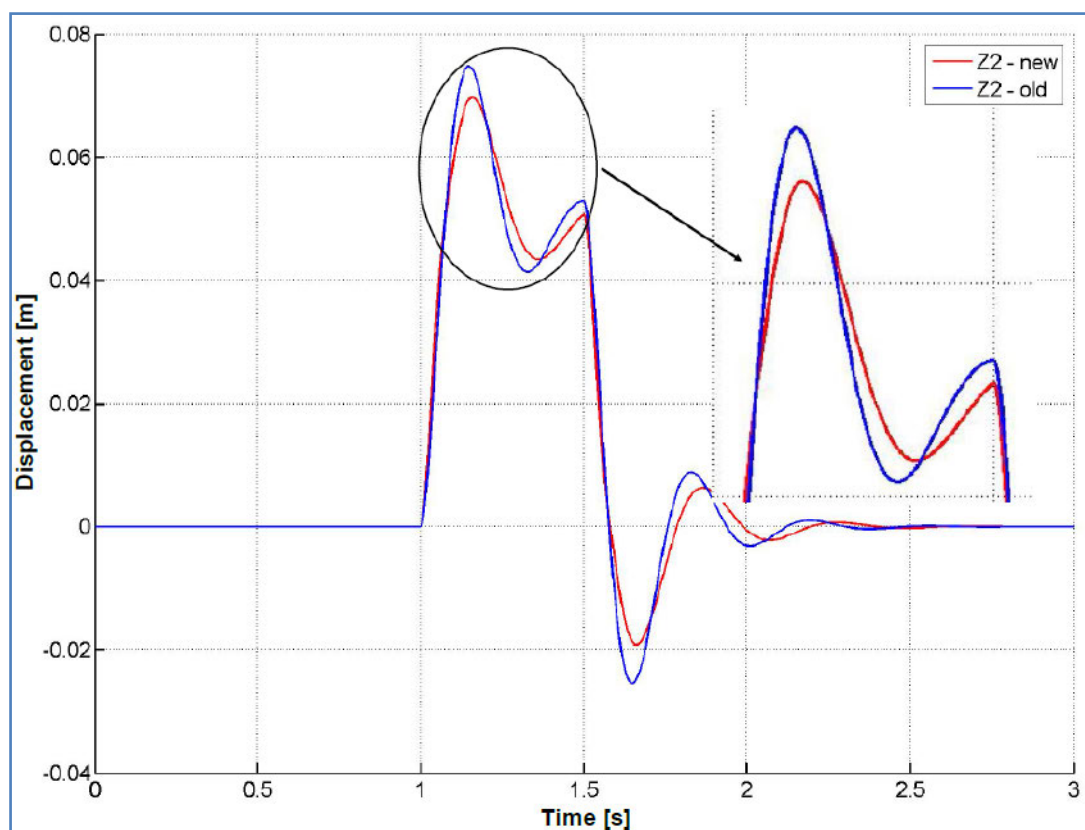


**Figure 4-2:** The simulation of half-car model to calculate rolling and displacement.



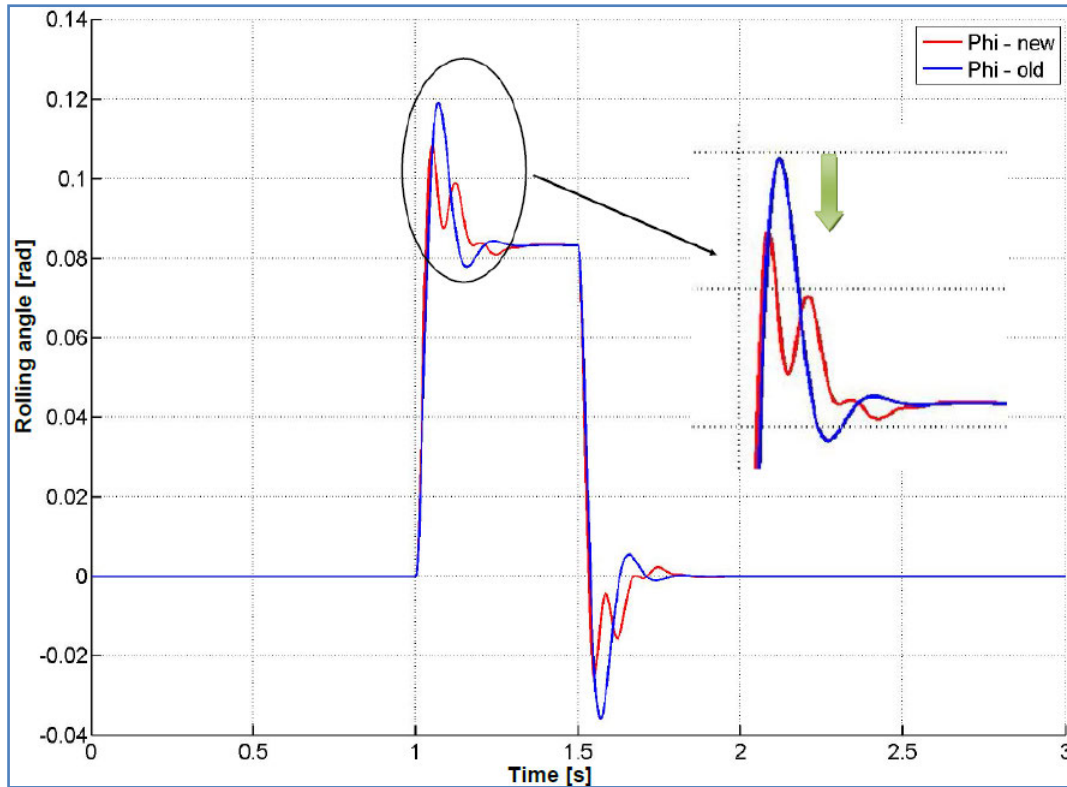
### 4.3 Advantage Results on Half-car Model

The **Figure 4-3** shows the results that then half-car model employing inerter effects to the sprung mass displacement, in the time domain. From the results, it was verified that the displacement is reduced by comparison between base and parallel suspension in half-car model models. The red line in new model apply inerter which has an advanced compare with blue line is conventional one. It means that an optimal algorithm allows the change in the structure of suspension parameters to obtain the minimum vertical displacement values.



**Figure 4-3:** The result of sprung mass displacement compare old and new half-car model.

For the half-car model, the results were confirmed that the inerter is added to affect the roll angle, the time histories of the body roll angles are shown in **Figure 4-4** respectively. From the results, it was verified that the rolling angle is reduced by comparison among each models.



**Figure 4-4:** The result of rolling angle compare old and new half-car model.

The old model presented as blue curve line while the red line is new one. It shows that the peak point of rolling angle reduce when use parallel suspension on half-car model. Comparing old-model and new-model we found that the rolling angle summary as below.

**Table 4-2:** The comparison rolling angle peak point results.

Rolling peak	Result (rad)	Improvement
$\varphi_{old}$	0.114	0%
$\varphi_{new}$	0.098	14.03%

The table shows that with inerter components employ to passive suspension system as a parallel structure, the rolling angle will be reduced. We fix inerter parameter  $b$  then constant spring and damper parameter, the rolling value reduce 14 percent.

#### **4.4 Summary and Comments**

This chapter has considered the half-car active suspension design problem. By applying the road disturbance response, the displacement can be improved so the advantage for rolling angle is satisfactory. A suspension system with inerter employing parallel applies to half-car model was verified that the modified model has better results compare with original model in this case study. The conditions under the half-car model structure can be decomposed into two quarter-cars were investigated, this mean we will focus to analyze quarter-car model for multipurpose. An optimal design which allows further improvement of the rolling angle will be discussed on the next chapter.



## **CHAPTER 5**

### **VERIFICATION INERTER DESIGN APPLY ON SUSPENSION SYSTEM**

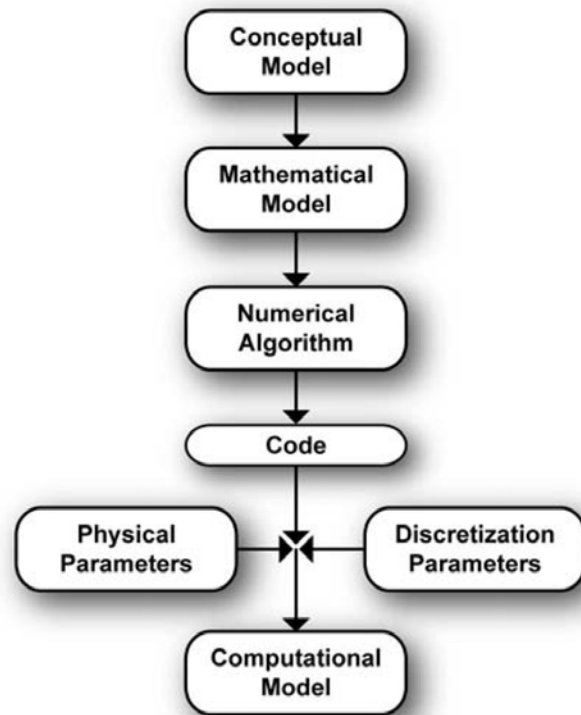
This chapter, describes the activities involved in developing the computational inerter model, starting with the formulation of the conceptual and mathematical models, then revising these models in the simulation resulting model. The description of the model development activities begins with the assumption that the reality of interest, the intended use of the model, the response features of interest, and the accuracy requirements have been clearly defined.

A verification process is introduced to estimate the passive suspension is the simple system that can be improved displacement stability depend on the sensitivity of the system in both mathematical and computational model. To improve displacement stability, this study proposes a design new passive suspension system taking with new inerter mechanism contribution. These quarter-car model with variable stiffness, damping and inerter suspension system is constructed verified in advanced.

#### **5.1 Inerter Model Analysis**

In general, the system model (conceptual to computational) is built up from subassembly, assembly, and component models. **Figure 5-1** illustrates the path from a conceptual model to a computational model. This conceptual model can be described with differential calculus to produce a mathematical model. The equations can be solved by various numerical algorithms or using the finite element method. The

numerical algorithm is programmed into a software package, here called a code with the specification of physical and discretization parameters, the computational model is created.



**Figure 5-1:** Path from conceptual model to computational model [29].

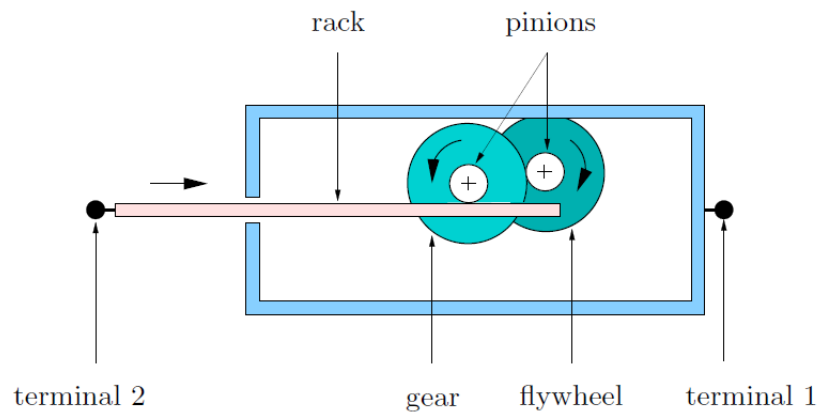
### 5.1.1 Conceptual Inerter Model

The conceptual model is defined as the idealized representation of the solid mechanics behavior of the reality of interest. The model include those mechanisms that impact the key mechanical and physical processes that will be of interest for the intended use of the model. The activity of conceptual model development involves formulating a mechanics-based representation of the reality of interest that is amenable to mathematical and computational modeling and that is expected to produce results with adequate accuracy for the intended use. Essentially, it is defining the modeling approach.

The formulation of the conceptual model is important to the overall model development process because many fundamental assumptions are made that influence

interpretation of the simulation results. These assumptions include the determination of how many separate parts or components will be included in the model, the approach to modeling the material behavior, the elimination of unimportant detail features in the geometry, and the selection of interface and boundary types, e.g., fixed, pinned, contact, friction, etc. If an important mechanical phenomenon is omitted from the conceptual model, the resulting simulations might not be adequate for the intended use of the model.

In previous study, an inerter was defined as a mechanical two-terminal, one-port device with the property that the equal and opposite force applied at the nodes is proportional to the relative acceleration between the nodes through a rack, pinion, and gears.



**Figure 5-2:** Theory structural inerter element [18].

To approximately model the dynamics of the device of **Figure 5-2**, let  $r_1$  be the radius of the rack pinion,  $r_2$  the radius of the gear wheel,  $r_3$  the radius of the flywheel pinion,  $\gamma$  the radius of gyration of the flywheel,  $m$  the mass of the flywheel.

The following relation holds:

$$F = b(\dot{v}_2 - \dot{v}_1) \quad \text{Eq. 5-1}$$

The constant of proportionality  $b$  is called the inertance,

And has units of kilograms:

$$b = m\alpha_1^2\alpha_2^2 \quad \text{Eq. 5-2}$$

Where  $\alpha_1 = \gamma/r_3$  and  $\alpha_2 = r_2/r_1$ .

It stored energy equal:

$$E = (1/2)b(v_2 - v_1)^2 \quad \text{Eq. 5-3}$$

## 5.2 Mathematical Model

The development of the mathematical model consists of specifying the mathematical descriptions of the mechanics represented in the conceptual model. In the mathematical model, principles of mechanics, the material behavior, interface properties, loads, and boundary conditions are cast into equations and mathematical statements. The specification of the mathematical model then allows the model input parameters to be defined. The model input parameters describe the various user-specified inputs to the model, such as material constants, road disturbance, and friction coefficient are fixed. The domain of interest can then be expressed in terms of these parameters.

On literature review, it show that inerter component is presented as b value in mass unit. For example, in gear type of inerter we have:

$$b = m\alpha_1^2\alpha_2^2$$

Where  $\alpha_1 = \gamma/r_3$  and  $\alpha_2 = r_2/r_1$ .

Therefore, in mathematical model, b value is constant so we do not define for inerter component as gear inside. Thus we assumption that inerter ignore all coefficient of fraction inside, we only define for quarter-car suspension as follow. For the quarter-car model, the suspension admittance function which relates the suspension force to the strut velocity through spring, damper and inerter.

The module of sprung mass body was represented by these equations:



$$M\ddot{Z}_2(t) = F_k(t) + F_c(t) + F_b(t) \quad \text{Eq. 5-4}$$

Where:

$$F_k(t) = k(Z_1(t) - Z_2(t)) \quad \text{Eq. 5-5}$$

$$F_c(t) = c(\dot{Z}_1(t) - \dot{Z}_2(t)) \quad \text{Eq. 5-6}$$

$$F_b(t) = b(\ddot{Z}_1(t) - \ddot{Z}_2(t)) \quad \text{Eq. 5-7}$$

The un-sprung mass module equation:

$$m\ddot{Z}_1(t) = F_{kt}(t) - (F_k(t) + F_c(t) + F_b(t)) \quad \text{Eq. 5-8}$$

Where:

$$F_{kt}(t) = k_t(Z_0(t) - Z_1(t)) \quad \text{Eq. 5-9}$$

The equations of motion in the Laplace transformed domains are:

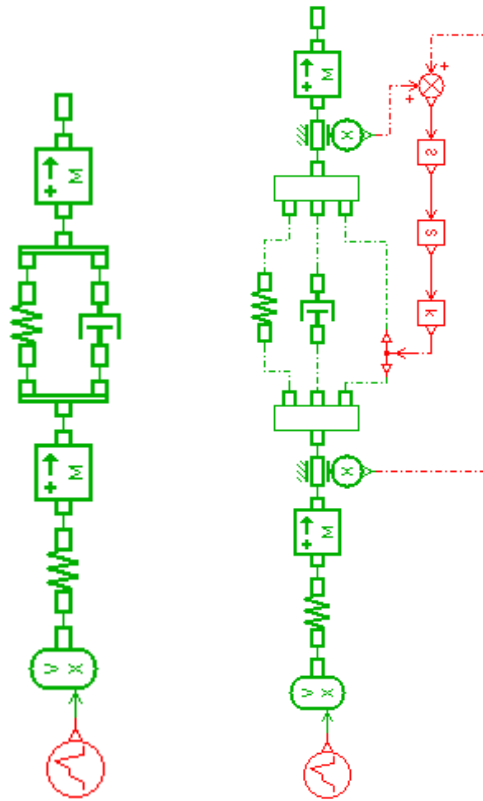
$$M_s s^2 \widehat{Z}_s = -sQ(s)(\widehat{Z}_s - \widehat{Z}_u) \quad \text{Eq. 5-10}$$

$$M_u s^2 \widehat{Z}_u = sQ(s)(\widehat{Z}_s - \widehat{Z}_u) + k_t(\widehat{Z}_r - \widehat{Z}_u) \quad \text{Eq. 5-11}$$

$$Q(s) = Y_k + Y_c + Y_b = \frac{k}{s} + c + bs \quad \text{Eq. 5-12}$$

In this research, we integrated inerter mechanism that applied on passive suspension system. First, we use conventional suspension model with initial parameter from formula car. Second, base on mathematical model, we apply inerter on suspension system in parallel structure show on **Figure 5-3**. Then we focus to analyze the effects of inerter on the system as displacement of sprung mass and tire deflection.

Furthermore, this mathematical model used fixed initial conditions such as b value under mass unit which there is no parameter present for factor and coefficients inside. Changing the b value means change prototype of inerter mechanism in respectively. Thus mathematical model is the simple model then we try to verify that it can be work same the real one correctly.



**Figure 5-3:** The conventional and parallel mathematical quarter-car model.

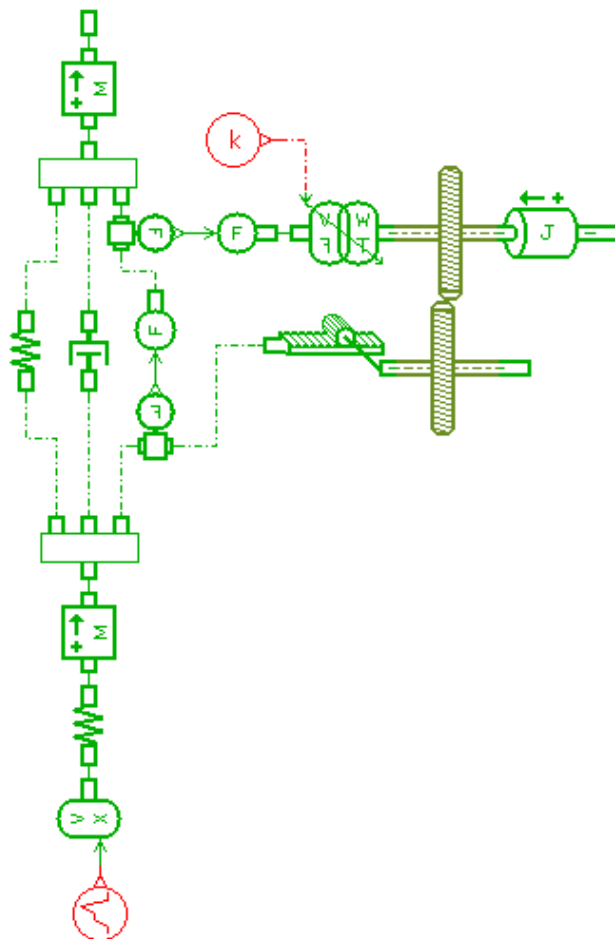
### 5.3 Computational Model

The computational model is the numerical implementation of the mathematical model that will be solved on a computer to yield the computational predictions (simulation results) of the system response. As defined herein, the computational model includes the type and degree of spatial discretization of the component inside, the temporal discretization of the governing equations, the solution algorithms to be used to solve the governing equations, and many coefficients criteria for the numerical solutions.

The computational model can be simple or complicated. Though an analyst might be tempted to jump directly from a component description of the reality of interest to the development of a computational model, it is valuable to think through the process of conceptual modeling, mathematical modeling, and computational

modeling to have a thorough understanding of what assumptions and mathematical simplifications underlie the computational model.

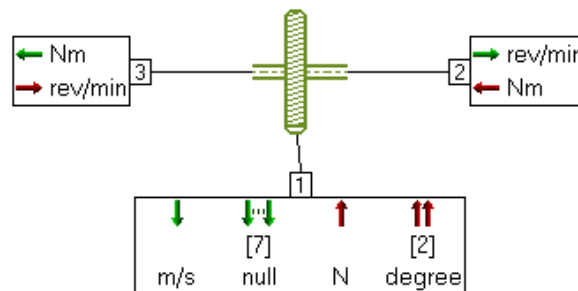
We design computational quarter-car model with more detail of inerter components in gear, rack, pinion, flywheel and friction parameter show in **Figure 5-4**, where  $M$  is mass,  $F$  is force signal,  $V$  is velocity,  $X$  is displacement,  $W$  is angular velocity,  $T$  is torque and  $J$  is rotary load. Each of them works on difference initial frictions or efficient rate. Furthermore, we integrated inerter mechanism which applied on passive suspension system. For each model, we have to calibrate to closing optimization inertance value. Each of them has difference characteristics on working as frictions or efficient rate so they can effect to simulation results.



**Figure 5-4:** The computational parallel suspension on quarter-car model.

### 5.3.1 Inerter Modal Parameter

Commonly, at some stage of validation, the modeler will find that the computational model needs revisions to achieve the desired accuracy or to account for new requirements. In a general sense, there are two classes of possible revisions to the mathematical and computational models. The first class of revisions covers updates to parameters in the mathematical or computational model that are determined by calibrating the computational model to experimental data, e.g., additional component parameters, modal damping coefficients for linear vibration, or friction coefficients for a mechanical interface. The second class of revisions covers changes to the form of the mathematical or conceptual model to improve the description of the mechanics of interest so that better agreement with the reference computational data can be achieved. The classes of gear inerter parameter are discussed below.



**Figure 5-5:** Gear component with 3 ports.

**Table 5-1:** Gear component parameters index.

Title	Variable name	Unit	Value
Radius of gear wheel	$r_2$	mm	50
Radius of flywheel pinion	$r_3$	mm	10
Width of tooth face	b	mm	15

Immersed gear height	h	mm	0
Poisson's ratio	pois	null	0.3
Young's modulus	Ey	N/m <sup>2</sup>	2.1e+11
Coefficient of viscous friction	vis	Nm/(rev/min)	0



**Figure 5-6:** Helical rack and pinion.

**Table 5-2:** Helical rack and pinion component parameters index.

Title	Variable name	Unit	Value
Radius of the pinion	$r_1$	mm	10
Helix angle	alpha	degree	5
Pinion axis angle	beta	degree	0
Contact stiffness	k	N/m	1e+009
Contact damping	damp	N/(m/s)	1e+006
Static coefficient	must	null	0.12
Friction coefficient	musl	null	0.1
Stribeck constant	astrib	m/s	0.001
Stick displacement threshold	dtrel	mm	0.001
Equivalent viscous friction during stiction	rtors	N/(m/s)	100000



**Figure 5-7:** Rotary load with two shafts without friction.

**Table 5-3:** Rotary parameter .

Title	Variable name	Unit	Value
Moment of inertia	I	$g \cdot m^2$	0.04

### 5.3.2 Updates to Model Parameters

Revision by parametric model calibration is extensively used in the field of linear structural dynamics to bring computational predictions into better agreement with measured response quantities such as modal frequencies. This revision process is commonly known as model updating, model tuning, parameter calibration, and parameter estimation. The process allows the most common sources of modeling difficulties in linear structural dynamics compliance in joints, energy loss/damping, unmeasured excitations, uncertain boundary conditions,...to be represented as simple mechanical models.

It is important that model development activities be documented to facilitate reuse of the model. The documentation should explain the rationale for model development with modeling assumptions and describe the conceptual, mathematical, and computational models. The description of the mathematical model should include assumptions about the mechanics of interest and the sources of information for the model parameters. The description of the computational model should include

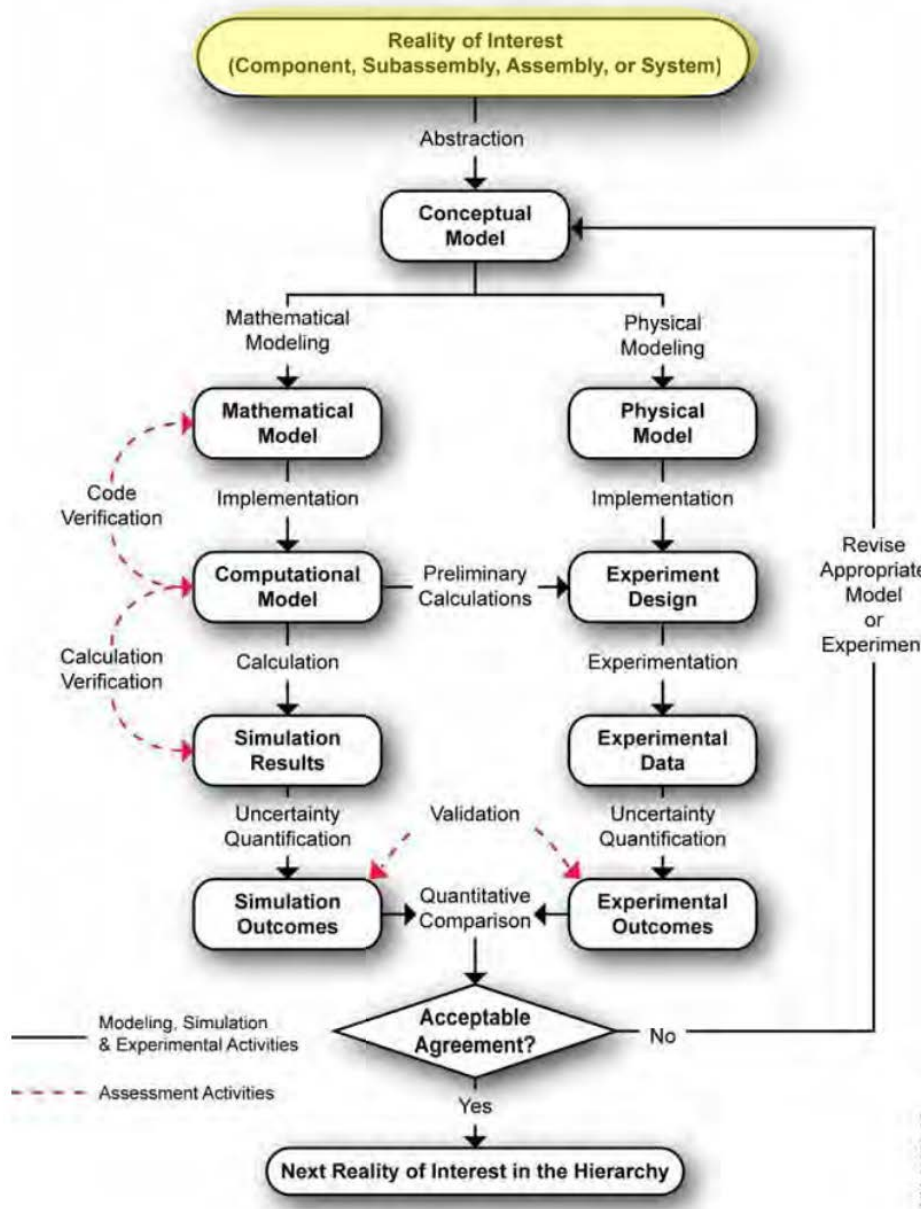
discretization assumptions, computational parameters, and other parameters of interest.

Parametric model calibration, however, determines only the model's fitting ability, not its predictive capability. Data used for model calibration must remain independent of data used to assess the predictive capability of the model. We will discuss about revised modal parameter in next chapter after optimization processing.

#### **5.4 Verification Process**

Once the elements of the physical system's hierarchy (whether one or many tiers) have been defined and prioritized, a systematic approach can be followed for quantifying confidence in model predictions through the logical combination of hierarchical model building, focused laboratory and field experimentation, and uncertainty quantification. This process is discussed below. **Figure 5-8** identifies the activities and products in the recommended Verification & Validation approach for computational solid mechanics. The activities are denoted by simple text, such as "mathematical modeling" and "physical modeling"; the products of these activities are highlighted in rounded boxes, e.g., the mathematical model is the product (or output) of the mathematical modeling activity. Modelers follow the left branch to develop, exercise, and evaluate the model.

Experimenters follow the right branch to obtain the relevant experimental data via physical testing. Modelers and experimenters collaborate in developing the conceptual model, conducting preliminary calculations for the design of experiments, and specifying initial and boundary conditions for calculations for validation.



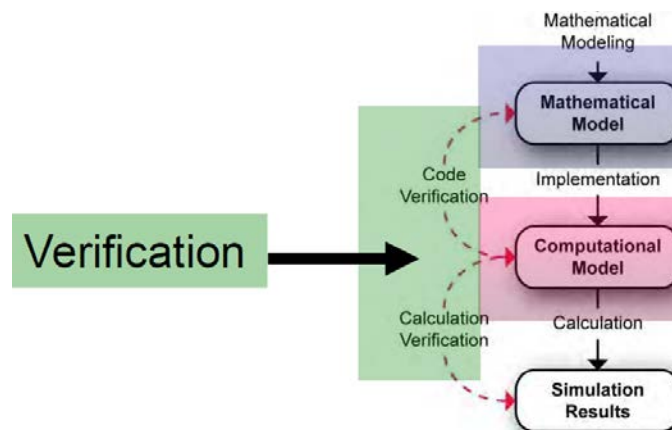
**Figure 5-8:** Verification & Validation activities and products [29].

This thesis focuses to verification process on the left branch without experimental for validation process. The process of verification assesses the fidelity of the computational model to the mathematical model. The mathematical model is commonly a set of partial differential equations and the associated boundary conditions, initial conditions, and constitutive equations. The computational model is the numerical implementation of the mathematical model, usually in the form of



numerical discretization, solution algorithms, and convergence criteria. Verification assessments consider issues related to numerical analysis, software quality engineering, programming errors in the computer code, and numerical error estimation.

Verification is composed of two fundamental activities: code verification and calculation verification show on **Figure 5-9**. Code verification is the assessment activity for ensuring, to the degree necessary, that there are no programming errors in a computer code and that the numerical algorithms for solving the discrete equations yield accurate solutions with respect to the true solutions of the partial differential equations.



**Figure 5-9:** Verification process [29].

A discussion of the differences and emphases of code verification and calculation verification is found in References [30] [31].

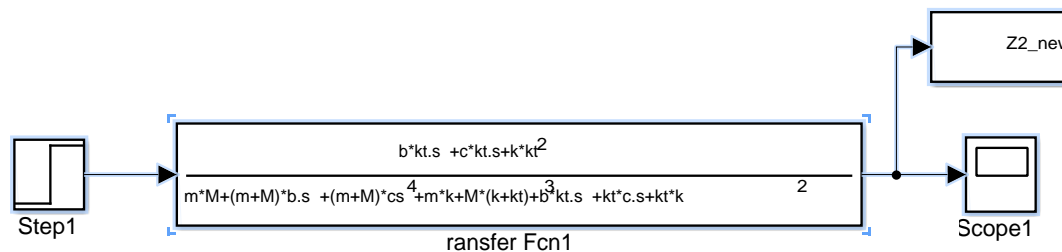
#### 5.4.1 Code Verification

The assessment activity of code verification can be logically segregated into two parts:

First is numerical code verification, which focuses on the underlying mathematical correctness and specific implementations of discrete algorithms for solving partial differential equations.

The second the software quality engineering or software quality assurance, which address such matters as configuration management, version control, code architecture, documentation, and regression testing [32].

Although modal equation users are typically not directly involved in developing and producing the modeling software they use, it is important that these users provide feedback to the developers to ensure that the best software engineering practices are consistently employed for the codes they use. Otherwise, unnecessary faults in the code may impact simulation results intermittently and unpredictably.



**Figure 5-10:** Quarter-car employing inerter represent in mathematical model.

#### 5.4.2 Calculation Verification

Calculation verification is applied to a computational model that is intended to predict validation results. Thus, each computational model developed in a validation hierarchy would be subject to calculation verification. The goal of calculation verification is to estimate the numerical error associated with the discretization. In most cases, exercising the computational model with multiple meshes is required to estimate this error.

The two basic categories of approaches for estimating the error in a numerical solution to a complex set of partial differential equations are a priori and a posteriori:

A priori approaches use only information about the numerical algorithm that approximates the partial differential operators and the given initial and boundary conditions [33] [34].

A posteriori error estimation approaches use all of the a priori information plus the results from two or more numerical solutions to the same problem.

The discussion here focuses on a posteriori error estimates because they can provide quantitative assessments of numerical error in practical cases of nonlinear partial differential equations. So we will compare mathematical and computational model in frequency domain.

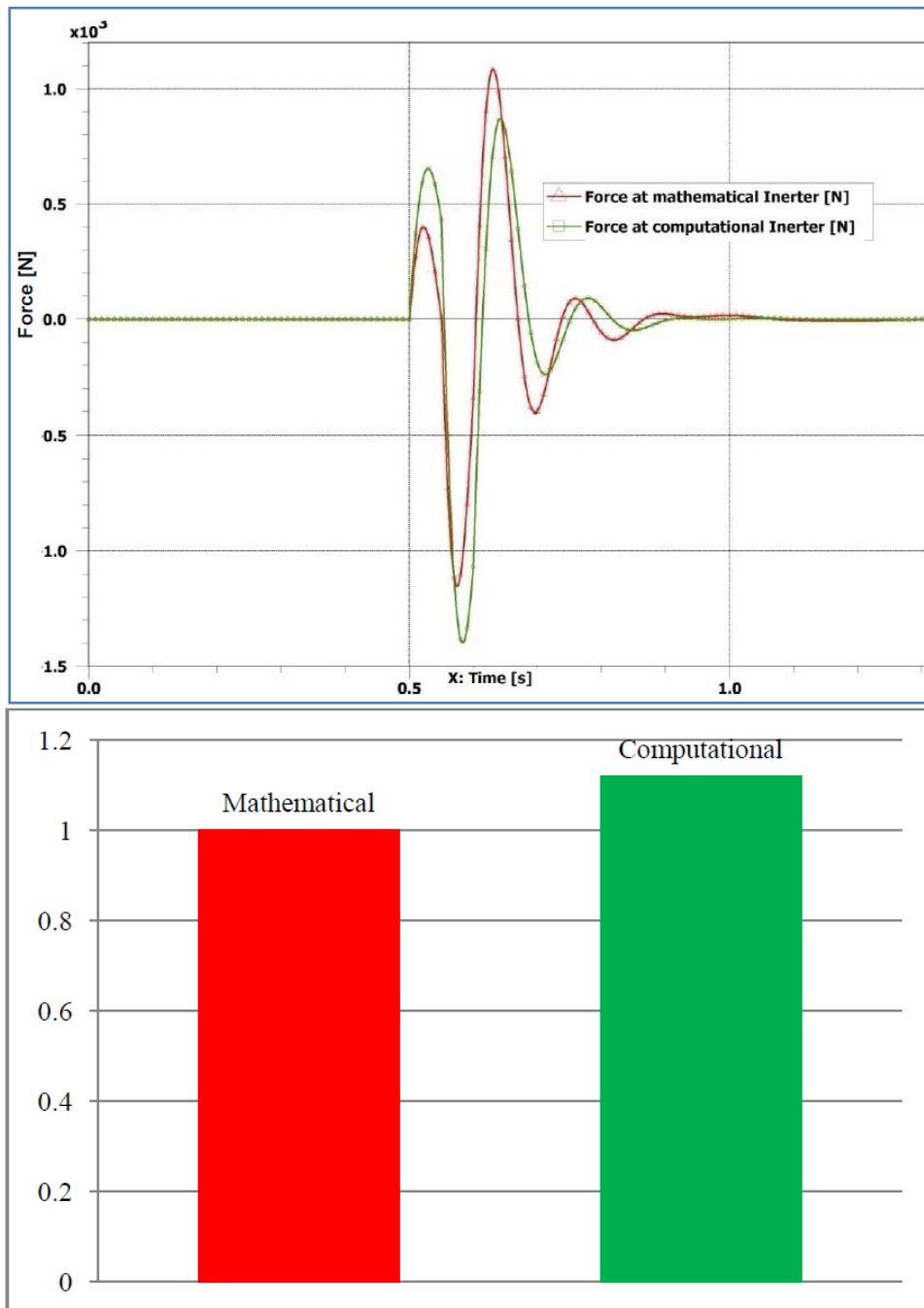
#### 5.4.3 Verification Results

We need to be an integral part of the verification process to facilitate for using of the model. They should explain the rationale and limitations of the code verification and calculation verification activities. It should include descriptions of the estimation techniques employed, the results of consistency tests, and the analytical solutions and numerical solutions used. An acceptable computational systems should also be described.

We initiate the software and choose the statistical test with mathematical and computational model. Next, we select the type of analysis, first is the force apply to inerter and the second is output at sprung mass displacement in the more detail. We intentionally select road disturbance is statistical power which introduces relatively for the normal road bump.

We proceed by selecting a relatively large effect size of factors and coefficient in computational inerter model as well as initial conditional running programs.

Finally, we command the software to commence computation and we obtain the results depicted in **Figure 5-11**. As can be seen, the force output at inerter component is the same shape with a little bit difference value at some points, but totally value is approximate in RMS estimate.

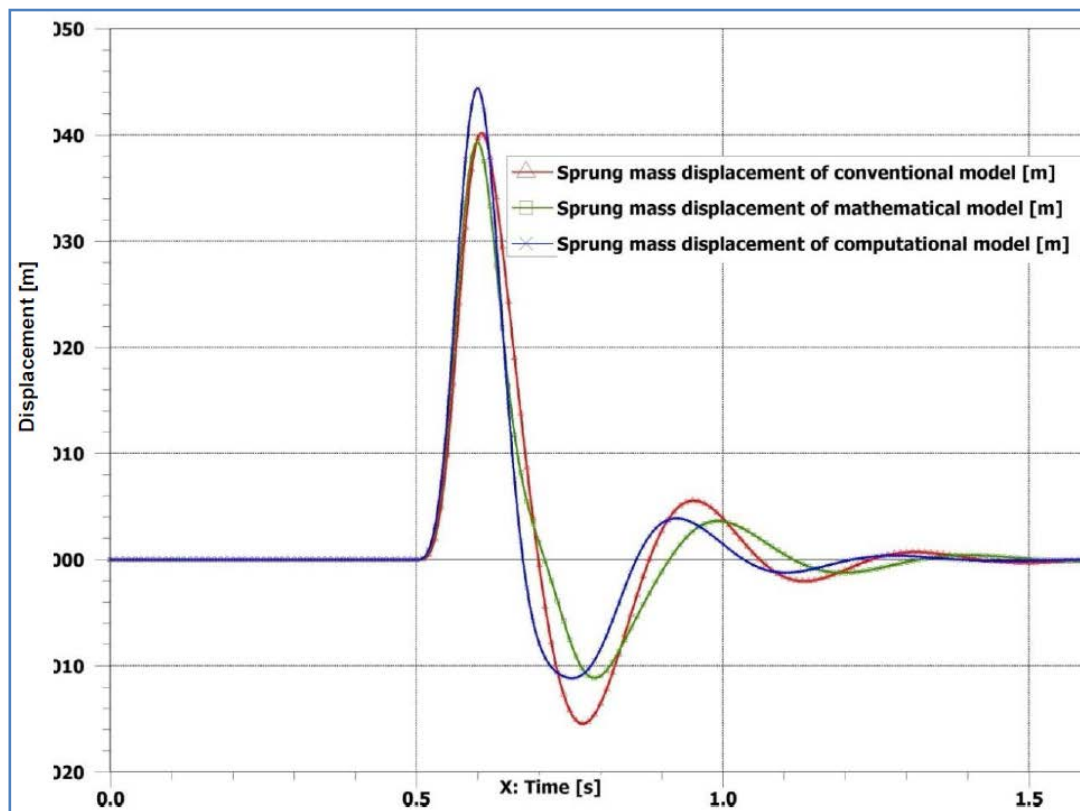


**Figure 5-11:** Comparison force apply on computational and mathematical Inerter.

**Table 5-4:** Comparison RMS force apply to mathematical and computational inerter respectively.

Model	RMS_Force [N]	Changeable
Mathematical Inerter model	9187	0
Computational Inerter model	10277	11.8%

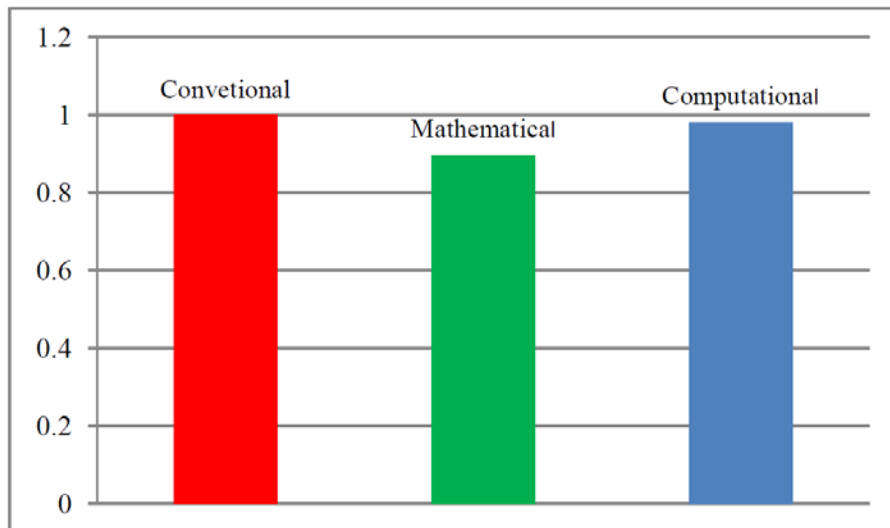
Post test analysis shown on output results of sprung mass displacement on **Figure 5-12**. Many ways of analyzing the results after tests have been performed. In this case such a design, we examine the result of displacement in time domain, we like to analyze the results of the tests in order to determine the joint effects of the factors on the success or failure of computational and mathematical tests.



**Figure 5-12:** Comparison sprung mass displacement among conventional, mathematical and computational model.

**Figure 5-13** showed that the inerter has an advance on applying suspension system. While the suspension without inerter has high displacement of sprung-mass, then the system applied inerter has a smaller one. The computational model has frictions inside, included mass components in inerter mechanism so the line curves are unlike at the same time.

**Table 5-5** show the comparison  $RMS(Z_s)$  among conventional, mathematical and computational model. While mathematical has more than 10% of improvement compare with conventional model then computational has small advantage about 2%. We show some reasons for this case: first is delay phase of computational is bigger than mathematical, second the computational model has some factor of friction and coefficient inside while the mathematical model has no factor.



**Figure 5-13:** Comparison RMS sprung mass displacement among conventional, mathematical and computational model.

The sum of roots mean squares as well as the statistic for testing for no differences in treatment means often provide rough but reliable indicators as to the relative importance of each factor or combination. The identified significant variability displacement leads to the conclusion that this area may contain more of a

potential for hidden system defects. In this case, it shown that a difference results still exist because of extra modal parameter add in inerter component. Therefore, we have some extra comparison after optimization process on time and other relevant resources, we should add supplementary for tests adjusting parameters in the initial locations of the suspension then modifying parameter to improving system.

**Table 5-5:** Comparison improvement RMS sprung mass displacement of conventional, mathematical and computational model in respectively.

Model	RMS( $Z_s$ ) [m]	Improvement
Conventional model	0.369	0%
Mathematical model	0.331	10.31%
Computational model	0.362	1.83%

## 5.5 Summary and Comments

In this chapter, we developed the verification process to numerically calculate the suspension model for quarter-car model, which is useful for estimate complex systems. We applied the procedure to the linear quarter-car model with conceptual inerter model employment. The mathematical model figure out with assumption of simple theories as b value was defined.

Furthermore, the computational model simulations were obtained after implementing the detail factors and coefficients inside the inerter mechanism. It is noticed that all the computational models we have completed in the numerical models were based on our experience, and a trial and error exist because sometimes it had difference assumption conditions. The results shown that mathematical and computational model work on the same shapes of force apply to inerter and also had advanced on RMS displacement. It is verified that mathematical model performance

is correctly working theories. It is importance for optimization process before we verify studying methodology.



## **CHAPTER 6**

### **OPTIMIZATION PROCESS APPLY ON SUSPENSION WITH INERTER**

#### **6.1 Response Surface Methodology (RSM) Introduction**

Response surface methodology (RSM) is a collection of statistical and mathematical techniques useful for developing, improving, and optimizing processes. It also has important applications in the design, development, and formulation of new products, as well as in the improvement of existing product designs.

The most extensive applications of RSM are in the industrial world, particularly in situations where several input variables potentially influence some performance measure or quality characteristic of the product or process. This performance measure or quality characteristic is called the response. It is typically measured on a continuous scale, although attribute responses, ranks, and sensory responses are not unusual. Most real-world applications of RSM will involve more than one response. The input variables are sometimes called independent variables, and they are subject to the control of the engineer or scientist, at least for purposes of a test or an experiment [35].

The origin of RSM is the seminal paper by Box and Wilson. They also describe the application of RSM to chemical processes. This paper had a profound impact on industrial applications of experimental design, and was the motivation of much of the research in the field. There have also been four review papers published

on RSM [36] [37] [38] [39]. The monograph by Myers [40] was the first book devoted exclusively to RSM.

In practice, complex process optimization problems such as this can often be solved by superimposing appropriate response surface contours. However, it is not unusual to encounter problems with more than two process variables and more complex response requirements to satisfy. In such problems, other optimization methods that are more effective than overlaying contour plots will be necessary.

### 6.1.1 Approximating Response Functions

In general, suppose that the scientist or engineer (whom we will refer to as the experimenter) is concerned with a product, process, or system involving a response  $y$  that depends on the controllable input variables  $\xi_1, \xi_2, \dots, \xi_k$ . The relationship is

$$y = f(\xi_1, \xi_2, \dots, \xi_k) + \varepsilon$$

where the form of the true response function  $f$  is unknown and perhaps very complicated, and  $\varepsilon$  is a term that represents other sources of variability not accounted for in  $f$ . Thus  $\varepsilon$  includes effects such as measurement error on the response, other sources of variation that are inherent in the process or system (background noise, or common/special cause variation in the language of statistical process control), the effect of other (possibly unknown) variables, and so on. We will treat  $\varepsilon$  as a statistical error, often assuming it to have a normal distribution with mean zero and variance  $\sigma^2$ . If the mean of  $\varepsilon$  is zero, then

$$E(y) \equiv \eta = E[f(\xi_1, \xi_2, \dots, \xi_k)] + E(\varepsilon) = f(\xi_1, \xi_2, \dots, \xi_k)$$

The variables  $\xi_1, \xi_2, \dots, \xi_k$  are usually called the natural variables, because they are expressed in the natural units of measurement, such as degrees Celsius ( $^{\circ}\text{C}$ ), pounds per square inch (psi), or grams per liter for concentration. In much RSM work it is convenient to transform the natural variables to coded variables  $x_1, x_2, \dots, x_k$ ,

which are usually defined to be dimensionless with mean zero and the same spread or standard deviation.

In terms of the coded variables, the true response function is now written as

$$\eta = f(x_1, x_2, \dots, x_k)$$

Because the form of the true response function  $f$  is unknown, we must approximate it. In fact, successful use of RSM is critically dependent upon the experimenter's ability to develop a suitable approximation for  $f$ . Usually, a low-order polynomial in some relatively small region of the independent variable space is appropriate. In many cases, either a first-order or a second-order model is used.

#### 6.1.2 The Sequential Nature of RSM

Most applications of RSM are sequential in nature. That is, at first some ideas are generated concerning which factors or variables are likely to be important in the response surface study. This usually leads to an experiment designed to investigate these factors with a view toward eliminating the unimportant ones. This type of experiment is usually called a screening experiment. Often at the outset of a response surface study there is a rather long list of variables that could be important in explaining the response. The objective of factor screening is to reduce this list of candidate variables to a relative few so that subsequent experiments will be more efficient and require fewer runs or tests. We refer to a screening experiment as phase zero of a response surface study. You should never undertake a response surface analysis until a screening experiment has been performed to identify the important factors.

Once the important independent variables are identified, phase one of the response surface study begins. In this phase, the experimenter's objective is to determine if the current levels or settings of the independent variables result in a value

of the response that is near the optimum, or if the process is operating in some other region that is possibly remote from the optimum. If the current settings or levels of the independent variables are not consistent with optimum performance, then the experimenter must determine a set of adjustments to the process variables that will move the process toward the optimum. This phase of response surface methodology makes considerable use of the first-order model and an optimization technique called the method of steepest ascent.

Phase two of a response surface study begins when the process is near the optimum. At this point the experimenter usually wants a model that will accurately approximate the true response function within a relatively small region around the optimum. Because the true response surface usually exhibits curvature near the optimum, a second-order model or very occasionally some higher-order polynomial will be used. Once an appropriate approximating model has been obtained, this model may be analyzed to determine the optimum conditions for the process.

### 6.1.3 RSM and the Philosophy of Quality Improvement

During the last few decades, industrial organizations in the United States and Europe have become keenly interested in quality and process improvement. Statistical methods, including statistical process control (SPC) and design of experiments, play a key role in this activity. Quality improvement is most effective when it occurs early in the product and process development cycle. It is very difficult and often expensive to manufacture a poorly designed product. Industries such as semiconductors and electronics, aerospace, automotive, biotechnology and pharmaceuticals, medical devices, chemical, and process industries are all examples where experimental design methodology has resulted in shorter design and development time for new products,

as well as products that are easier to manufacture, have higher reliability, have enhanced field performance, and meet or exceed customer requirements.

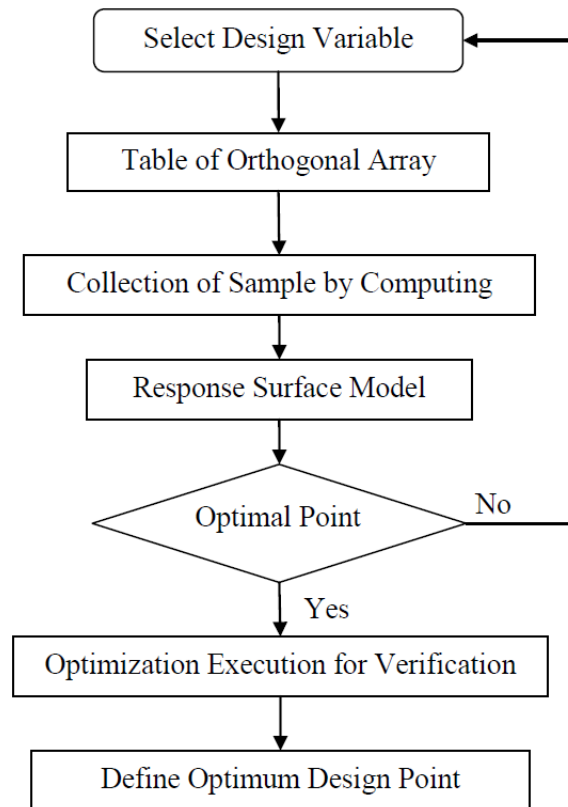
RSM is an important branch of experimental design in this regard. RSM is a critical technology in developing new processes, optimizing their performance, and improving the design and/or formulation of new products. It is often an important concurrent engineering tool, in that product design, process development, quality, manufacturing engineering, and operations personnel often work together in a team environment to apply RSM. The objectives of quality improvement, including reduction of variability and improved product and process performance, can often be accomplished directly using RSM.

#### 6.1.4 Product Design and Formulation

Many product design and development activities involve formulation problems, in which two or more ingredients are mixed together. There are many industrial problems where the response variables of interest in the product are a function of the proportions of the different ingredients used in its formulation. This is a special type of response surface problem called a mixture problem.

While we traditionally think of mixture problems in the product design or formulation environment, they occur in many other settings. Consider plasma etching of silicon wafers, a common manufacturing process in the semiconductor industry. Etching is usually accomplished by introducing a blend of gases inside a chamber containing the wafers. The measured responses include the etch rate, the uniformity of the etch, and the selectivity (a measure of the relative etch rates of the different materials on the wafer). All of these responses are a function of the proportions of the different ingredients blended together in the etching chamber.

### 6.1.5 Optimization Chart Flow

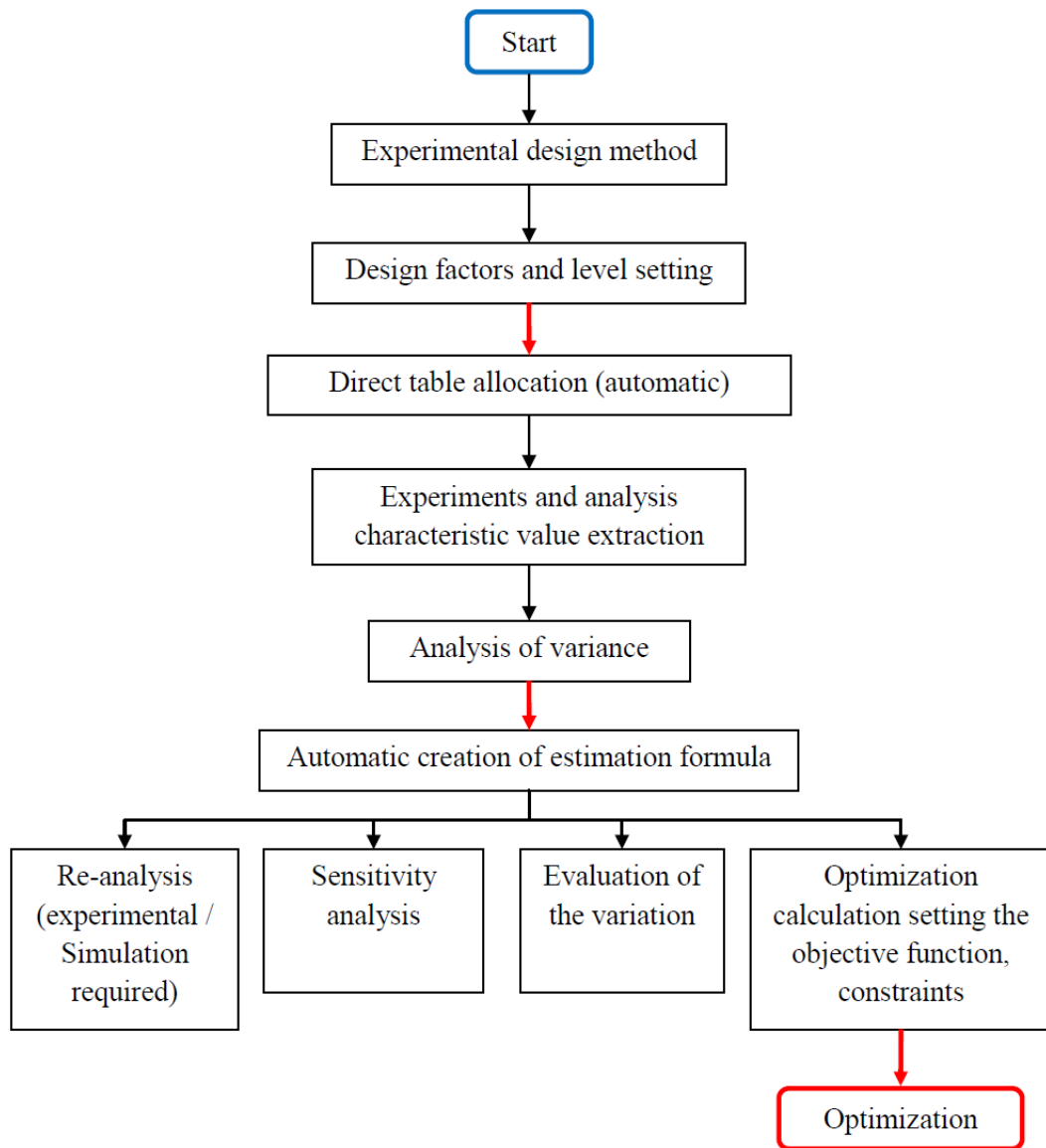


**Figure 6-1:** The response surface methodology optimization chart flow.

### 6.1.6 Optimization Process

Normally, if you do not achieve the design goal that was repeated trial and error of the design change, you have to experiments and analysis again in conventional laboratory analysis method. It not only is inefficient but also spend the time and cost. The this problem was solved in one fell swoop statistical design by support of computing software, that the reason we use mathematical model to evaluation. We utilize the experimental design on computer, to determine the estimated equation characteristics evaluated, in order to optimize in mathematical programming. It can reduce to a minimum the number of experiments and analysis. The benefits of this method are: system was also applied to both linear and nonlinear

phenomena, system design production efficiency is dramatically improved, it can be introduced economical system to all development and production sites, integrated system obtained a variety of design and analysis information and feel free to simple system in use.



**Figure 6-2:** The approximate optimization process.

## 6.2 Optimization Quarter-car Model

In this section we will focus to a single aspect of performance is related to the dynamics problem. We used the structure parameter which represented the following design variables:  $k$ ,  $c$ ,  $b$ , and  $k_t$ , with lower and upper boundaries show in **Table 6-1**. Simulation on mathematical quarter-car model was carried out to enable evaluation of vehicle performance measures. The resulted root-mean-squared (RMS) parameters, namely the  $RMS(Z_s)$  sprung mass displacement and  $RMS(Z_{t-def})$  tire deflection were taken into consideration under constraint function of  $RMS(Z_{sus})$  suspension deflection limitation.

**Table 6-1:** The boundary of design variables.

Lower	Parameter	Upper boundary	Unit
18000	$k$	30000	$[Nm^{-1}]$
600	$c$	1800	$[Nsm^{-1}]$
5	$b$	35	$[kg]$
50000	$k_t$	90000	$[Nm^{-1}]$

### 6.2.1 Optimal Displacement:

The objective function is represented for root-mean-squared of sprung mass displacement is:

$$RMS(Z_s) = f(k, c, b, k_t) \rightarrow \text{Min} \quad \text{Eq. 6-1}$$

Under the synthetic assumption, we can figure out this equation:



$$\begin{aligned}
\text{RMS}(Z_s) = & -0.886 + 1.24e - 04 * k - 2.56e - 09 * k^2 \\
& + 2.59e - 03 * c - 1.18e - 06 * c^2 - 5.47e \\
& - 03 * b + 8.43e - 05 * b^2 + 2.14e - 07 * k_t \\
& - 1.94e - 12 * k_t^2 - 2.61e - 07 * k * c \\
& + 1.16e - 10 * k * c^2 + 5.69e - 12 * k^2 * c \\
& - 2.53e - 15 * k^2 * c^2 - 1.31e - 07 * k * b \\
& + 1.30e - 09 * k * b^2 + 1.40e - 12 * k^2 * b \\
& - 3.73e - 14 * k^2 * b^2 + 6.14e - 06 * c * b \\
& - 6.65e - 08 * c * b^2 - 1.55e - 09 * c^2 * b \\
& + 1.58e - 11 * c^2 * b^2
\end{aligned} \tag{Eq. 6-2}$$

The constrained functions were represented by the suspension deflection:

$$\text{Min}\{\text{RMS}|Z_{\text{sus}}|\} \leq \text{RMS}(Z_{\text{sus}}(k, c, b, k_t)) \leq \text{Max}\{\text{RMS}|Z_{\text{sus}}|\} \tag{Eq. 6-3}$$

To calculating RMS( $Z_s$ ) and RMS( $Z_{\text{sus}}$ ), we used Orthogonal Arrays (OA) of Design of Experimental with L27 (313) then, we have:

$$\text{Min}\{\text{RMS}|Z_{\text{sus}}|\} = 0.0223 \text{ [m]} \tag{Eq. 6-4}$$

$$\text{Max}\{\text{RMS}|Z_{\text{sus}}|\} = 0.0474 \text{ [m]} \tag{Eq. 6-5}$$

We introduce the approximate optimization method, Sequential Quadratic Programming (SQP) with Response Surface Method (RSM). We made RSM using the OA to optimize modal parameters of the passive suspension system with inerter. The new modal parameters are represented for optimization suspension system called optimization model. In order to verify the effectiveness of the proposed optimal method, the numerical simulations were carried out. The vertical displacement optimization results were measured over various fixed structure suspensions. The optimization was performed for  $k_{\text{opt}}$ ,  $c_{\text{opt}}$ ,  $b_{\text{opt}}$  and  $k_{t-\text{opt}}$  ranging from boundary conditions. The modal parameter results were obtained by fixed-structure is presented in **Table 6-2**.

**Table 6-2:** The comparative modal parameters to optimal sprung mass displacement.

Parameter	k	c	b	k <sub>t</sub>
Base model	24000	1200	0	70000
Parallel model	24000	1200	20	70000
Optimization model	19091	1255	29.5	86363
Unit	[Nm <sup>-1</sup> ]	[Nsm <sup>-1</sup> ]	[kg]	[Nm <sup>-1</sup> ]

### 6.2.2 Optimal Tire Deflection:

The same method, we can optimal tire deflection in respectively. The objective function is represented for root-mean-squared of tire deflection is:

$$\text{RMS}(Z_{t-\text{def}}) = f(k, c, b, k_t) \rightarrow \text{Min} \quad \text{Eq. 6-6}$$

Under the synthetic assumption, we can figure out this equation:

$$\begin{aligned} \text{RMS}(Z_{t-\text{def}}) = & -1.841 + 1.81e - 04 * k - 4.06e - 09 * k^2 \\ & + 4.83e - 03 * c - 2.23e - 06 * c^2 + 1.20e \\ & - 02 * b - 3.49e - 05 * b^2 + 9.08e - 07 * k_t \\ & - 8.68e - 12 * k_t^2 - 4.37e - 07 * k * c \\ & + 2.02e - 10 * k * c^2 + 9.57e - 12 * k^2 * c \\ & - 4.36e - 15 * k^2 * c^2 + 2.36e - 07 * k * b \\ & - 1.31e - 09 * k * b^2 - 8.50e - 12 * k^2 * b \\ & + 6.73e - 14 * k^2 * b^2 - 1.21e - 05 * c * b \\ & + 7.94e - 08 * c * b^2 + 3.33e - 09 * c^2 * b \\ & - 2.77e - 11 * c^2 * b^2 \end{aligned} \quad \text{Eq. 6-7}$$

The constrained functions were represented by the suspension deflection:

$$\text{Min}\{\text{RMS}|Z_{\text{sus}}|\} \leq \text{RMS}(Z_{\text{sus}}(k, c, b, k_t)) \leq \text{Max}\{\text{RMS}|Z_{\text{sus}}|\} \quad \text{Eq. 6-8}$$

We used Orthogonal Arrays (OA) of Design of Experimental with L<sub>27</sub> (313)

then, we have:

$$\text{Min}\{\text{RMS}|Z_{\text{sus}}|\} = 0.0223 \text{ [m]} \quad \text{Eq. 6-9}$$

$$\text{Max}\{\text{RMS}|Z_{\text{sus}}|\} = 0.0474 \text{ [m]} \quad \text{Eq. 6-10}$$

The modal parameter results were obtained in **Table 6-3**.

**Table 6-3:** The comparative modal parameters to optimal tire deflection.

Parameter	k	c	b	$k_t$
Base model	24000	1200	0	70000
Parallel model	24000	1200	20	70000
Optimization model	24545	819	5	86363
Unit	$[\text{Nm}^{-1}]$	$[\text{Nsm}^{-1}]$	$[\text{kg}]$	$[\text{Nm}^{-1}]$

### 6.2.3 Optimal Both Displacement and Tire Deflection:

Optimal solutions for mixed performance of sprung mass displacement and tire deflection: Optimal performance solutions for  $\text{RMS}(Z_s)$  and  $\text{RMS}(Z_{t-\text{def}})$  individually for parallel suspension network has been computed above. Furthermore, it is also important to consider combined optimal vehicle performance across different measures. Here we present the results for a mixed  $\text{RMS}(Z_s)$  and  $\text{RMS}(Z_{t-\text{def}})$  measure:

$$\text{RMS}(\bar{Z}) = (1 - \alpha)\text{RMS}(Z_s) + \alpha\text{RMS}(Z_{t-\text{def}}) \quad \text{Eq. 6-11}$$

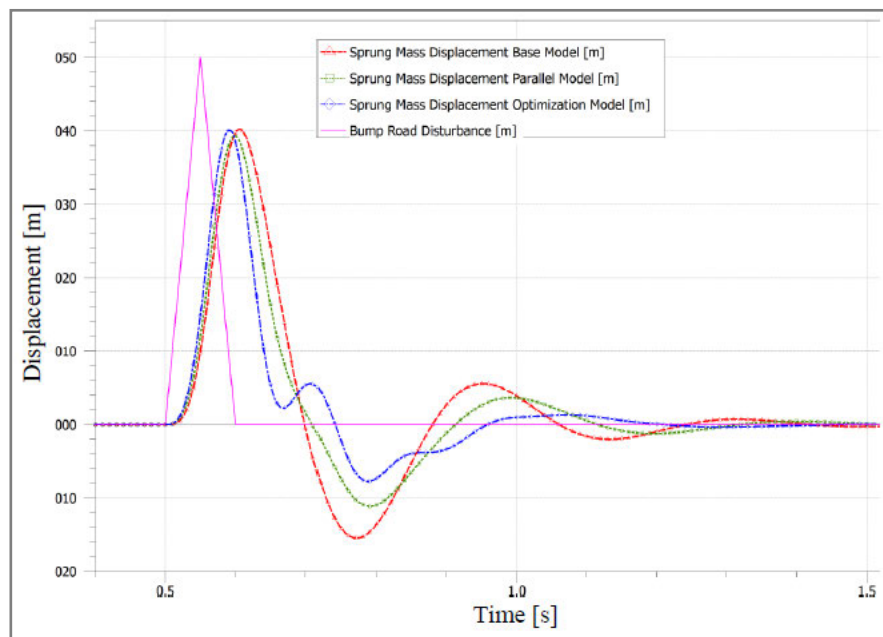
where  $\alpha \in [0,1]$  is a weighting between  $\text{RMS}(Z_s)$  and  $\text{RMS}(Z_{t-\text{def}})$ .

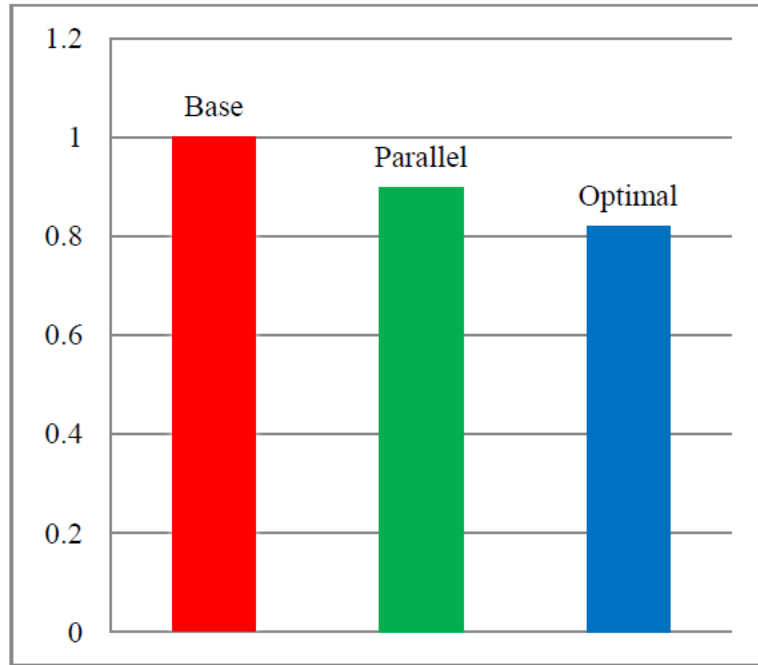
**Eq. 6-11** can be optimized with respect to the suspension parameters. The resulting optimal solutions are drawn for a particular  $Z_s$  and  $Z_{t-\text{def}}$ . We use the same method SQP with RSM, we optimize modal parameters of the passive suspension system with inerter. The modal parameter results to optimal both displacement and tire deflection are presented in **Table 6-4**.

**Table 6-4:** The comparative modal parameters to optimal both displacement and tire deflection.

Parameter	k	c	b	$k_t$
Base model	24000	1200	0	70000
Optimization model	21818	1037	5	86363
Unit	$[\text{Nm}^{-1}]$	$[\text{Nsm}^{-1}]$	$[\text{kg}]$	$[\text{Nm}^{-1}]$

**Figure 6-2** shows the results that the suspension system with inerter effects to the sprung mass displacement, the time histories of the displacement in respectively. From the results, it was verified that the displacement is reduced by comparison between base and parallel models. The optimization result is presented as circle symbol curve suggesting that the structure of the suspension optimize from the stiffness, damper and inerter get the best result for displacement. An encouraging feature of the optimization algorithm that it allows the change in the structure of suspension parameters varies in order to obtain the minimum vertical displacement values.





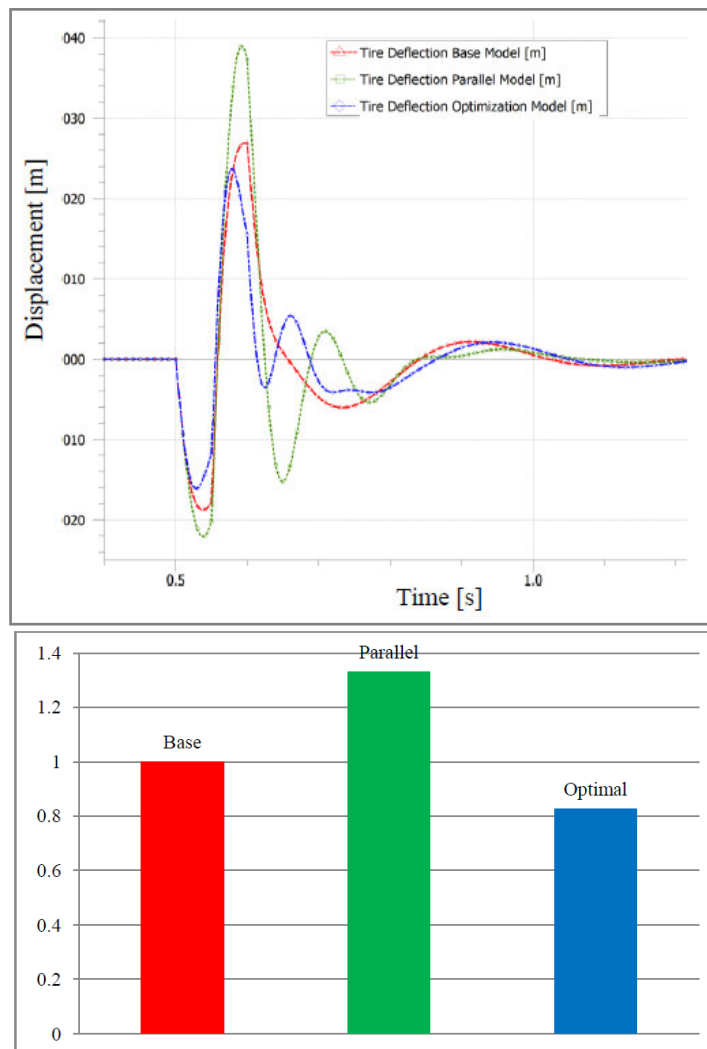
**Figure 6-3:** Comparative sprung mass displacement of base, parallel and optimal model in respectively.

Comparing between base and optimization model, we found that correspondences between these RMS of displacement variables of sprung mass is summarized below. If we only apply inerter to base suspension system, we can get a better RMS displacement improve about 10 percent, while we modify the system with optimal parameters, this value reduce more than 18 percent. These results verified with new suspension system could be accomplished that the body displacement dynamics can be reduced with employment inerter component.

**Table 6-5:** Comparison the RMS sprung mass displacement results.

Model	RMS( $Z_s$ ) [m]	Improvement
Base model	0.369	0%
Parallel model	0.331	10.32%
Optimization model	0.302	18.00%

**Figure 6-3** shows that sprung mass displacement is good at almost parameters of parallel model then the tire deflection is hard to get better RMS value. If we only apply inerter to base model under parallel suspension with no change of other parameters, the RMS value of tire deflection is increase more than 33 percent compare with base model. It means that tire deflection is not good for tire grip to contact the road.



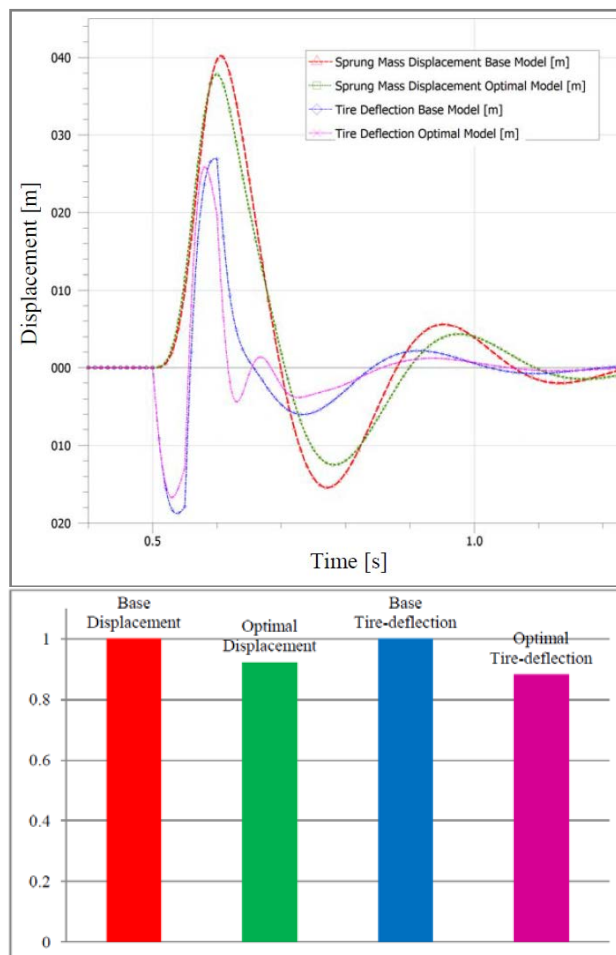
**Figure 6-4:** Comparative tire deflection of base, parallel and optimal model in respectively.

Otherwise, we optimal this value by changr the quarter ca parameter, the  $RMS(Z_{t-def})$  get better value by reduce around 17 percent shown on **Table 6-6**. Therefore, inerter still have advanced effect to the tire deflection in this case study.

**Table 6-6:** Comparison the RMS tire deflection results.

Model	RMS( $Z_{t-def}$ ) [m]	Improvement
Base model	0.206	0%
Parallel model	0.274	-33.06%
Optimization model	0.170	17.29%

In general, it can be seen that suspension with inerter offer performance advantages over conventional suspension for both RMS( $Z_s$ ) and RMS( $Z_{t-def}$ ) combined. The **Figure 6-4** shows that not only sprung mass displacement improves but also tire deflection reduces.



**Figure 6-5:** Comparative sprung mass displacement and tire deflection of base and optimal quarter-car model in respectively.

Although, both RMS displacement and tire deflection value are reduce slightly compare with individual optimization, near 8 percent in Table 8 compare to 18 percent in Table 6 for sprung mass displacement; and 12 percent in Table 8 compare to 17 percent in **Table 6-7** of tire deflection improvement. All of that it shows the advanced results for vehicle oscillation when we apply inerter on suspension system.

**Table 6-7:** Comparison both RMS sprung mass displacement and tire deflection results.

Model	RMS( $Z_s$ ) [m]	Improvement	RMS( $Z_{t-def}$ ) [m]	Improvement
Base model	0.369	0%	0.206	0%
Optimization model	0.339	7.84%	0.181	11.94%

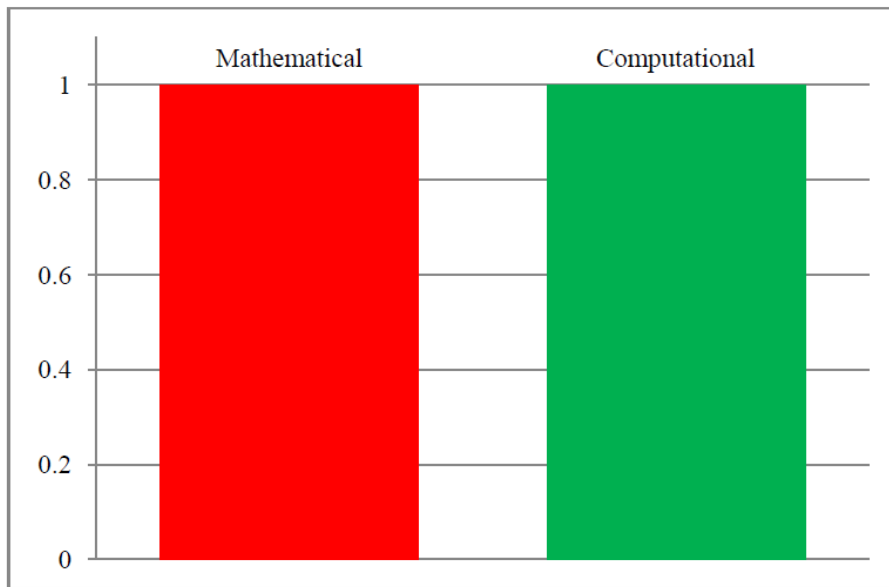
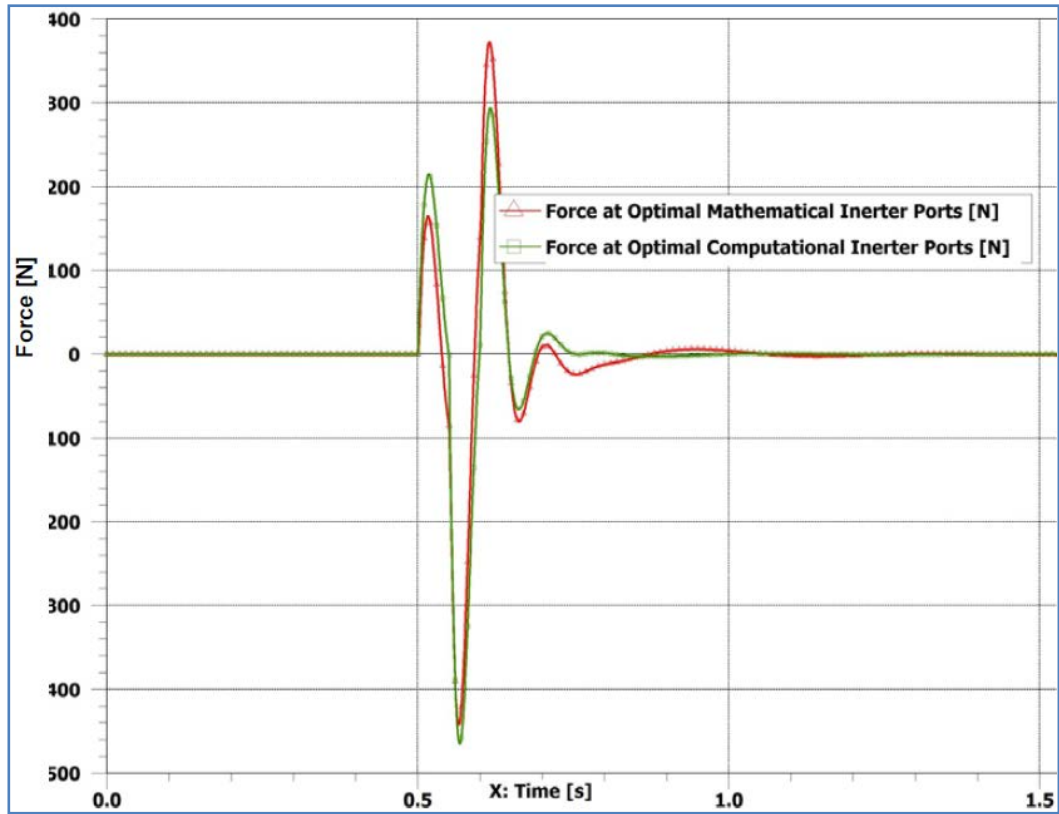
In summary, the results showed that suspension with inerter was not only have better displacement but also tire deflection. The conventional spring and damper always resulted in very normal vibration behavior, but the use of inerter can reduce the oscillation. In this studying, an optimal design to achieve variables stiffness, damping and inerter in suspension system with better results for both comfort and road holding.

### 6.3 Verification Optimal Modal Parameter

#### 6.3.1 Verification Force Apply to Inerter

The **Figure 6-6** shown that the force output at inerter component is the same shape and RMS value between mathematical and computational inerter mechanism with optimal value. At some points, the values are difference because of additional factors and coefficients inside computational model while the mathematical present with constant value in mass unit.





**Figure 6-6:** Comparison RMS force between optimization of mathematical and computational inerter.

The **Table 6-8** shows clearly that the root mean square of force apply to inerter component change only 0.03% after optimization process. This value has an advantage compare with 11.8% difference before optimization shown on Table ... On

the other hands, we reduce b value from initial to optimal parameter so the RMS force reduce from close 10000 N to near 2800 N in respectively. And the red line of mathematical model is closer to the green line of computational model. It verified that the input value of both model is table and the mathematical model is the simple model working correctly.

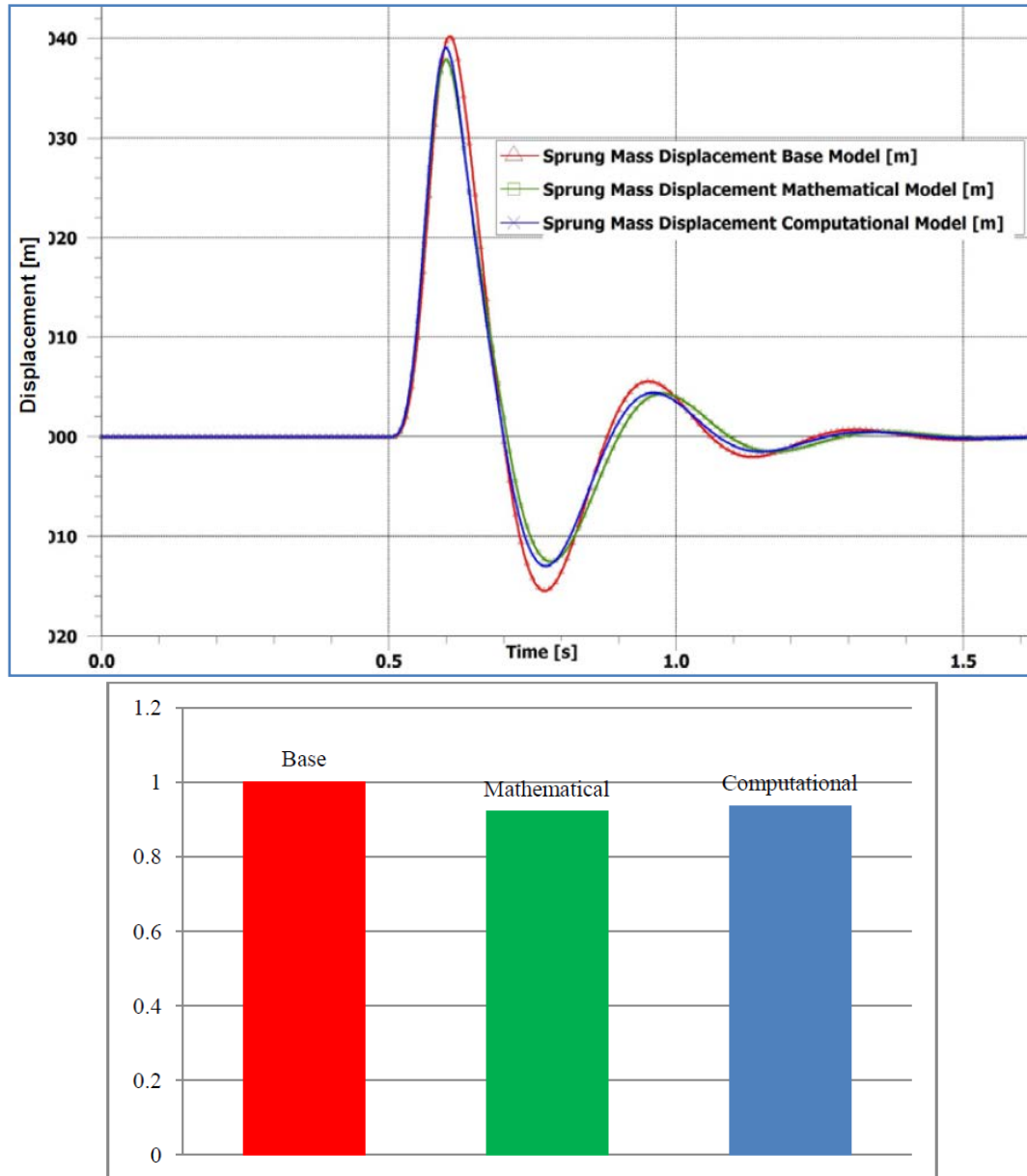
**Table 6-8:** Comparison RMS force apply to optimal mathematical and computational inerter respectively.

Model	RMS_Force [N]	Changeable
Optimal Mathematical Inerter model	2808	0
Optimal Computational Inerter model	2809	0.03%

### 6.3.2 Verification Sprung mass Displacement

For the post test analysis, we analyze output results of sprung mass displacement and tire deflection compare between mathematical and computational model in optimal parameters. Many ways of analyzing the results after tests have been performed, but we focus to the result of displacement and tire deflection in time domain which present for comfortable and handing on car.

**Figure 6-7** showed that both mathematical and computational model have advantages compare with conventional model about sprung mass displacement. While the suspension without inerter has high displacement of sprung-mass, then the system applied inerter has a smaller one. The computational model has frictions inside, included mass components in inerter mechanism so the line curves are unlike with mathematical model at the same time.



**Figure 6-7:** Comparison RMS sprung mass displacement among conventional, mathematical and computational model respectively.

**Table 6-9** shows the comparison  $RMS(Z_s)$  among conventional, mathematical and computational model in optimal parameters, clearly that the optimal model has total advantage compare with conventional model. We have to trade off between comfortable and handling so the displacement improvement near 8% lower than 10% of mathematical without optimization. But the computational model has more improvement 6.29% compare with computational model without optimization has

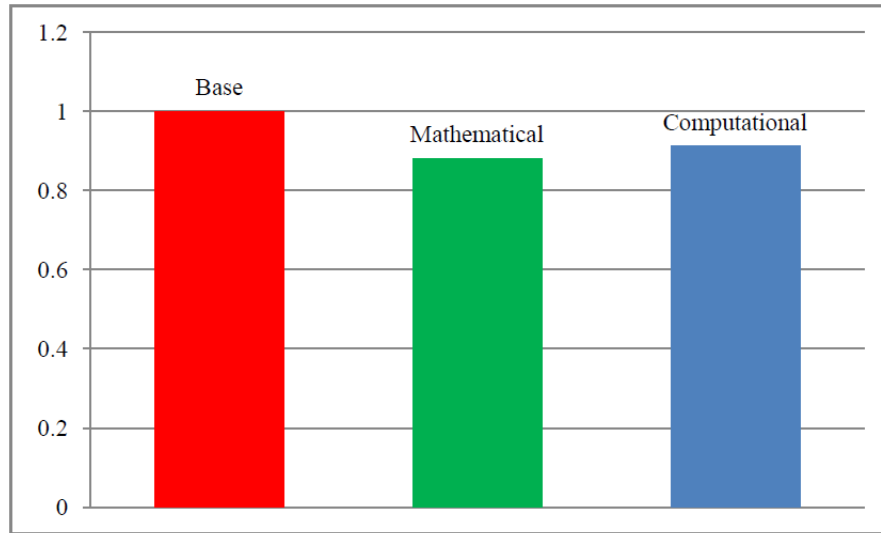
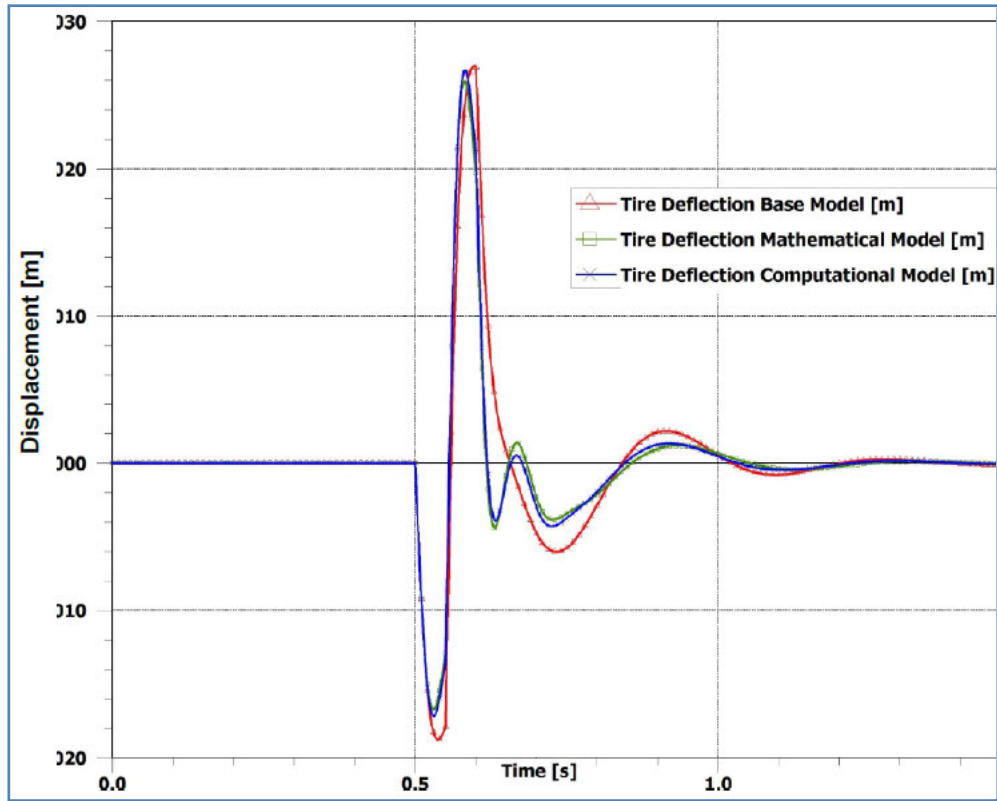
small advantage about 2%. The importance point is the improvement of both mathematical and computational model is closed after using optimization process. It verified that the mathematical model has the same properties with computational model, so we can estimate output value under both model.

**Table 6-9:** Comparison RMS of sprung displacement among conventional and optimal mathematical, optimal computational inerter respectively.

Model	RMS( $Z_s$ ) [m]	Improvement
Conventional Model	0.369	0
Mathematical Inerter model	0.340	7.84%
Computational Inerter model	0.345	6.29%

### 6.3.3 Verification Tire Deflection

From another point of view, the **Figure 6-8** showed the comparison of tire deflection between mathematical and computational model, both of them have advantages compare with conventional model. While the suspension without inerter has high tire deflection then the systems applied inerter have better results. In this case, it still has a difference between computational model and mathematical model, because of the frictions inside and coefficients of inerter mechanism.



**Figure 6-8:** Comparison RMS tire deflection among conventional, mathematical and computational model respectively.

The roots mean squares of tire deflection present on **Table 6-10**, it shown that a difference results still exist because of extra modal parameter add in inerter component. The comparison  $RMS(Z_{t-def})$  among conventional, mathematical and computational model in optimal parameters is difference. While the tire deflection of

mathematical model improvement near 12% more than only 8.78% improvement of computational model respectively. The totally, the improvement tire deflection of both mathematical and computational model is close after using optimization process. It verified that the mathematical and computational models can estimate each other. Furthermore, we can add supplementary for tests adjusting parameters in the initial locations of the suspension then modifying parameter to improving system.

**Table 6-10:** Comparison RMS of tire deflection among conventional and optimal mathematical, optimal computational inerter respectively.

Model	RMS( $Z_{t-def}$ ) [m]	Improvement
Conventional Model	0.206	0
Mathematical Inerter model	0.181	11.94%
Computational Inerter model	0.188	8.78%

#### 6.4 Optimization Half-car Model

For the optimization of rolling, in this section we will focus on a single aspect of performance is related to the rolling problem. We used the structure parameter which represented the following design variables:  $k$ ,  $c$ ,  $b$ , and  $k_t$ , with lower and upper boundaries showed below.

**Table 6-11:** The boundary of design variables.

Lower boundary	Parameter	Upper boundary	Unit
20000	$k$	28000	N/m
1000	$c$	1400	Ns/m
10	$b$	30	kg
60000	$k_t$	80000	N/m

The objective function is represented for the rolling angle modes as:

$$\varphi = \varphi(k, c, b, k_t) \rightarrow \text{Min} \quad \text{Eq. 6-12}$$

Under the synthetic assumption of basic passive half-car model, we can figure out this rolling equation:

$$\begin{aligned} \varphi = & 0.159 - 5.236(e - 07)k + 2.118(e - 11)k^2 \\ & - 1.35(e - 5)c + 1.138(e - 08)c^2 \\ & - 1.136(e - 06)k_t + 6.555(e - 12)k_t^2 \\ & - 7.75(e - 4)b + 2.838(e - 05)b^2 \end{aligned} \quad \text{Eq. 6-13}$$

Constrain functions were represented by the body displacement modes under boundaries above. In this case, the results show:

$$\text{Min}\{\text{Max } Z_2\} \leq Z_2(k, c, b, k_t) \leq \text{Max}\{\text{Max } Z_2\} \quad \text{Eq. 6-14}$$

To calculating Max Z2, we used Orthogonal Arrays (OA) of Design of Experimental with L27 (313) then:

$$\text{Min}\{\text{Max } Z_2\} = 0.0641 \text{ (m)} \quad \text{Eq. 6-15}$$

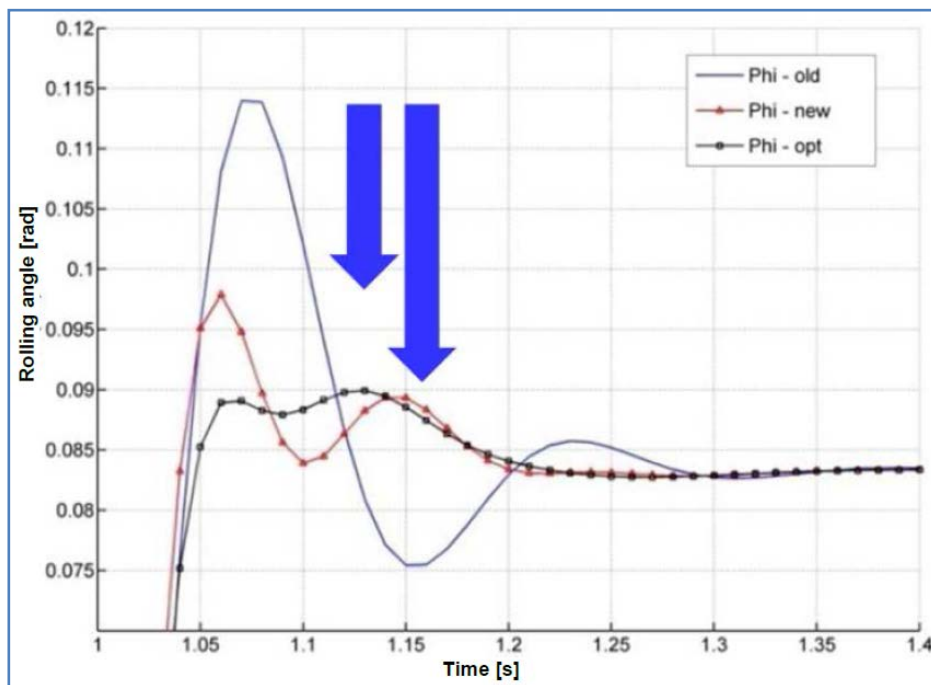
$$\text{Max}\{\text{Max } Z_2\} = 0.0755 \text{ (m)} \quad \text{Eq. 6-16}$$

With the same optimal methods, we introduce the approximate optimization method, Sequential Quadratic Programming (SQP) with Response Surface Method (RSM). We made RSM using the OA to optimize modal parameters for half-car model. The new modal parameters are represented for optimization suspension system and they called:  $k_{\text{opt}}$ ,  $c_{\text{opt}}$ ,  $b_{\text{opt}}$  and  $k_{t-\text{opt}}$ .

**Table 6-12:** The comparative modal parameters for half-car model.

Parameter	k	c	b	$k_t$
old_model	24000	1200	X	70000
new_model	24000	1200	20	70000
opt_model	20727	1036	16.63	78182
Unit	N/m	Ns/m	kg	N/m

For the half-car model, the results were confirmed that the inerter is added to affect the roll angle, the time histories of the body roll angles are shown in **Figure 6-9**, respectively. From the results, it was verified that the rolling angle is reduced by comparison among each models.



**Figure 6-9:** Results of optimization rolling angle for half-car models.

The optimization result is presented as circle-symbol curve suggesting that the structure used the optimal parameters of stiffness, damper and inerter. Comparing among old-model, new-model and opt-model we found that the rolling angle is reduced, as summarized below in **Table 6-13**.

**Table 6-13:** The comparison rolling peak results.

Rolling peak	Result (rad)	Improvement
$\varphi_{old}$	0.114	0%
$\varphi_{new}$	0.098	14.03%
$\varphi_{opt}$	0.090	21.05%



The table shows that with inerter components are employed to passive suspension system as a parallel structure, the rolling angle will be reduced. We just use for a simple and fix inerter parameter  $b$ , the rolling value reduce 14 percent, while it will be reduced more than 21 percent if we optimal suspension parameter. In conclusion, the inerter component has an advanced effect to the suspension system in general and in passive suspension system in particular.

## **6.5 Summary and Comments**

In this chapter, we introduce optimization process using response surface methodology. This is last step for designing and improving production. We used the quarter-car and half-car model with inerter employ under the road disturbance responses to estimate displacement, tire deflection and rolling angle. Through system analysis, it was shown that the performance requirements can be achieved with optimization process. Furthermore, a verification process will be confirm system again, it shown the better results of system in small gap between mathematical and computational model. It is strongly verify that we optimization on mathematical model is correctly in this thesis.



## **CHAPTER 7**

### **CONCLUSIONS**

#### **7.1 Contributions of Dissertation**

We summary the main contributions of this dissertation:

In general, comfort improvement has been a very active research field in the last decade as a consequence, most of the issues are active and semi-active suspension control concerns the handling of stroke limitations which is linked to the comfort objective. However, the aim of this dissertation was to discuss the passive suspension employing inerter in necessary focus another trend of vehicle oscillation research. In this thesis, an innovative optimal performance bound is computed for both comfort and road-holding improvement objectives in the passive network employing inerter mechanism.

In chapter 3, a general theorem for suspension system was developed. The passive suspension was considered that is possible application of the inerter. In frequency response function domain, the parallel suspension system is carried out and can be designed to improve vehicle dynamics in low frequency. The results showed that suspension with inerter was not only have better displacement but also tire deflection. The conventional spring and damper always resulted in very normal vibration behavior, but the use of inerter can reduce the oscillation.

In chapter 4, we applied the theorems developed in chapter 3 to the linear half-car model. The results showed that suspension with inerter was not only have

better displacement but also have smaller rolling angle of sprung mass body on quarter-car and half-car model in respectively. In the next chapter, we developed an algorithm for the numerical calculation of the suspension module in parallel structure with inerter. Hence it is possible to apply this model design to complex systems.

In chapter 5, we developed the verification process to numerically calculate the suspension model for quarter-car model, which is useful for estimate complex systems. We applied the procedure to the linear quarter-car model with conceptual inerter model employment. The mathematical model figure out with assumption of simple theories with constant  $b$  value to compare with the computational model implements the detail factors and coefficients inside the inerter mechanism. It is noticed that all the computational models we have completed in the numerical models were based on a real model. The results shown that mathematical and computational models work on the same shapes of force apply to inerter and also had advanced on RMS displacement compare with conventional model. It is verified that mathematical model performance is correctly working theories, thus it is importance for optimization process on the next steps.

In the last chapter, we introduce optimization process using response surface methodology which an optimal design to achieve variables stiffness, damping and inerter in suspension system with better results for both comfort and road holding. It was showed that conventional spring and damper always resulted in very normal vibration behavior, but the use of inerter can reduce the oscillation. Through system analysis, it was shown that the performance requirements can be achieved with optimization process. On the other hands, a verification process will be confirm system again, it shown the better results of system in small gap between mathematical and computational model. It is strongly verify that we optimization on mathematical

model is correctly in this thesis. Furthermore, an optimal design to achieve variables stiffness, damping and inerter in suspension system achieved better results for rolling with road disturbance in half-car model. These simulations confirmed that ride comfort in the same frequency domain with basic suspension system while the body car rolling was improved.

Throughout this dissertation, computing software was used for simulation of vehicle models in combination with the theoretical work. Therefore, verification and optimization process approach should be very useful to solve vehicle oscillation problems.

## **7.2 Future Research**

In this dissertation, first step to figure out the trend to develop suspension oscillation employing inerter on passive system. We can combine this component with other strut as semi-active or electrical inerter inside the system. Base on these advantage of optimization results; we verify that the suspension with a controllable inerter under simple conditions can apply on normal car.

We will integrate other types of inerter which can be controlled, and apply on suspension system for large dynamic stability. We should construct some physical modeling for suspension systems then it will be validated with mathematical modeling. We can integrate controllable inerter mechanism to optimizing suspension system for other dynamics stability focus to interactive left side and right side, also study with other dynamic attitudes on full-car model.



## APPENDIX A

### SIMULATION FOR QUARTER-CAR MODEL USING MATLAB R2014

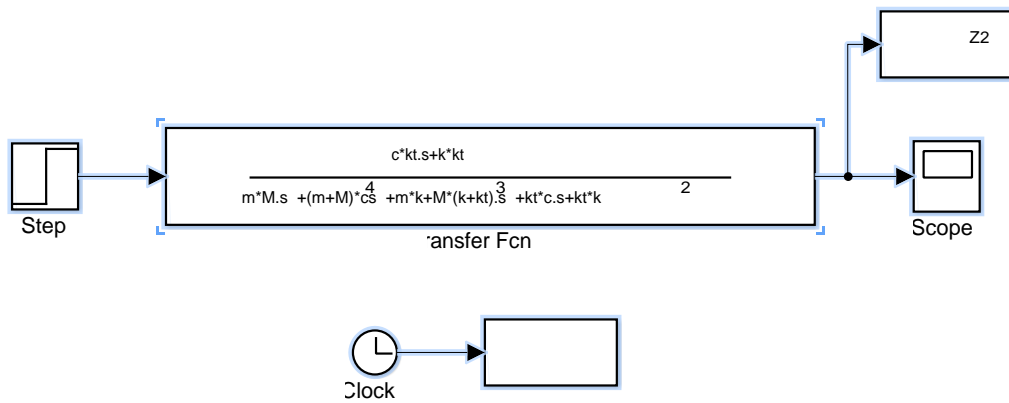


Figure A-1: Simulink of conventional quarter-car model.

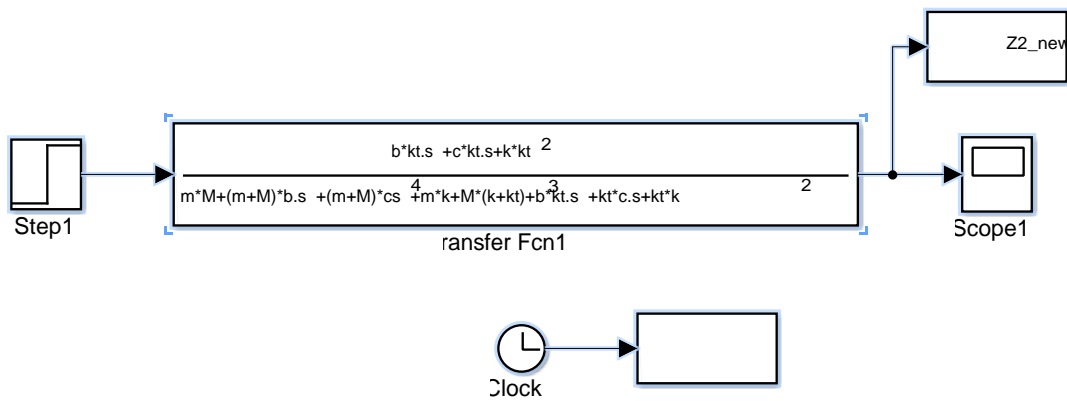


Figure A-2: Simulink of new and optimal quarter-car model.

#### A.1 Function for Quarter-car Model

```
clear all
close all
clc
% Half Car Modal Parameters
```

```

M = 126;      %kg
m = 12;       %kg
g = 9.8;      %m/s^2
a = 0.6;      %m
%
kt= 70000;    %N/m
k= 24000;     %N/m
c = 1200;     %Ns/m
b = 20;       %kg
%
H0_L= 0;      %m
H0_R= 0.1;    %m

sim('Quarter_Model_Conventional')
figure(1)
hold on
plot(t,Z2,'r')
xlabel('t(s)')
ylabel('Z2 (m)')
grid on

sim('Quarter_Model_New')
figure(1)
hold on
plot(t,Z2_new,'b')
xlabel('t(s)')
ylabel('Z2_new')
grid on

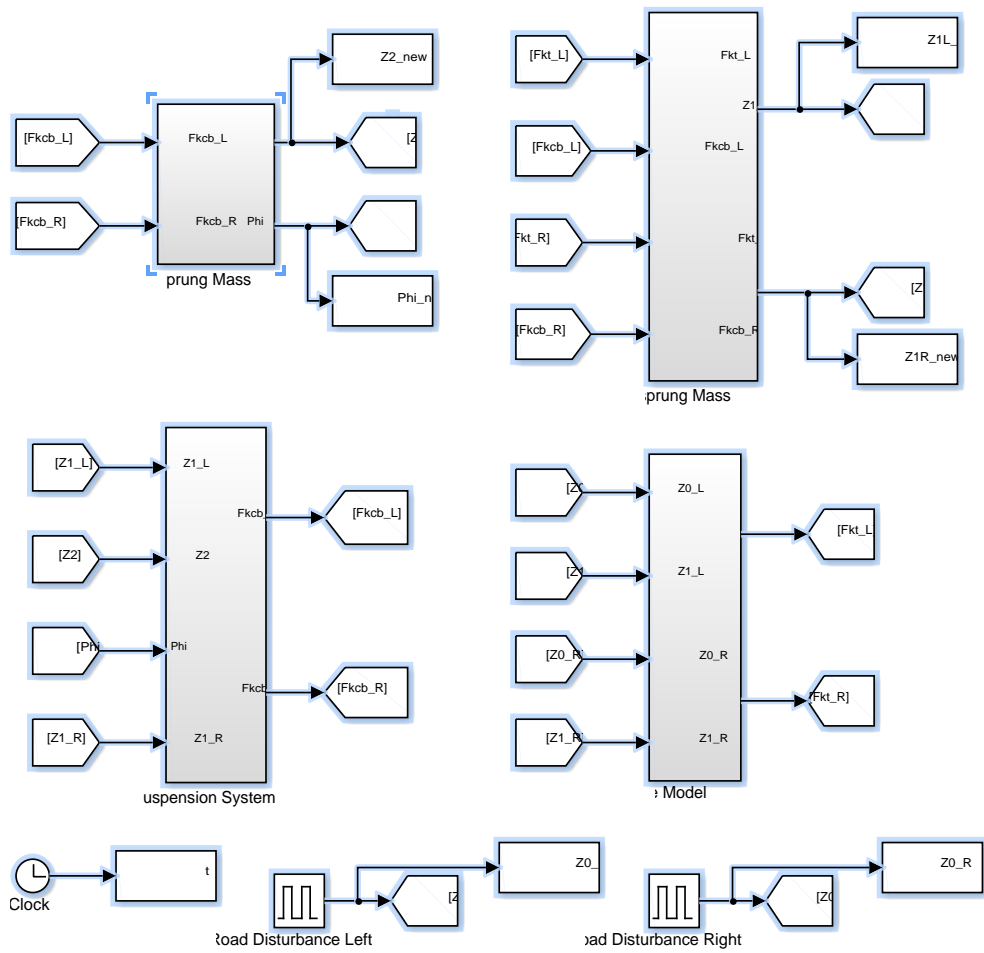
sim('Quarter_Model_Optimization')
figure(1)
hold on
plot(t,Z2_new,'m')
xlabel('t(s)')
ylabel('Z2_opt')
grid on

```

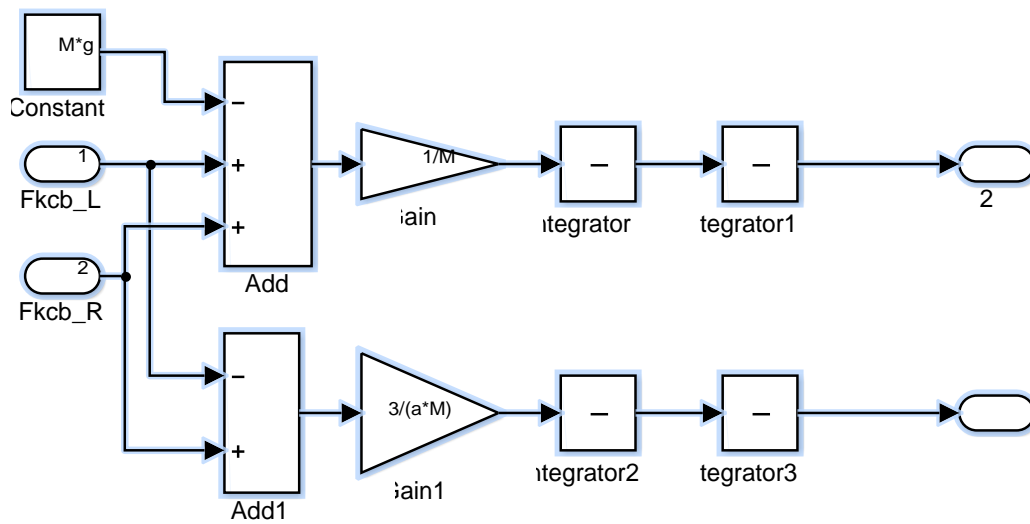


## APPENDIX B

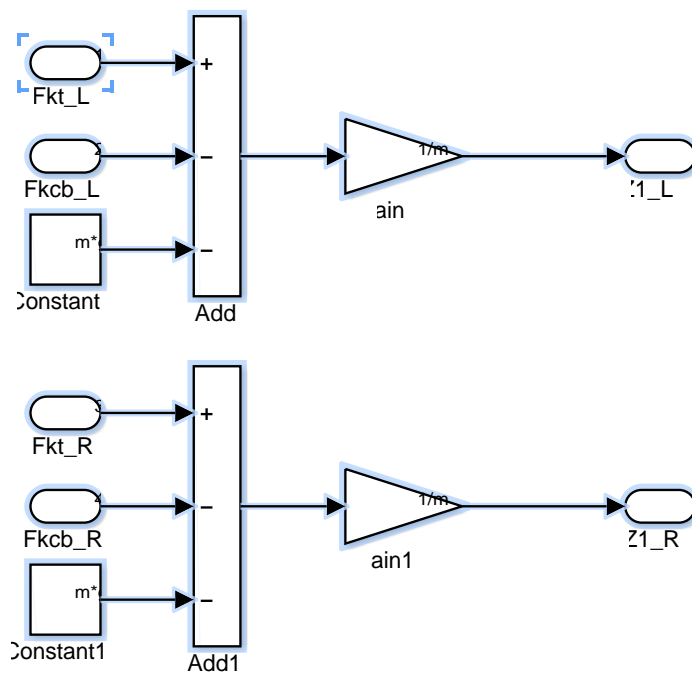
### SIMULATION FOR HALF-CAR MODEL USING MATLAB R2014



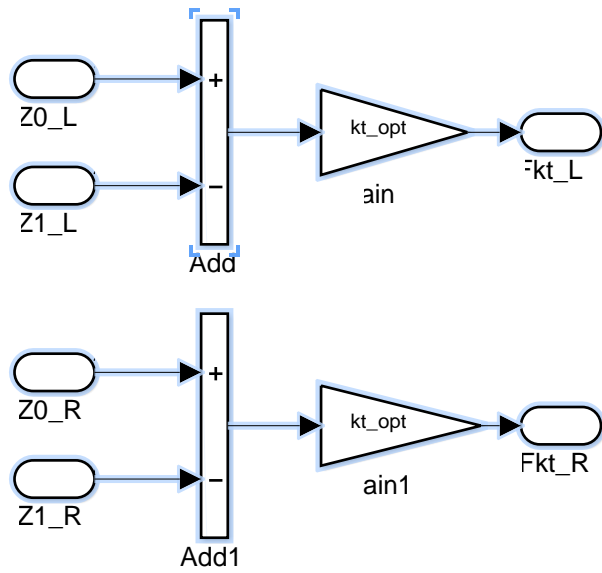
**Figure B-3:** Simulink of half-car model.



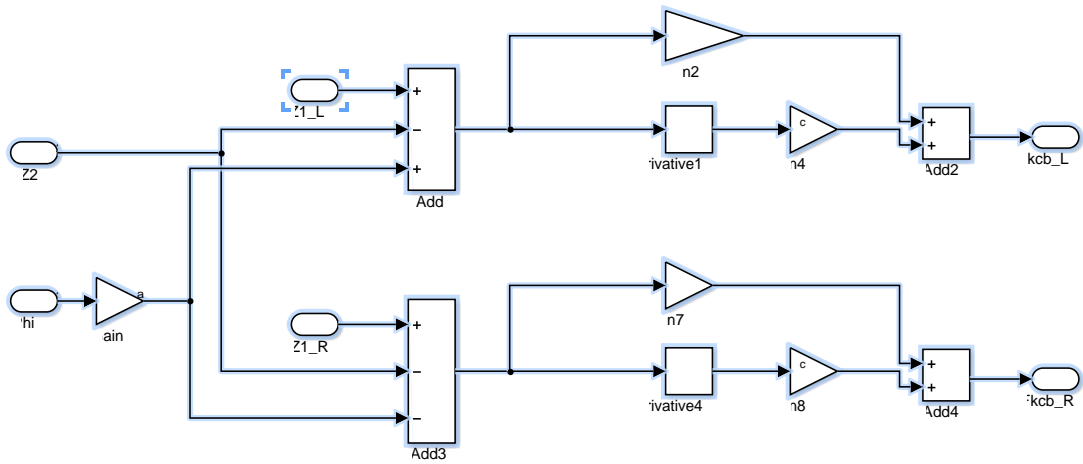
**Figure B-4:** Simulink of sprung mass module.



**Figure B-5:** Simulink of un-sprung mass module.



**Figure B-6:** Simulink of tire module.



**Figure B-7:** Simulink of conventional suspension module.

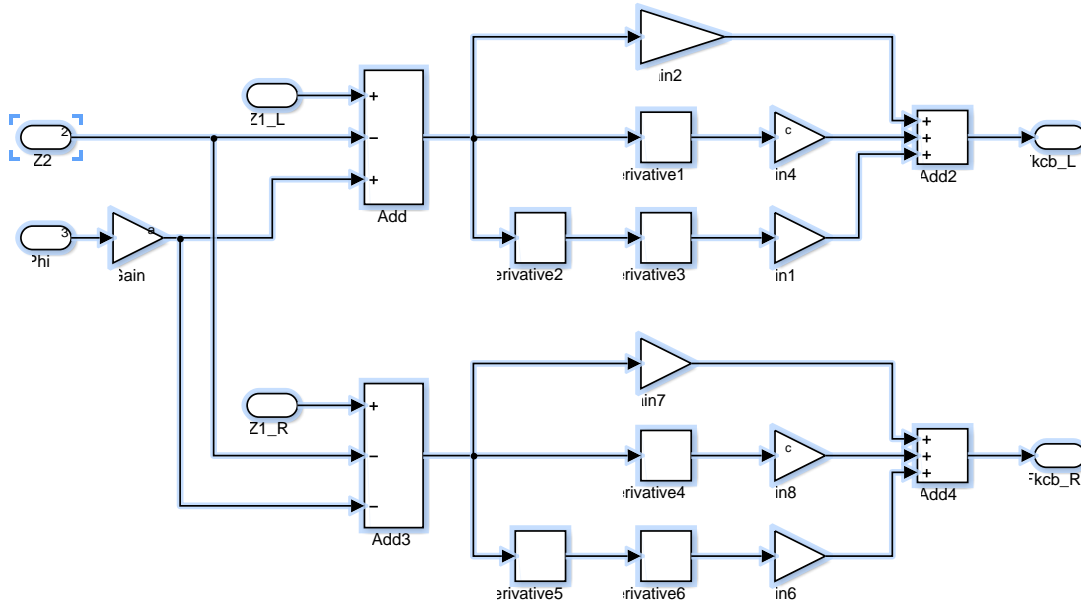


Figure B-8: Simulink of new parallel suspension module.

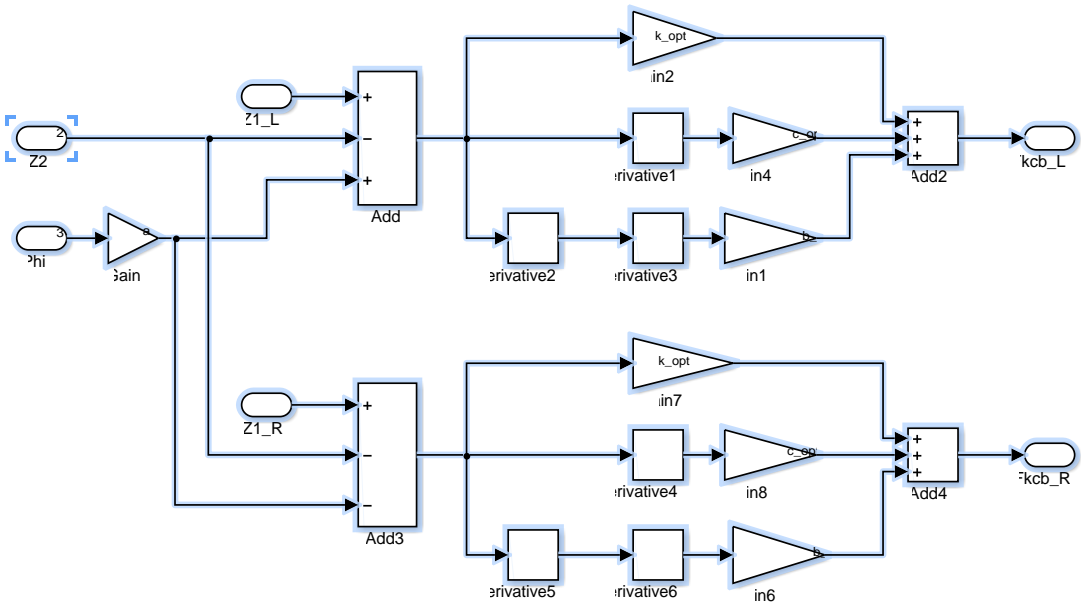


Figure B-9: Simulink of optimal suspension module.

### B.1 Function for Half-car Model

```

clear all
close all
clc
% Half Car Modal Parameters
M = 126; %kg

```

```

m = 12;      %kg
g = 9.8;    %m/s^2
a = 0.6;    %m
kt= 70000;  %N/m
k= 24000;   %N/m
c = 1200;   %Ns/m
b = 20;     %kg
%
kt_opt= 78182; %N/m
k_opt = 20727; %N/m
c_opt = 1036; %Ns/m
b_opt = 13.63; %kg
%
H0_L= 0; %m
H0_R= 0.1; %m
% Run Simulation
sim('Half_Car_Rolling_Old')
sim('Half_Car_Rolling_New')
sim('Half_Car_Rolling_Opt')
% Comparative Results Z2
figure(1)
hold on
plot(t,Z2_old,'b')
plot(t,Z2_new,'r')
plot(t,Z2_opt,'k')
xlabel('t(s)')
ylabel('Z2 (m)')
grid on
% Comparative Results Phi
figure(2)
hold on
plot(t,Phi_old,'b')
plot(t,Phi_new,'r')
plot(t,Phi_opt,'k')
xlabel('t(s)')
ylabel('Phi (rad)')
grid on
% Road Disturbance
figure(3)
hold on
plot(t,Z0_L,'b')
plot(t,Z0_R,'g')
xlabel('t(s)')
ylabel('Z0 (m)')
grid on

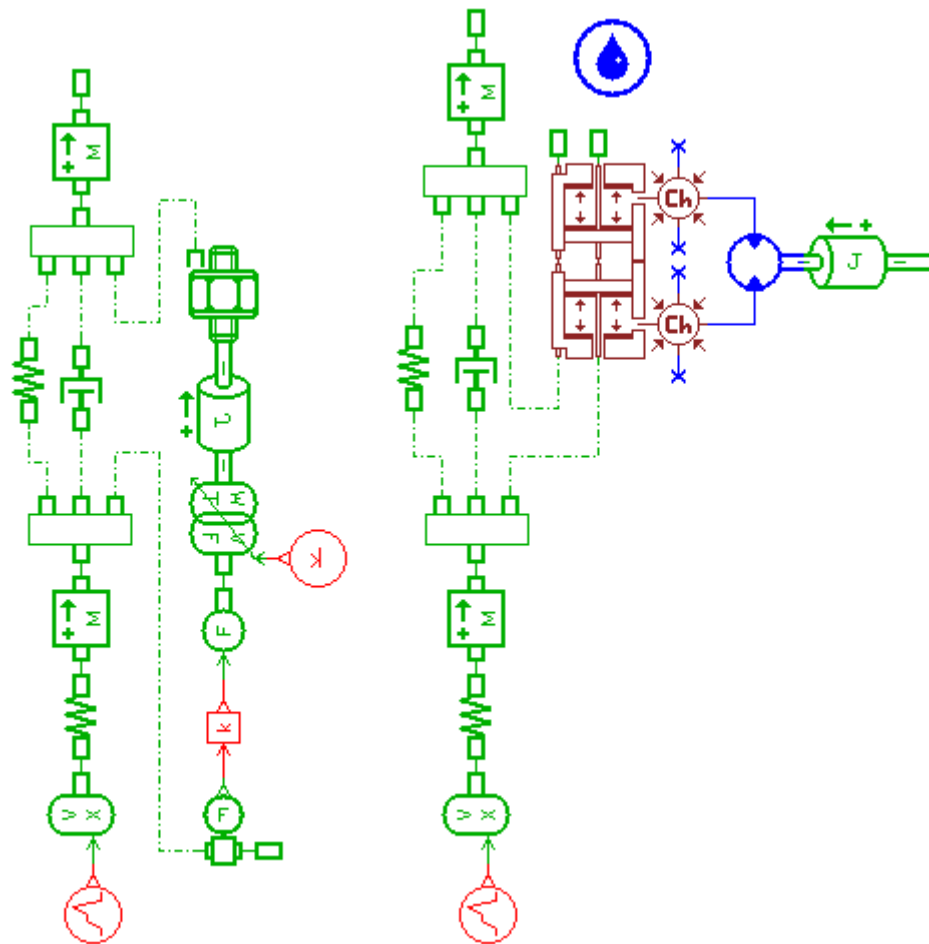
% Comparative Results MaxValue
maxPhi_old = max(abs(Phi_old))
maxPhi_new = max(abs(Phi_new))
maxPhi_opt = max(abs(Phi_opt))
maxZ2_old = max(abs(Z2_old))
maxZ2_new = max(abs(Z2_new))
maxZ2_opt = max(abs(Z2_opt))

```



## APPENDIX C

### COMPUTATIONAL QUARTER-CAR MODEL AMESIM REV 11 SL11



**Figure C-10:** The computational quarter-car model with screw inerter and hydraulic inerter in respectively.

## **APPENDIX D**

### **SOFTWARE USE IN THIS DISSERTATION**

**D.1 Matlab & Simulink: Version R2014.**

**D.2 AMESim Rev 11 SL11**



## BIBLIOGRAPHY

- [1] Bosch, *Automotive Handbook*, 8th ed.: SAE International, 2011.
- [2] M. Chiaberge, *New Trends and Developments in Automotive System Engineering*.: First published, 2011.
- [3] J. F. Gardner, and J. L. Shearer B. T. Kulakowski, *Dynamic Modeling and Control of Engineering Systems*, Third edition ed.: Cambridge University Press, 2007.
- [4] T. Gillespie, "Fundamental of vehicle dynamics," in *Society of Automotive Engineers*, 1992.
- [5] A. Zin, "Robust automotive suspension control toward global chassis control," Laboratoire d'Automatique de Grenoble (now GIPSA-lab), Grenoble, France, Ph.D. Thesis 2005.
- [6] C., Sename, O., and Dugard, L. Poussot-Vassal, "Attitude and handling improvements based on optimal skyhook and feedforward strategy with semi-active suspensions," *International Journal of Vehicle Autonomous Systems*, vol. 6(3–4), pp. 308–329, 2009.
- [7] D. and Isermann, R. Fischer, "Mechatronic semi-active and active vehicle suspensions," in *Control Engineering Practice*, 2003, pp. 1353–1367.
- [8] G., Peter, T., Gissinger, G., and Basset, M. Girardin, "Modélisation non linéaire du confort dynamique d'un véhicule," in *Proceedings of the 17th Conférence Internationale*, Bordeaux, France, 2006.
- [9] C. Poussot-Vassal, C. Spelta, O. Sename, L. Dugard S. M. Savaresi, *Semi-Active Suspension Control Design for Vehicles*.: Published by Elsevier Ltd, 2010.
- [10] C., Velenis, E., Tsiotras, P., and Gissinger, G. Canudas, "Dynamic tire friction models for road/tire longitudinal interaction," in *Vehicle System Dynamics*, 2003, pp. 189–226.
- [11] U. and Nielsen, L. Kiencke, "Automotive Control Systems," in *Springer-Verlag*, 2000.
- [12] M. Tanelli, "Active Braking Control Systems Design for Road Vehicles,"

dipartimento di Elettronica e Informazione, Milano, Italy, Ph.D. thesis 2007.

- [13] E., Tsiotras, P., Canudas, C., and Sorine, M. Velenis, "Dynamic tire friction models for combined longitudinal and lateral vehicle motion," in *Vehicle System Dynamics*, 2005, pp. 43(1):3–29.
- [14] M. C. Smith, "Synthesis of Mechanical Networks: The Inerter," *IEEE Transactions on Automatic Control*, vol. 47, Nov.10 2002.
- [15] M. S. Hsu, W. J. Su, and T. C. Lin F. C. Wang, "Screw Type Inerter Mechanism," U.S Patent 0108510, 2009.
- [16] T. C. Lin F. C. Wang, "Hydraulic Inerter Mechanism," U.S Patent 0139225, 2009.
- [17] M. C. Smith, "Passive Network Synthesis Revisited," Department of Engineering, University of Cambridge, Cambridge, U.K, Semi-plenary Lecture 2003.
- [18] Malcolm C. Smith, "The Inerter Concept and Its Application," Department of Engineering, University of Cambridge, Cambridge U.K, Plenary Lecture 2003.
- [19] C. Papageorgiou, F. Scheibe, F. C. Wang, and M. C. Smith M. Z. Q. Chen, "The Missing Mechanical Circuit Element," no. IEEE Circuits and Systems Magazine, 2009.
- [20] D. Sammier, "Sur la modélisation et la commande des suspensions automobiles," Laboratoire d'Automatique de Grenoble, Grenoble, France, Ph.D.Thesis 2001.
- [21] T. Gillespie, "Fundamental of vehicle dynamics," in *Society of Automotive Engineers*, 1992.
- [22] D., Sename, O., and Dugard, L. Sammier, "Skyhook and  $H_\infty$  control of active vehicle suspensions: some practical aspects," in *Vehicle System Dynamics*, 2003, pp. 39(4):279–308.
- [23] A. T. Murphy, and H. H. Richardson J. L. Shearer, *Introduction to System Dynamics.*: Addison-Wesley, 1967.
- [24] J. C. Schönfeld, "Analogy of hydraulic, mechanical, acoustic and electrical," *Appl. Sci. Res*, vol. vol. 3, pp. 417–450, 1954.
- [25] D. L. Margolis, and R. C. Rosenberg D. C. Karnopp, "System Dynamics: Modeling and Simulation of Mechatronic Systems," in *Wiley*, New York, 2000.
- [26] F. C. Wang and W. J. Su, "Inerter Nonlinearities and the Impact on Suspension Control," in *American Control Conference*, Seattle, Washington, USA, 2008.

- [27] T. Uemura, "Proposed Suspension System that Aims to Achieve Both ride Comfort and Maneuverability," Shibaura Institute of Technology, Master Thesis 2009.
- [28] Jyuro Izumi, "Combined environmental testing for equipment used on automobiles - Overview and test approach," ESPEC Technology Report No. 6,.
- [29] David Moorcroft, "Model Verification and Validation Process," Federal Aviation, CBA Meeting 2012.
- [30] P. J. Roache, "Verification and Validation in Computational Science and Engineering," in *Hermosa Publishers*, Albuquerque, NM, 1998.
- [31] P. J. Roache, "Verification of Codes and Calculations," *AIAA Journal*, vol. 5, no. 36, pp. 696–702, 1998.
- [32] W. L., and Trucano, T. G. Oberkampf, "Verification and Validation in Computational Fluid Dynamics," in *Progress in Aerospace Sciences*, 2002, pp. 209–272.
- [33] J. H., and Peric, M. Ferziger, "Computational Methods for Fluid Dynamics," in *Springer Verlag*, New York, 1996.
- [34] J. T. Oden, "Error Estimation and Control in Computational Fluid Dynamics," in *The Mathematics of Finite Elements and Applications*, New York, 1994, pp. 1–23.
- [35] Douglas C. Montgomery, Christine M. Anderson-Cook Raymond H. Myers, *Response surface methodology : process and product optimization using designed experiments*, 3rd ed. New Jersey, Canada: John Wiley & Sons, Inc, 2009.
- [36] W. J., and Hunter, W. G. Hill, "A Review of Response Surface Methodology: A Literature Review," in *Technometrics*, 1996, pp. 571–590.
- [37] R., and Pike, D. J. Mead, "A Review of Response Surface Methodology from a Biometric Viewpoint," in *Biometrics*, 1975, pp. 803–851.
- [38] R. H., Khuri, A. I., and Carter, W. H. Myers, "Response Surface Methodology: 1966–1988," in *Technometrics*, 1989, pp. 137–157.
- [39] R. H., Montgomery, D. C., Vining, G. G., Borror, C. M., and Kowalski, S. M. Myers, "Response Surface Methodology: A Retrospective and Literature Survey," in *Journal of Quality Technology*, 2004, pp. 53–77.
- [40] R. H. Myers, *Response Surface Methodology*. Canada: Blacksburg, VA, 1976.

- [41] M. C. Smith and F. C. Wang, "Performance Benefits in Passive Vehicle Suspensions Employing Inerters," in *Proceedings of the 42nd IEEE, Conference on Decision and Control*, Maui, Hawaii USA, 2003.
- [42] F. C. Wang and W. J. Su, "Inerter Nonlinearities and the Impact on Suspension Control," in *American Control Conference*, Seattle, Washington, USA, 2008.
- [43] J. Izumi, "Combined Environmental Testing for Equipment used on Automobiles," ESPEC Technology Report No. 6, Overview and Test Approach.
- [44] R. K., and Nachtsheim, C. J. Meyers, "Constructing Exact D-Optimal Experimental Designs by Simulated Annealing," in *American Journal of Mathematical and Management Sciences*, 1988, pp. 329–359.

## LIST OF PUBLICATION

- [P.1] **Thanh-Tung TRAN**, Hiroshi HASEGAWA "*Advanced Passive Suspension with Inerter Devices and Optimization Design for Vehicle Oscillation*", International Journal of Materials Science and Engineering (IJMSE, ISSN: 2315-4527).
- [P2] **Thanh-Tung TRAN**, Chiaki HORI and Hiroshi HASEGAWA "*Integrated Inerter Design and Application to Optimal Vehicle Suspension System*", International Journal of Computer-Aided technologies (IJCAx, ISSN: 2349-218X) Vol.1, No.2/3, Oct.2014.
- [P3] **Thanh-Tung TRAN**, Hiroshi HASEGAWA "*Verification and Optimization Advantage of Inerter Devices Apply to Grounded Vehicle Dynamics*", Thematic Conference on Multi-body Dynamics, Jun.2015 Barcelona.
- [P4] **Thanh-Tung TRAN**, Hiroshi HASEGAWA "*Advanced Passive Suspension with Inerter Devices and Optimization Design for Vehicle Oscillation*", ICCMA 2014, Dec.2014 Dubai, UAE.
- [P5] **Thanh-Tung TRAN**, Chiaki HORI and Hiroshi HASEGAWA "*Verification and optimization of Formula SAE suspension employing Inerter mechanism*", MOVIC 2014, Aug.2014 Sapporo, Japan.
- [P6] **Thanh-Tung TRAN**, Hiroshi HASEGAWA "*Integrated Optimization Design for Vehicle Dynamics Considering Suspension with Inerter*", APVC2013, Jun.2013, ICC Jeju, Korea.
- [P7] **Thanh-Tung TRAN**, Hiroshi HASEGAWA "*Integrated Inerter Design and Application on Vehicle Suspension*", ICMDT2013, May.2013 BEXCO, Pusan, Korea.
- [P8] **Thanh-Tung TRAN**, Chiaki HORI and Hiroshi HASEGAWA "*Simulation Passive Suspension System with Inerter to Optimize Rolling*", SEATUC, Mar.2013 Bandung, Indonesia.